Glucocorticoid Receptor Promoter Expression and Apoptosis Induction in Small Cell Lung Cancer

by

Nimisha Singh

Submitted in fulfilment of the academic requirements for the degree of Master of Science in the School of Life Sciences, Department of Biological and Conservational Sciences, University of KwaZulu-Natal, Durban

February 2013

As the candidate's supervisor I have approved this thesis/dissertation for submission.

Signed: _____ Name: Dr. Paula Sommer Date: _____

Abstract

Lung cancer is the most common cancer worldwide and is the fourth leading cause of death in South Africa. Lung cancer is categorised into two types; non-small cell lung cancer and small cell lung cancer (SCLC). SCLC constitutes 20% of all lung cancers and is considered to be an aggressive tumour as it gains chemo-resistance and exhibits early metastasis in diagnosed patients. SCLC cells originate from the neuroendocrine cells of the bronchoepithelium and are known to secrete the neuropeptide, proopiomelanocortin (POMC). POMC undergoes proteolytic cleavage to produce the adrenocorticotropin hormone (ACTH). ACTH stimulates the production of the steroid hormone, glucocorticoid hormone (GC), through the hypothalamus-pituitary-adrenal (HPA) axis. The produced GCs mediate a negative feedback system of the HPA axis to sequester ACTH production. SCLC cells are insensitive to this negative feedback stimulus. GCs elicit their actions through the glucocorticoid receptor (GR). Studies have shown that SCLC cells have a reduced expression of GR which perpetuates the GC-insensitivity. Importantly, over-expression of exogenous GR in SCLC cells leads to cell death by apoptosis. It was postulated that SCLC cells select against GR expression for longevity. Cancer cells are known to alter/silence the expression of tumour suppressor genes by a mechanism known as methylation. Methylation occurs when the enzyme, DNA methyltransferase 1, adds a methyl group to a cytosine present in a guanine-cytosine rich region of the gene (CpG island). The GR gene has a 5'-untranslated exon 1 region that consists of eight promoter regions (1A-1J), in these promoter regions are many CpG islands that have the potential to be methylated.

The first aim of this study was to determine the promoter/s utilised by SCLC cells to express the GR protein. Conventional PCR revealed that all three cell lines predominantly utilise promoters 1B and 1C for GR expression. Bioinformatic analysis revealed that these promoters contain putative CpG islands and new data suggests that the GR is silenced by methylation and that treatment with a de-methylating agent results in GR re-expression. To determine which promoter is responsible for GR re-expression after de-methylation, the SCLC cell line, DMS79, as well as two control cell lines, A549 and HEK cells, were treated with the de-methylating agent, 5-aza-2'-deoxycytidine, for 72 hours. qPCR analyses revealed that all three cell lines expressed promoters 1B and 1C with A549 cells showing no evidence of methylation. The HEK cells showed methylation in promoter 1C and not promoter 1B. The SCLC cells showed

methylation in both promoter 1B and 1C, however, only promoter 1B showed a significant increase in transcript levels.

SCLC cells are induced to undergo GC-mediated apoptosis when GR expression is restored however the mechanism utilised by the GR to induce the apoptotic cascade is unknown. The GR structure is divided into three domains; ligand binding domain (LBD), DNA binding domain (DBD) and amino terminal domain (NTD). The second aim of this study was to determine the component of the GR that induces apoptosis of SCLC cells. HEK and SCLC cells were infected with empty virus and various GR construct viruses; containing either a wild-type GR, ligand binding mutant, DNA binding mutant or a transactivation mutant (NTD); for 72 hours. Both cell lines were quantified for apoptosis and cell death using microscopic analyses. In HEK cells, it was shown that apoptosis occurred in cells expressing the wild-type GR, the DNA binding mutant and transactivation mutant constructs but apoptosis was reduced in cells expressing the ligand binding viruses. This indicates that the LBD may be necessary for inducing apoptosis in HEK cells. In DMS79 cells, apoptosis occurred in cells expressing the wild-type GR, ligand binding mutant and the DNA binding mutant constructs. There was less apoptotic activity exhibited in the transactivation constructs which indicates the NTD may be necessary for apoptosis induction in these cells.

The NTD of the GR is responsible for interaction with other transcription factors to mediate GR transcriptional activity and this study has shown that the transactivation domain plays a necessary role in apoptosis induction. An analysis of the various pathways the GR interacts with through the NTD domain could lead to the identification of the pathway which triggers apoptosis in SCLC cells. This discovery, together with knowledge of promoter methylation and expression may contribute to the development of new, more effective therapies for SCLC.

Preface

The experimental work described in this dissertation was carried out in the School of Life Sciences, Department of Biological and Conservation Sciences, University of KwaZulu-Natal, Westville, from January 2011 to January 2013, under the supervision of Dr. Paula Sommer.

These studies represent original work by the author and have not otherwise been submitted in any form for any degree or diploma to any tertiary institution. Where use has been made of the work of others it is duly acknowledged in the text.

_____ _____

Nimisha Singh Date

Plagiarism declaration

I, Nimisha Singh, declare that

1. The research reported in this thesis, except where otherwise indicated, is my original research.

2. This thesis has not been submitted for any degree or examination at any other university.

3. This thesis does not contain other persons' data, pictures, graphs or other information, unless specifically acknowledged as being sourced from other persons.

4. This thesis does not contain other persons' writing, unless specifically acknowledged as being sourced from other researchers. Where other written sources have been quoted, then:
a. Their words have been re-written but the general information attributed to them has been referenced

b. Where their exact words have been used, then their writing has been placed in italics and inside quotation marks, and referenced.

5. This thesis does not contain text, graphics or tables copied and pasted from the Internet, unless specifically acknowledged, and the source being detailed in the thesis and in the References sections.

Signed: _____ Date: _____

Nimisha Singh

Table of Contents

List of Tables

List of Figures

List of Abbrevations

^{o}C – degrees Celsius

ACTH – Adrenocorticotropin Hormone

AF1/2 – Activation Factor 1 or 2

AP-1/2 – Activating Protein 1 or 2

CRH – Corticotropin-releasing Hormone

DBD – DNA Binding Domain

DNMT – DNA Methyltransferase enzyme

FADD – Fas Associated Death Domain

GC – Glucocorticoid Hormone

GR – Glucocorticoid Receptor

GRE – Glucocorticoid Response Element

hIAP2 – Human Inhibitor of Apoptosis 2 Gene

HPA – Hypothalamic-Pituitary-Adrenal Axis

Hsp – Heat Shock Protein

IAP – Inhibitor of Apoptosis Protein

LBD – Ligand Binding Domain

MAPK – Mitogen Activated Protein Kinases

NLS1/2 – Nuclear Localisation Signal 1 or 2

NPC – Nuclear Pore Complex

NSCLC – Non-Small Cell Lung Cancer

NTD – N-Terminal Domain

PCR – Polymerase Chain Reaction

POMC – Proopiomelanocortin Hormone

RT – Reverse Transcriptase

SCLC – Small Cell Lung Cancer

SGK – Serum-Glucocorticoid-regulated Kinase

qPCR – Real Time Quantitative Polymerase Chain Reaction

WHO – World Health Organisation

Acknowledgements

I would firstly like to thank my supervisor, Dr. Paula Sommer, for her help and guidance during my entire MSc experience. Thank you for sharing in all the stressful events that came with the project and helping me to remain level headed.

I would like to thank Dr. Dalene Vosloo and Dr. Paula Watt for the use of laboratory equipment.

My thanks go out to the Staff of Westville Electron Microscope Unit for the guidance in the use of facilities.

A special thank you is given to Shirley Mackellar of the Pietermaritzburg Electron Microscope Unit for teaching me how to use the confocal microscope and the support during my learning experience.

I would like to thank my mother for her constant motivation, support and encouragement for pursuing an MSc degree.

A big thank you to Zenzele Silla for not only being a great laboratory colleague but being a caring friend never failing in giving support and assistance to me in my time of need.

I thank Kerryn Houston for being my laboratory partner in crime and being a good friend.

To Roxanne Wheeler, without your quirky, loud and craziness I think that the lab work would have been a much more arduous task to perform.

To my friends; Natasha Rambaran, Ellisha Pillay, Ashlin Munsamy, Kashmira Raghu, Shivanee Pillay and Yanasivan Kisten; I thank you for your constant support and advice through this MSc experience.

I would like to thank the NRF for their support.

1. Introduction and Literature Review

1.1. Lung Cancer

At the end of the 20th century lung cancer was considered as one of the leading causes of deaths (Alberg *et al*., 2007). Today, lung cancer is the most common cancer worldwide (Panani and Roussous, 2006). According to World Health Organisation (WHO), 7.6 million cancer deaths were recorded in 2008 with 63% occurring in developing countries. In South Africa, lung cancer is the fourth leading cause of deaths (Bello *et al*., 2011). Tobacco/cigarette smoking is the major cause of lung cancer with only 20% of cases attributed to occupational exposure to carcinogenic agents, genetic predisposition and dietary intake (Ihde, 1995; Dresler *et al*., 2000; Panani and Roussos, 2006; Alberg *et al*., 2007; Bello *et al*., 2011). Lung cancer has also presented in passive smokers and non smokers (Alberg *et al*., 2007).

Overall, the patient has a prognosis of a 5 year survival rate dependent on type and stage of diagnosis (Hirsch *et al*., 2001; Alberg *et al*., 2007). Inefficient early stage diagnostics and lack of successful metastatic disease treatments further diminishes a patient's prognosis (Alberg *et al*., 2007; Hirsch *et al*., 2001). Patients diagnosed with Stage IA disease (small tumours at or less than the size of 3 cm with no metastasis) have a 60% chance of survival after 5 years while, for patients with stages II – IV, survival rates decrease from 40% to less than 5% (Mountain, 2000; Hirsch *et al*., 2001). Stage II is classified as the presence of primary tumours and metastasis into the peribronchial lymph node. Stage III is classified as tumours of any size present in the chest, pleura, diaphragm and bronchi and metastasis to lymph nodes. Stage IV includes tumours of various sizes and metastasis into the lymph nodes as well as distant metastases (Mountain, 2000). The incidence of lung cancer in men has started to decrease gradually but in women, continues to increase steadily (Ihde, 1995; Dresler *et al*., 2000; Alberg *et al*., 2007; Bello *et al*., 2011). This is due to women having a higher sensitivity to tobacco carcinogens than men (Dresler *et al*., 2000). The ability to metabolize tobacco carcinogens with detoxification enzymes is altered in females where the phase one detoxification enzymes promotes the activation of carcinogens. Tobacco carcinogens are known to alter gene expression and metabolism of various hormones/enzymes in the body. This may create a delay in metabolism, as in the case of detoxification, creating DNA adducts resulting in cancer development (Dresler, 2000). This factor coupled with increasing number of female smokers accredits the increase in cancer mortality in women (Dresler *et al*., 2000; Bello *et al*., 2011).

Lung cancer is considered as the end stage of a multistep process of carcinogenesis (Hirsch *et al*., 2001; Panani and Roussos, 2006). The process starts with a normal bronchial epithelial cell possessing a premalignant lesion that changes into an invasive carcinoma. This may occur due to chronic exposure to tobacco carcinogens that lead to genetic and epigenetic damages causing alterations in the expression of tumour suppressor genes and oncogenes (Hirsch *et al*., 2001; Panani and Roussos, 2006). Lung cancer can be classified according to histological features using conventional light microscopy (Alberg *et al*., 2007). Broadly, lung cancer is classified as 80% non-small cell lung cancer (NSCLC) and 20% small cell lung cancer (SCLC) (Ihde, 1995; Panani and Roussos, 2006). NSCLC comprises of squamous cell carcinoma, adenocarcinoma, large cell carcinomas and bronchoalveolar carcinomas (Panani and Roussos, 2006; Alberg *et al*., 2007).

1.2. Small Cell Lung Cancer (SCLC)

1.2.1. Characteristics and Prognosis

SCLC is considered an aggressive tumour with 90% of diagnosed cases strongly linked to cigarette smoking (Simon and Wagner, 2003; Jackman and Johnson, 2005). The risk of SCLC development in smokers is directly proportional to the number of cigarettes smoked. Cessation of smoking decreases a smoker's chances of developing SCLC (Jackman and Johnson, 2005). Patients with SCLC are initially highly responsive to chemotherapy however possess the tendency to gain chemo-resistance with widespread metastases occurring. This results in a prognosis of a less than 5% chance of survival past 5 years (Jackman and Johnson, 2005; Sommer *et al*., 2010). SCLC presents as a submucosal malignancy where there are hilar masses and hilar and mediastinal adenopathy (Ihde, 1995; Jackman and Johnson, 2005). The Veterans Administration Lung Group has categorised SCLC into two stages; limited-stage or extensive-stage disease (Ihde *et al*., 1995; Simon and Wagner, 2003; Jackman and Johnson, 2005). Limited-stage disease is considered to have hilar and mediastinal nodes that are restricted to an ipsilateral hemithorax with one radiotherapy port. Extensive-stage disease is defined as any metastasis beyond the limited-stage boundary (Simon and Wagner, 2003; Jackman and Johnson, 2005). About 70% of patients diagnosed and treated with extensive-stage diseases have a prognosis of 7-12 months and 2% chance of a survival rate past 5 years. Patients with limited-stage disease have a survival period of 23 months and a 12-17% chance of a 5 year survival (Jackman and Johnson, 2005).

SCLC cells are histologically distinguished into two classes; 90% are the typical small cell carcinoma while the remaining 10% are mixed with one of the NSCLC types (Jackman and Johnson, 2005). According to the WHO, classification SCLC is a tumour with small cells that are round/oval/spindle-shaped containing scarce cytoplasm, ill-defined cell borders, fine granular chromatin and absent or inconspicuous nucleoli (Jackman and Johnson, 2005). SCLC cells are known to have neuroendocrine properties by ectopically secreting neuropeptide hormones causing paraneoplastic syndromes and neurological complications of the central nervous system in patients (Jackman and Johnson, 2005).

1.2.2. Ectopic Secretion of Adrenocorticotropin Hormone (ACTH)

SCLC is derived from the neuroendocrine cells of the bronchoepithelium (Hopkins-Donaldson *et al*., 2003). SCLC cells secrete neuropeptide hormones that cause the paraneoplastic syndrome, Cushing's syndrome, in 2-5% of patients due to over-activity of the adrenal cortex (Munck *et al*., 1984; Ray *et al*., 1994; Jackman and Johnson, 2005). SCLC cells ectopically secrete the ACTH precursor gene, proopiomelanocortin (POMC) (Ray *et al*., 1994; 1996). The POMC protein undergoes proteolytic cleavage to produce ACTH, β-endorphin, β-lipotropin and other peptides (Munck *et al*., 1984). Fifty percent of patients exhibit aberrant production of ACTH resulting in elevated cortisol levels (Ray *et al*., 1994; 1996). This ectopic secretion of ACTH peptides by SCLC cells is insensitive to the normal negative feedback system elicited by circulating glucocorticoids (GCs) on ACTH produced by the pituitary (Munck *et al*., 1984; Ray *et al*., 1994; 1996; O'Connor *et al*., 2000). This insensitivity is evidence of GC resistance in SCLC cells (Ray *et al*., 1994; 1996; Sommer *et al*., 2007; 2010).

1.3. Hypothalamus-Pituitary-Adrenal Axis

The hypothalamus-pituitary-adrenal (HPA) axis is one of the peripheral mechanisms of the stress system (O'Connor *et al*., 2000). Normal ACTH production is controlled by the HPA axis (Ray *et al*., 1994; 1996; Zhou and Cidlowski, 2005; Duma *et al*., 2006). In the event of stress, the hypothalamus produces and releases corticotrophin-releasing hormone (CRH) into the bloodstream. This stimulates the anterior pituitary to release ACTH which is transported in the peripheral circulation to the adrenal glands where it binds to specific receptors on the plasma membrane of adrenal cortex cells (Zhou and Cidlowski, 2005; Duma *et al*., 2006). The adrenal cortex is responsible for two types of activity; firstly to regulate salt and water metabolism and

secondly, to increase carbohydrate metabolism. The adrenal cortex synthesizes mineralocorticoids and GCs in response to both activities respectively (Munck *et al*., 1984). The adrenal cells are stimulated to produce and release GCs into the bloodstream. The circulating levels of GCs relay signals to the hypothalamus and pituitary to inhibit production of ACTH. The hypothalamus stops producing CRH therefore the anterior pituitary does not receive any signals and ceases ACTH production (Figure 1.1) (Munck *et al*., 1984; O'Conner *et al*., 2000; Tsigos and Chrousos, 2002; Duma *et al*., 2006). The purpose of the negative feedback system of GCs on ACTH is to limit the duration of tissue exposure to GCs thereby minimising catabolic, anti-reproductive and immunosuppressive effects of these hormones (Tsigos and Chrousos, 2002).

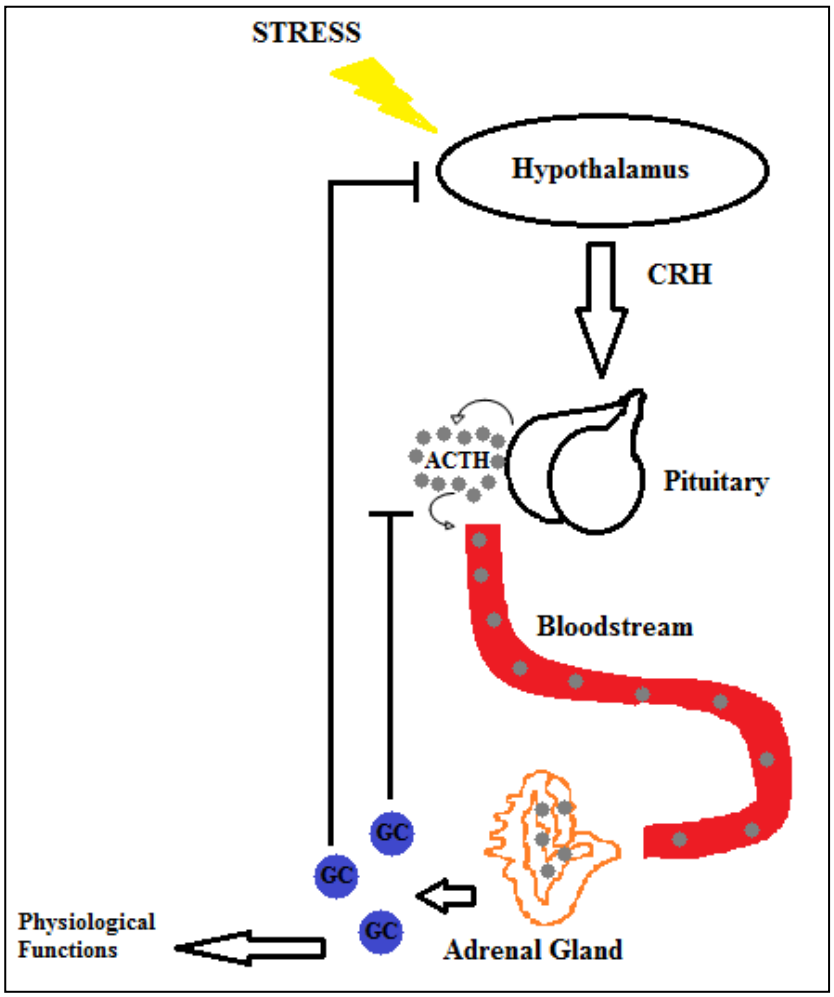

Figure 1.1: Illustration of HPA Axis and negative feedback system of GCs. CRH – Corticotrophin-releasing hormone, ACTH – Adrenocorticotropin hormone, GC – Glucocorticoid hormone (Constructed by author)

1.4. Glucocorticoid Hormone

When an individual experiences any physical or emotional stress that threatens the homeostasis of the body, a rapid increase in GC secretion occurs (Munck *et al*., 1984; Nunez and Vedeckis, 2002; Zhou and Cidlowski, 2005; Duma *et al*., 2006; Nicolaides *et al*., 2010; Kassi and Moutsatsou, 2011). GCs are an endogenously synthesised class of steroid hormones (Nunez and Vedeckis, 2002; Zhou and Cidlowski, 2005; Duma *et al*., 2006; Sommer *et al*., 2010). GCs are present in the circulatory system at basal levels which are sufficient to respond to stress and hormone stimuli thereby maintaining homeostasis (Munck *et al*., 1984, Turner *et al*., 2010). To maintain a basal level of GCs under normal conditions, CRH secretion follows a pulsatile circadian pattern with 2-3 secretory periods per hour (Tsigos and Chrousos, 2002). During a stressful event, the natural defences of the body are activated to neutralise the stress. Once the stressful event has been removed, the natural defences need to be inactivated. The increased secretion of GC levels during a stress event acts as the signal to switch off the natural defences. The inactivation serves to protect the body from the defence mechanisms overshooting and threatening homeostasis (Munck *et al*., 1984; O'Connor *et al*., 2000; Tsigos and Chrousos, 2002).

Due to the lipophilic property of the GC hormone, it is able to enter in any tissue by simple diffusion through the cell membrane thereby being involved in every cellular, molecular and physiological network (Zhou and Cidlowski, 2005; Duma *et al*., 2006; Nicolaides *et al*., 2010). Therefore, GCs are able to influence the biological functions of cells, tissues and organs including intermediary metabolism, reproduction, maintenance of vascular tone, immune and inflammatory regulation, effects on the central nervous system, development and programmed cell death (Munck *et al*., 1984; O'Connor *et al*., 2000; Zhou and Cidlowski, 2005; Duma *et al*., 2006; Nicolaides *et al*., 2010). GCs are the most potent steroid and are used clinically in many life-saving therapies including anti-inflammatory or immune-suppressive effects in asthma, dermatitis, rheumatoid arthritis, prevention of graft rejection, ulcerative colitis and allergic rhinitis (Munck *et al*., 1984; O'Connor, 2000; Schaaf and Cidlowski, 2003; Zhou and Cidlowski, 2005; Duma and Cidlowski, 2006).

GCs mediate their functions in the various tissues by binding to the ubiquitous cytoplasmic and nuclear receptor known as the glucocorticoid receptor (GR) (Munck *et al*., 1984; O'Connor *et*

al., 2000; Tsigos and Chrousos, 2002; Zhou and Cidlowski, 2005; Duma *et al*., 2006; Nicolaides *et al*., 2010; Sommer *et al*., 2010; Kassi and Moutsatsou, 2011).

1.5. Glucocorticoid Receptor

1.5.1 GC Activation of the GR

The GR can be found in every nucleated cell type in the body (Munck *et al*., 1984; O'Connor *et al*., 2000). In the absence of GCs, the GR resides in the cytoplasm where it is bound to a multimeric chaperone complex (Hittelman *et al*., 1999; Croxtall *et al*., 2002; Chen *et al*., 2008; Vandevyver *et al*., 2012). The multimeric chaperone complex guides the conformation of GR in an ATP-dependent manner from a low to a high hormone affinity. Newly synthesized GR is recognised by the heat shock protein 70 (hsp70) and binds to the ligand binding domain of the GR. The co-chaperone, hsp40, binds to hsp70 thereby priming the GR:hsp complex to bind to hsp90 dimers (Figure 1.2.a) (Vandevyver *et al*., 2012). Once hsp90 dimers bind to the GR complex, ATP binds and hsp70 and hsp40 dissociate from the complex and co-chaperone p23 binds and stabilizes hsp90 dimers to the GR (Figure 1.2.b). This stabilization allows for the maturation of the GR and for the ligand binding cleft to be open for GC binding. The immunophilin, FKBP51, binds to the hsp90 dimer thereby completing GR maturation which allows for the GR to bind GC hormone at a high affinity (Figure 1.2.b) (Duma *et al*., 2006; Vandevyver *et al*., 2012). The hypothesis was that once the GC ligand is bound, the GR undergoes a conformational change where phosphorylation of the GR and dissociation of hsp90 dimers and other factors occurs. As part of the conformational change, the GR dimerizes with another GR to form homodimers that translocate to the cell nucleus (Figure 1.2.c) (Hittelman *et al*., 1999; Croxtall *et al*., 2002; Chivers *et al*., 2006; Chen *et al*., 2008). However, several studies have indicated that the hsp90 complex is required for GR nuclear transport (Figure 1.2.d) (Vandevyver *et al*., 2012).

It is hypothesised that the GR moves along the microtubules of the cell's cytoskeleton, aided by immunophilins, to the nucleus. The GR enters the nucleus through a nuclear pore complex (Figure 1.2.d) (Vandevyver *et al*., 2012). In the nucleus, the homodimer GR recruits transcription factors and binds to specific palindromic DNA sequences known as glucocorticoid response elements (GRE). Depending on the type of GRE binds to the GR, that specific gene can either be activate or inactivate transcriptional activity (Figure 1.2.e)

(Hittelman *et al*., 1999; Chivers *et al*., 2006; Chen *et al*., 2008; Vandevyver *et al*., 2012). The GR can also repress transcription as a monomer by interacting with the transcription factors, nuclear factor κ-B and activator protein-1 (Vandevyver *et al*., 2012). The GR's influence on transcription occurs in a hormone dependent manner depending on the level of GCs present (Hittelman *et al*., 1999).

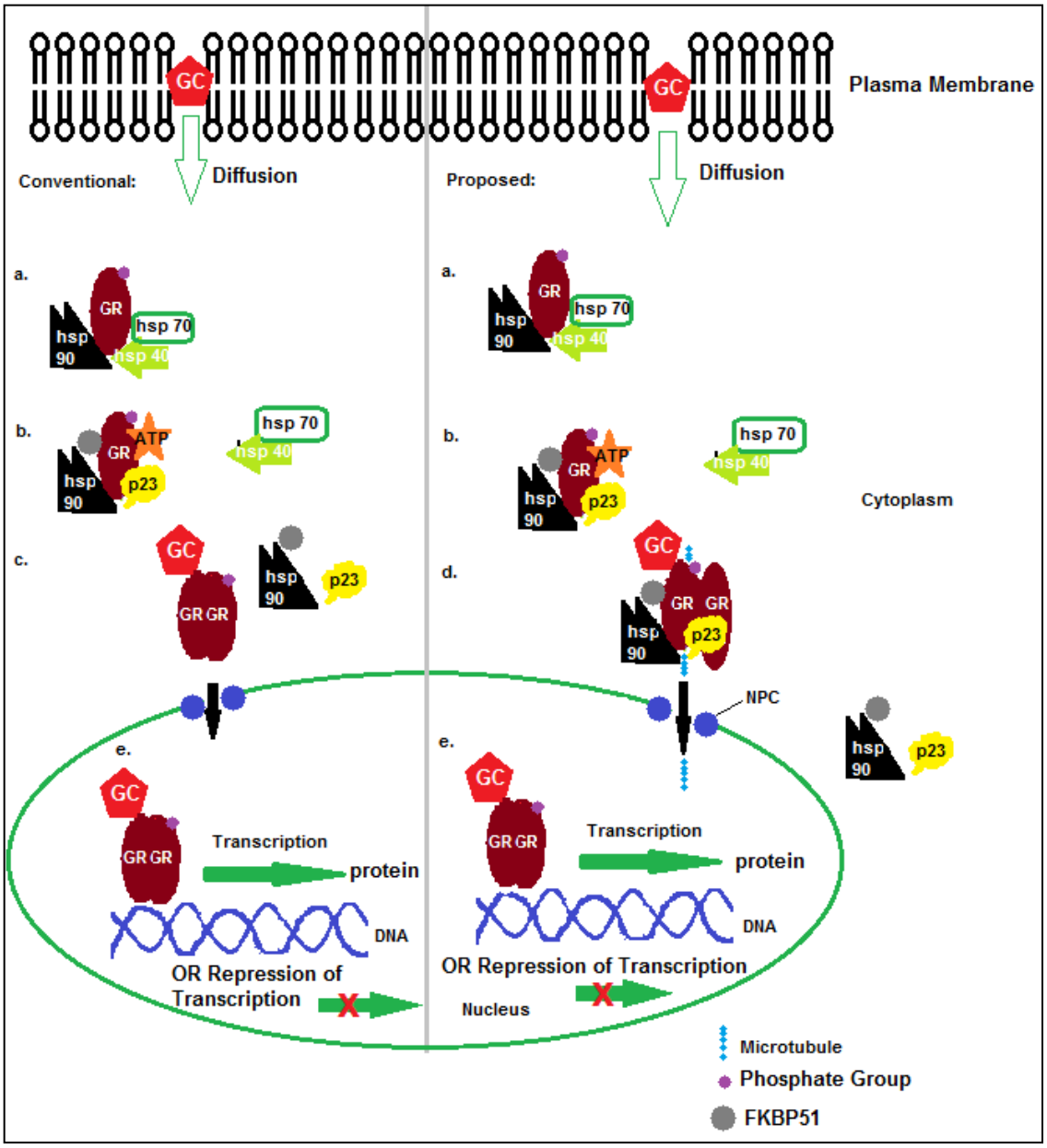

Figure 1.2: Signalling pathway of glucocorticoid receptor (GR) transcriptional activity; conventional hypothesis and proposed hypothesis by Vandevyver *et al*., 2012. GC: glucocorticoid hormone, NPC: nuclear pore complex, hsp: heat shock protein, p23: co-chaperone of hsp 90, FKBP51: immunophilin that binds to microtubules for nuclear translocation of GR complex. See text for detailed explanation (Constructed by author)

1.5.2. GR Structure

The GR belongs to the steroid/thyroid/retinoic acid nuclear receptor superfamily of transcription factors (O'Connor *et al*., 2000; Schaaf and Cidlowski, 2003; Nicolaides *et al*., 2010; Kassi and Moutsatsou, 2011). The GR gene is located in chromosome 5q31-q32 and has 9 exons. The first 8 exons are uniform while the 9^{th} exon can generate two highly homologous receptor isoforms, α and β (Alt *et al*., 2010; Turner *et al*., 2010). The GRα isoform has an additional 50 amino acids, thus producing a 777 amino acid protein. The GRβ isoform has an additional, non-homologous 15 amino acids producing a 742 amino acid protein (Alt *et al*., 2010; Nicolaides *et al*., 2010; Kassi and Moutsatsou, 2011). These isoforms are formed by alternative splicing of the GR mRNA (Kassi and Moutsatsou, 2011). The GRα resides in the cytoplasm of cells and serves as the classic GR responding to ligand binding (Nicolaides *et al*., 2010; Kassi and Moutsatsou, 2011). The exact function of GRβ is still unknown and many discrepancies have arisen from identifying its exact function (Schaaf and Cidlowski, 2003). It is believed that GRβ has inhibitory effects on GRα isoform (Schaaf and Cidlowski, 2003; Duma *et al*., 2006; Nicolaides *et al*., 2010). The first exon of the GR serves as a 5'-untranslated region (5'-UTR) housing 9 alternative first exons (Alt *et al*., 2010; Turner *et al*., 2010).

1.5.3. The 5'-Untranslated Region of the GR

1.5.3.1. Exon 1/Promoter Region

The 5'-UTR contains the untranslated exon 1 of the GR. It is believed that the first exon is responsible for the differential expression of GR protein (Turner *et al*., 2010). The GR exon 1 has 9 alternative first exons (Turner *et al*., 2010). The first exons are named as follows; 1A, 1B, 1C, 1D, 1E, 1F, 1H, 1I and 1J (Presul *et al*., 2007; Alt *et al*., 2010; Turner *et al*., 2010). The promoter region is categorised into two regions, the distal (30 kb upstream of exon 2) and proximal (5 kb upstream of exon 2) regions (Presul *et al*., 2007; Turner *et al*., 2010). Exons 1A and 1I are found in the proximal promoter region while exons 1B, 1C, 1D, 1E, 1F, 1H and 1J are found in the distal promoter region (Presul *et al*., 2007; Turner *et al*., 2010). Exon 1A is split into three exons, $1A_1$, $1A_2$ and $1A_3$, and exon 1I is found immediately after exon $1A_3$. In the distal promoter region, the first exons are in the order of 1D, 1J, 1E, 1B, 1F, 1C and 1H (Presul *et al*., 2007; Turner *et al*., 2006; 2010) (Figure 1.3). Exon 1C also has three exons; $1C_1$, $1C_2$ and $1C_3$. Exons 1A and 1C are considered to have splice variants and the utilisation of each variant is dependent on the cell type (Turner *et al*., 2010). For translational conformity among the different cell types of GR protein, the translation start site is in the common exon 2. Exon 2

has an in-frame stop codon upstream of the ATG start codon which ensures that the alternative first exons are not translated (Alt *et al*., 2010; Turner *et al*., 2006; Presul *et al*., 2007; Turner *et al*., 2010). Promoter usage is tissue-specific and influences the differential GR mRNA transcripts present by mRNA processing, stability, export and translation (Turner *et al*., 2010; Presul *et al*., 2007). Exon 1A is only expressed in thymocytes, hematopoietic cell lines and some regions of the brain (Presul *et al*., 2007; Alt *et al*., 2010) while exons 1B and 1C are used in almost all tissue types (Nunez and Vedeckis, 2002; Alt *et al*., 2010; Turner *et al*., 2010). The concentration of GR present in each cell type is critical in order for the cell to respond to GC stimulation in terms of type and magnitude of response (Nunez and Vedeckis, 2002). The first exons lack consensus TATA or CAAT boxes but contain highly guanine-cytosine rich regions (Nunez and Vedeckis, 2002; Turner *et al*., 2006; 2010; Alt *et al*., 2010).

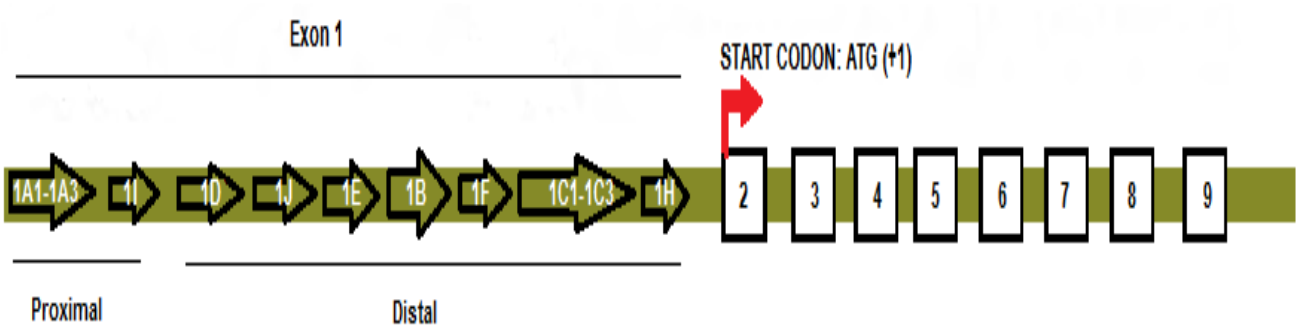

Figure 1.3: Structure of the GR gene with 9 alternative first exons followed by exons 2 - 9 (Adapted from Turner *et al*., 2010)

1.5.3.2. CpG Islands

When a cytosine is bound to a guanine by the phosphate bond, it is termed as a CpG dinucleotide. A CpG island can be defined as a region that contains clusters of CpG dinucleotides. A CpG island is usually greater than 200 bp long and the guanine-cytosine content should be more than 50% of that region (Jones and Laird, 1999; Turner *et al*., 2006; Cao-Lei *et al*., 2011). CpG islands consist of 1% of the human genome (Cao-Lei *et al*., 2011). CpG islands are found upstream of 60-70% of all genes that contain promoters (Cao-Lei *et al*., 2011). In the 5'-UTR of the GR, there are many CpG islands that span 3.1 kb upstream of exon 2 (Turner *et al*., 2006). These CpG islands have been shown to be highly conserved among the different species (Turner *et al*., 2006). As the GR lacks a TATA or TATA-like box or a CAAT

motif, it is thought that the CpG islands present in exon 1 of the GR have promoter activity (Nunez and Vedeckis, 2002; Schaaf and Cidlowski, 2003; Zhou and Cidlowski, 2005; Turner *et al*., 2010) acting as a transcription binding site for transcription factors (Duma *et al*., 2006; Alt *et al*., 2010; Turner *et al*., 2010; Cao-Lei *et al*., 2011). The transcription factor binding sites present in the CpG islands are for Activating Protein 1 and 2 (AP-1, AP-2), Ying Yang 1(YY1), Sp1, nuclear factor κB, CREB, NGFI-A, glucocorticoid response factor, IRF-1 and 2 and GREs (Duma *et al*., 2006; Turner *et al*., 2010; Alt *et al*., 2010). YY1 is a zinc finger transcription factor that can act as a repressor, activator or initiator of transcription. In the GR the promoter regions are named according to their respective first exons. Since the GR acts as a transcription factor, it can auto-regulate its own CpG islands present within the promoter region by binding to specific GREs (Turner *et al*., 2010). Promoters 1B and 1J have sites for Sp1 transcription factor (Alt *et al*., 2010; Turner *et al*., 2010) while promoter 1C has sites for Sp1, AP2, and YY1 transcription factors (Turner *et al*., 2010). Transcription factor YY1 and GREs can bind to promoter 1D region while promoter 1E can only bind GREs. Promoter 1F can bind to GREs, AP-1, Sp1, NGFI-A and GR DNA binding factor 1. GR DNA binding factor 1 acts as a repressor (Turner *et al*., 2010). Promoter 1A only binds the GR protein (Alt *et al*., 2010). All CpG islands of alternative exons found in the distal promoter region (1B-1J) are highly prone to methylation (Cao-Lei *et al*., 2011).

1.5.3.3. Methylation

DNA methylation occurs at a cytosine neighbouring 5' a guanosine residue (Jones and Laird, 1999; Baylin *et al*., 2004, Turner *et al*., 2010; Cao-Lei *et al*., 2011). This methylation is carried out by DNA methyltransferase (DNMT) 1 enzyme using S-adenosyl-methionine as the methyl donor (Jones and Laird, 1999; Baylin *et al*., 2004). The methyl group is attached at carbon 5 of the cytosine residue creating a 5-methyl cytosine. CpG dinucleotides are thought to be vulnerable to DNA methylation. A CpG dinucleotide can be methylated on both DNA strands effectively silencing transcription of the gene by preventing binding of transcription factors (Alt *et al*., 2010; Turner *et al*., 2010; Cao-Lei *et al*., 2011) (Figure 1.4).

DNA methylation is utilised as an epigenetic silencing mechanism by cells to regulate gene expression (Turner *et al*., 2010). However, cancer cells have adopted this mechanism to silence the expression of unwanted tumour suppressor genes thereby ensuring their immortality (Baylin *et al*., 2004). Cancer cells utilise DNMT1 to methylate CpG islands present within the

promoter region of tumour suppressor genes. This methylation affects the binding affinity of transcription factors to the promoter region as the methyl group obstructs the major groove of the DNA helix. This prevents initiation of transcription (Jones and Laird, 1999; Baylin *et al*., 2004; Kay *et al*., 2011) (Figure 1.4).

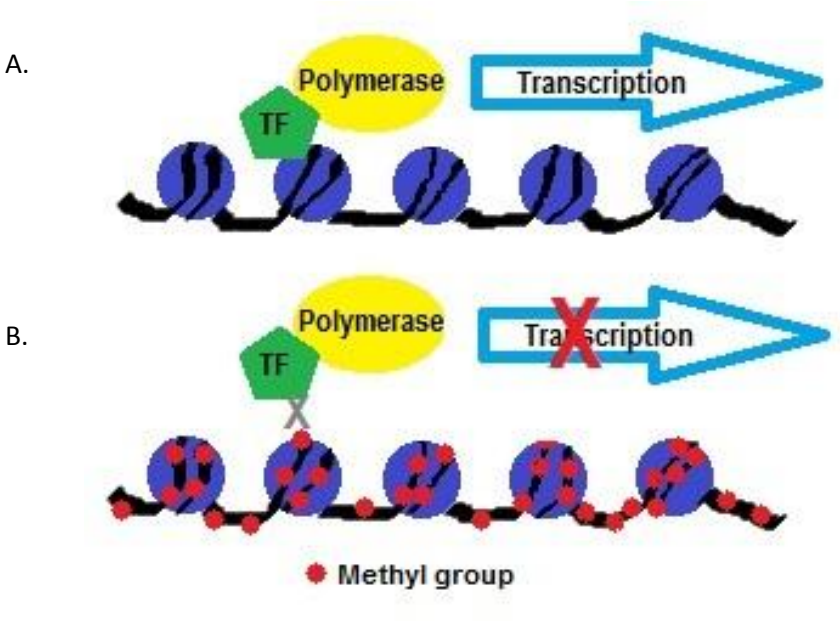

Figure 1.4: DNA methylation of promoter region of gene inhibits transcription. A. Gene undergoing normal transcription in the absence of methyl groups. B. DNA methylation has occurred and methyl groups are an obstruction to transcription complex binding to the target gene. TF: transcription factor

1.5.4. Domains of the Glucocorticoid Receptor

The GR protein can be divided into three major functional domains, namely the amino-terminal (NTD) encoded by exon 2, DNA-binding domain (DBD) encoded by exons 3 and 4, ligand-binding domain/C-terminal (LBD) encoded by exons 5-9 and a hinge region (Zhou and Cidlowski, 2005; Nicolaides *et al*., 2010; Kassi and Moutsatsou, 2011) (Figure 1.5).

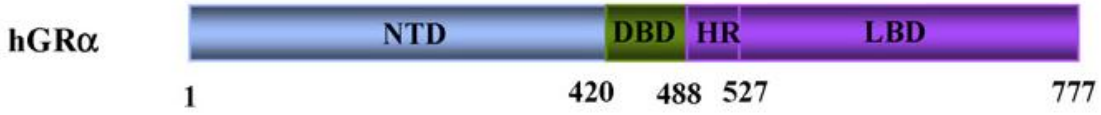

Figure 1.5: Domains of the GR protein (Taken from Nicolaides *et al*., 2010) NTD – N terminal domain, DBD – DNA binding domain, HR-Hinge region, LBD – Ligand binding domain. 1-777 are amino acid numbers

1.5.4.1. N-terminal Domain (NTD)

The size and homology of the sequence of the NTD region is the most variable domain of the nuclear hormone receptors. The GR NTD region differs between species (Kumar and Thompson, 2005). The first 420 amino acids of the GR protein encodes the NTD in which the active transcriptional activation factor 1 (AF1) region is present for maximal transcriptional enhancement (Schaaf and Cidlowski, 2003; Kumar and Thompson, 2005; Zhou and Cidlowski, 2005; Duma *et al*., 2006; Nicolaides *et al*., 2010). The transcription enhancement ability of AF1 region is cell or coactivator dependent (Kumar and Thompson, 2005). The AF1 region is located between amino acids 77 to 262 (Schaaf and Cidlowski, 2003; Garza *et al*., 2010). This domain is considered a constitutive and GC independent domain that has direct interaction with factors responsible for transcription initiation. The AF1 domain has three serine residues where p38-mitogen-activated protein kinases (MAPK) add phosphate groups (Schaaf and Cidlowski, 2003; Duma *et al*., 2006; Garza *et al*., 2010). Phosphorylation of the AF1 region post ligand binding results in GR translocation to the nucleus and regulates binding affinity of transcription factors to their co-activators and DNA (Schaaf and Cidlowski, 2003; Duma *et al*., 2006; Garza *et al*., 2010). This phosphorylation may be a mechanism for other signalling pathways to influence GC signalling at a post-translational level (Duma *et al*., 2006). In the AF1 region, serine 211 and serine 226 are phosphorylated upon ligand binding and are believed to be important for GR transcriptional activity (Kumar and Thompson, 2005; Garza *et al*., 2010; Vandevyver *et al*., 2012). This phosphorylation renders a conformational change creating a functionally folded active structure of AF1 region. The newly folded surface forms the basis for the multi-protein assemblies to physically interact with the AF1 region for a GR-mediated regulation of transcription and chromatin remodelling (Hittelman *et al*., 1999; Kumar and Thompson, 2005; Garza *et al*., 2010). This folding is considered spontaneous as the AF1 region folding can compensate for the amount of transcription factors and coregulators available and the type of GRE sequence is present (Kumar and Thompson, 2005; Garza *et al*., 2010). The

folded AF1 structure is in direct contact with RNA polymerase II, transcription factor IID, CREB-binding protein and TATA box binding protein (Hittelman *et al*., 1999; Kumar and Thompson, 2005; Duma *et al*., 2006). The AF1 can recruit both positive and negative GREs for transcription (Hittelman *et al*., 1999).

1.5.4.2. DNA Binding Domain (DBD)

The DBD can be found between amino acids 421 and 488. This domain is highly conserved among all nuclear hormone receptors and contains two zinc finger motifs (Schaaf and Cidlowski, 2003; Kumar and Thompson, 2005; Duma *et al*., 2006; Turner *et al*., 2008; Garza *et al*., 2010; Nicolaides *et al*., 2010). The zinc finger motifs are formed by two highly conserved groups of four cysteine residues. Each group has a zinc atom bound hence zinc fingers. These fingers result in the formation of a tertiary structure with three helices present. The DBD has three amino acids, located in the first zinc finger, that have contact with specific bases within GREs for GR:DNA site binding specificity (Kumar and Thompson, 2005). This binding occurs in the major groove of GRE. The second zinc finger is responsible for stabilizing the DBD:GRE interactions and binds to the minor groove of GREs. Five amino acids in the second zinc finger play an important role in receptor homodimerization and conferring high affinity binding at GREs (Kumar and Thompson, 2005; Zhou and Cidlowski, 2005). As a homodimer the GR is able to bind to GREs which are DNA specific sequences that regulate transcription by keeping the GR in the major groove of the α-helix of DNA (Hittelman *et al*., 1999; Schaaf and Cidlowski, 2003; Chen *et al*., 2008; Kassi and Moutsatsou, 2011). The type of GRE the DBD binds to will initiate transcription to either activate or repress the target gene (Schaaf and Cidlowski, 2003; Chen *et al*., 2008). It has been shown that the DBD:GRE interaction can result in conformational change in the AF1 structure of the NTD. This greatly enhances the interaction between AF1 and the TATA box binding protein (Kumar and Thompson, 2005). The DBD contains part of a nuclear localisation signal (NLS1) domain responsible for GR nuclear translocation upon ligand binding (Schaaf and Cidlowski, 2003; Duma *et al*., 2006; Vandevyver *et al*., 2012). The GR nuclear translocation occurs rapidly with a half time ranging between 4 to 6 minutes. NLS1 has a bipartite structure and consists of 28 amino acids. The NLS1 is situated near the DBD-hinge boundary (Vandevyver *et al*., 2012). In the absence of GC, the NLS1 function is inhibited by the LBD (Schaaf and Cidlowski, 2003).

1.5.4.3. Ligand Binding Domain (LBD)

The LBD is found between amino acids 527 and 777 (Schaaf and Cidlowski, 2003; Duma *et al*., 2006; Garza *et al*., 2010; Nicolaides *et al*., 2010). The LBD is a moderately conserved region responsible for recognition and binding of ligand, chaperones and proteins. The LDB contains 12 helices and 4 small β-strands that fold into three helices forming the sides and top of a globule. This globule contains a central pocket for ligand binding (Kumar and Thompson, 2005; Nicolaides *et al*., 2010). It is believed that helix 12 is important for activating gene transcription and serves as a bridge between the receptor and transcription initiation complex by tethering through the TATA box binding protein to the TATA box (Kumar and Thompson, 2005). This domain houses the ligand-dependent transcriptional activation function 2 (AF2) in a hydrophobic pocket in helix 12 (Kumar and Thompson, 2005; Lavery and McEwan, 2005; Zhou and Cidlowski, 2005, Nicolaides *et al*., 2010). AF2 is GC dependent where ligand binding promotes folding for the formation of a surface that permits protein-protein contact (Hittelman *et al*., 1999; Kumar and Thompson, 2005; Nicolaides *et al*., 2010). The protein-protein interactions are with the cytosolic chaperones or co-regulators, depending the absence or presence of a ligand respectively (Hittelman *et al*., 1999; Kumar and Thompson, 2005; Zhou and Cidlowski, 2005). When cytosolic GRα is unbound, it is a large heteromeric complex containing heat shock protein 90 (hsp90) and the p23 chaperone (Hittelman *et al*., 1999; Schaaf and Cidlowski, 2003). Hsp90 plays a central role in formation of the complex and is bound to the LBD of the GR (Schaaf and Cidlowski, 2003; Nicolaides *et al*., 2010). This association allows for the GR to maintain its conformation in order to bind to GCs however it is transcriptionally inactive (Schaaf and Cidlowski, 2003; Nicolaides *et al*., 2010). The LBD can bind agonist and antagonist ligands (Lavery and McEwan, 2005). The LBD has the second nuclear localisation signal 2 (NLS2) however its function is unknown (Duma *et al*., 2006; Nicolaides *et al*., 2010). The NLS2 region also participates in GR nuclear translocation but at a slower rate with a half time between 45 to 60 minutes and full nuclear localisation is not accomplished (Vandevyver *et al*., 2012). Upon GC-ligand binding and nuclear translocation of the GR, the GR affects the various functions elicited by the hormone. One such function is the inhibition of cell proliferation by arresting cells at the G_1 phase of the cell cycle. This results in cells being signalled for programme cell death, known as apoptosis, as seen in lymphocytes (O'Connor *et al*., 2000; Sommer *et al*., 2007).

1.6. Apoptosis

Apoptosis is a type of programmed cell death that is used by an organism to remove unwanted or harmful cells (Dieken and Miesfeld, 1992; Elmore, 2007; Bhola and Simon, 2009). Apoptosis is utilised during normal development and aging to regulate cell populations in tissue, in defence mechanisms to remove tissue damaged by disease or toxins and in immune reactions (Elmore, 2007). Characteristically, apoptosis is associated with DNA fragmentation, plasma membrane blebbing, nuclear and cytoplasmic condensation and margination of chromosomes into distinct masses (Dieken and Miesfeld, 1992; Elmore, 2007; Bhola and Simon, 2009). The final stage of apoptosis involves breaking up of the cell into apoptotic bodies that are ingested by macrophages (Dieken and Miesfeld, 1992; Elmore, 2007).

Apoptosis can be mediated by two main pathways. These are the intrinsic and extrinsic pathways with both pathways converging at the execution step (Elmore, 2007). The apoptotic pathways are controlled by a family of proteins known as caspases. Under normal conditions these enzymes are in an inactive form known as procaspases (Elmore, 2007). Once caspases are activated, they are able to activate other caspases resulting in a proteolytic casacade that speeds up apoptotic signalling. There are ten caspases involved in the apoptotic pathways and are categorised as either initiator, executioner or inflammatory casapases. Caspases 2, 8, 9 and 10 are initiator caspases while capases 3, 6 and 7 are executioners. Caspases 1, 4 and 5 are considered to be inflammatory (Elmore, 2007; Johnstone *et al*., 2002).

1.6.1. Intrinsic Pathway

The intrinsic pathway is a non-receptor pathway which is initiated by intracellular stimuli and targets the mitochondrial events within a cell. This stimulus can be exposure to a toxin, radiation or hypoxia and any other stress experienced by the body (Johnstone *et al*., 2002; Elmore, 2007). Such stresses interfere with the integrity of the mitochondrial membrane which results in the release of pro-apoptotic proteins cytochrome c, HtrA2 and Smac/DIABLO. Cytochrome-c binds to the scaffolding protein Apaf-1 and pro-caspase 9 to form an apoptosome (Johnstone *et al*., 2002; Elmore, 2007). The apoptosome formation results in the activation of caspase 9. Caspase 9 activates caspase 3 to elicit apoptosis of the cell (Johnstone *et al*., 2002; Elmore, 2007). Smac/DIABLO promote apoptosis by blocking the activity of a family of inhibitors of apoptosis proteins (IAP) (Johnstone *et al*., 2002; Elmore, 2007).

1.6.2. Extrinsic Pathway

The extrinsic pathway is a transmembrane receptor mediated interaction with death receptors from the tumour necrosis factor receptor super family. These receptors have an 80 amino acid cytosolic domain known as the death domain that is responsible for relaying death signals from the cell surface to the intracellular signalling pathways (Elmore, 2007). The extrinsic pathway is triggered when either Fas ligand or tumour necrosis factor α binds to their death receptor which results in the recruitment of cytosolic adapter proteins, Fas-associated death domain (FADD) or tumour necrosis factor-associated death domain proteins respectively (Johnstone *et al*., 2002; Elmore, 2007). FADD binds to procaspase 8 that results in a catalytic activation of the enzyme to caspase 8. Caspase 8 in turn activates caspase 3 and in a cascade manner activates capases 6 and 7 which results in apoptosis of the cell (Johnstone *et al*., 2002; Elmore, 2007).

1.7. Re-expression of Glucocorticoid Receptor in SCLC

1.7.1. Exogenous expression of GR

SCLC cells have shown to be insensitive to the negative feedback system of GCs indicating GC resistance (Ray *et al*., 1994; 1996; Sommer *et al*., 2007; 2010). The inability of GCs to inhibit ACTH production in SCLC prompted Sommer and colleagues (2007) to investigate GR expression in SCLC cells. They confirmed that SCLC cells were insensitive to GC administration which, in turn, did not affect cell proliferation. It is known that GCs can arrest proliferation at the G1 phase and signal cells for apoptosis. Thus, GC insensitivity in SCLC cell could confer a survival technique (Sommer *et al*., 2007). The aim of the 2007 study was to restore GR expression within SCLC cell lines. SCLC cells were transfected with GR-expressing plasmids which conferred GC sensitivity in a few SCLC cell lines. The DMS79 and COR L24 cell lines were still GC resistant. This prompted an investigation to over-express the GR in SCLC cells by infecting cells with a GR expressing retrovirus. Over-expression of the GR in SCLC cell lines only induced massive apoptosis, indicating that SCLC cells select for negligible GR levels as GR protein itself elicited cell death. Similar effects were seen in an *in vivo* xenograft study suggesting that GR expression is pro-apoptotic for SCLCs and that loss of GR expression favoured SCLC longevity (Sommer *et al*., 2010).

1.7.2. Endogenous re-expression of GR

The studies discussed above involved GR over-expression (Sommer *et al*., 2007; 2010). If exogenous over-expression of the GR in SCLC cells leads to cell death by apoptosis then it is postulated that SCLC cells would select not to express the GR protein. Many cancer types are known to down-regulate any gene exhibiting tumour suppressor activity (Jones and Laird, 1999; Baylin *et al*., 2004). Cancer cells tend to silence these genes in order to gain immortality. One mechanism utilised is methylation of promoter regions of genes (Jones and Laird, 1999; Baylin *et al*., 2004). It is believed that the reduced expression of GR displayed in SCLC could be attributed to epigenetic methylation of the CpG islands present in the promoter region (Duma *et al*., 2006; Alt *et al*., 2010; Turner *et al*., 2010). In theory if the methylation profiles were removed from the CpG islands of the promoter region of exon 1 of the GR, there should be an increased expression of GR protein in SCLC cells.

DNMT inhibitors can be used to remove methylation sites from the promoter region and have shown to be potent compounds in reactivating epigenetically silenced genes (Stresemann and Lyko, 2008). These DNMT inhibitors are cytosine analogues and once taken up by the cell, must be activated. After activation, the DNMT inhibitor is metabolically converted into 5-aza-2'-deoxycytidine-triphosphate. This construct can now serve as a substrate for DNA replication and allows for their incorporation into DNA where the DNMT inhibitor is substituted for cytosine. DNMT enzymes recognise it as a natural substrate and bind to it to initiate methylation (Christman, 2002; Streseman and Lyko, 2008). The carbon 5 of cytosine is substituted to a nitrogen residue in DNMT inhibitors and when DNMT enzyme binds, it is unable to detach as beta-elimination cannot occur. This results in the DNMT enzyme being irreversibly bound to the DNMT inhibitor which stops methylation from occurring (Christman, 2002; Streseman and Lyko, 2008).

Common DNMT inhibitors used for experiments are 5-azacytidine, 5-aza-2'-deoxycytidine and decitabine. For this study, 5-aza-2'-deoxycytidine (5-aza) was used. It was initially designed as a treatment for acute myelogenous leukemia however it interfered with normal cell processing due to its DNMT inhibitor properties. It was also noted that 5-aza was cytotoxic to cells which lead to the use of minimal levels that could confer its activity (Christman, 2002).

1.8. Aims and Objectives

Aim 1: To identify the promoters used for the re-expression of GR in SCLC cells.

The GR gene has been shown to be silenced by methylation where treatment with a DNMT inhibitor resulted in GR re-expression (Kay *et al*., 2011). The aim of this study is to determine which promoter is responsible for re-expression of the GR leading to apoptosis.

Aim 2: To identify the molecular events that cause GR-induced apoptosis of SCLC cells.

GCs are known to elicit apoptosis in lymphoid cells by arresting the cells in G1 phase of the cell cycle (Sommer *et al*., 2010). It has been shown that SCLC cells die by apoptosis when there is an over-expression of exogenous GR (Sommer *et al*., 2007) however the mechanism by which the GR elicits this apoptotic signal has not been elucidated. To determine which domain of the GR is necessary for inducing apoptosis, SCLC cells were infected with various GR constructs containing the wild-type GR and mutant constructs of each domain within the GR and the ability of each to induce apoptosis, determined.

Objective 1: The identification of the promoter/s responsible for GR re-expression in SCLC after reversal of silencing methylation.

Objective 2: To determine which domain is responsible for apoptosis induction, SCLC cells were spin-infected with retroviral constructs of GR and GR mutants.

Objective 2.1: To determine whether DNA binding (DBD) of GR is necessary for GR-induced apoptotic death of SCLC cells.

Objective 2.2: To determine whether transactivation (NTD) of GR is necessary for GR-induced apoptotic death of SCLC cells.

Objective 2.3: To determine whether ligand activation (LBD) is necessary for GR-induced apoptotic death of SCLC cells

2. Materials and Methods

2.1. Cell Culture

Culturing, sub-culturing and treatments of all cell lines were carried out in a class two, type A2 categorised laminar flow (Logic Labconco®). Cell lines were incubated at 37°C in a humidified Shel Lab 3552 CO_2 incubator (United Scientific (Pty) Ltd) supplemented with 5% CO_2. Three cell lines were used for experiments, a SCLC cell line (DMS79) and two control cell lines; human embryonic kidney (HEK) and non-small cell lung cancer (A549). These cell lines were obtained from the American Tissue Culture Collection (ATCC). Stock cultures were grown in 75 cm^3 tissue culture flasks (T75) (Corning). The adherent HEK and A549 cell lines were cultured in 10 ml of Dulbecco's Modified Eagles Medium (DMEM) supplemented with 10% inactivated foetal bovine serum (FBS) and 100 units/ml of penicillin/streptomycin (PAA). The non-adherent, suspension DMS79 cell line was cultured in 20 ml of RPMI 1640 medium with 10% inactivated FBS and 100 units/ml of penicillin/streptomycin (PAA).

Cell growth was observed using a Nikon inverted microscope at 40x and 100x magnification. When adherent cell lines were confluent, cells were passaged by adding 2 ml of 1x Trypsin-EDTA (PAA) (Appendix B.1) to the T75 flask and the cells incubated at 37°C until detachment. The equivalent amount of medium was used to neutralise the Trypsin-EDTA. Cells were subcultured at a density of $2x10^3$ cells/cm^2. Confluent DMS79 cells were allowed to settle by gravity to the bottom of an upright T75 flask and the excess medium was removed. The remaining medium containing the cells were pipetted into a 15ml centrifuge tube (Corning) and centrifuged at 1000 x *g* for 5 minutes in an Eppendorf 45180R centrifuge (Merck). The supernatant was discarded and pellet of cells was re-suspended in 1 ml of RPMI 1640 medium and passaged at approximately $2x10^5$ cells/ml.

2.2. De-methylation Treatment

2.2.1. Preparation of 5-Aza-2'-deoxycytidine

Fifty milligrams of 5-Aza-2'-deoxycytidine (5-aza) was purchased from Sigma-Aldrich. The 5-Aza stock solution was dissolved in a 1:1 ratio of filter sterilised water and filter sterilised

glacial acetic acid (Appendix B.2). The working solution was prepared by a 1:100 dilution of 5-Aza in the respective medium, that is 1 µl of 5-Aza stock was added to 99 µl of medium.

2.2.2. Treatment with 5-Aza

For experiments, HEK and A549 cell lines were grown in four 10 cm dishes. When the cells were between 60-70% confluent, they were treated with 0.5, 1 and 5 µmol/l of 5-aza. The fourth dish served as a vehicle control and was treated with a 0.5:100 dilution of glacial acetic acid. Cells were treated for 72 hours. DMS 79 cells were grown in four T75 flasks until 70% confluent and treated with 0.5, 1 and 5 µmol/l 5-aza and vehicle for 72 hours.

2.3. RNA Extraction

RNA was extracted from treated cells using a QIAGEN RNeasy kit according to the manufacturer's instructions for purification of total RNA from cells using spin technology. Adherent cells were trypsinised and pipetted into a 15 ml centrifuge tube. The dishes were washed with 1x phosphate buffered saline (PBS) (Appendix B.3) and pipetted into the centrifuge tube. DMS79 cells were harvested by the passaging method as described in section 2.1 and flasks were rinsed out with 1x PBS solution. Centrifuge tubes were centrifuged at 1000 x *g* for 5 minutes. The supernatant was discarded and the pellet of cells was re-suspended in 600 µl of RLT lysis buffer. Cells were homogenised by pipetting several times and vortexed on Vortex Genie 2 (Lasec SA (Pty) Ltd) at full power. The cell lysate was then passed through a QIAshredder (QIAGEN) at full speed in an Eppendorf 5418 centrifuge for a minute. The QIAshredder column was discarded and the collection tube containing the lysate was retained. 600 µl of 70% ethanol was added to the lysate and mixed by pipetting. The 1200 µl of solution was passed through an RNeasy spin column, placed in a 2 ml collection tube, at 8000 x *g* for 15 seconds. The flow through was discarded and 700 µl of RW1 buffer was pipetted into the spin column. The column was centrifuged at 8000 x *g* for 15 seconds and the flow through was discarded.

A volume of 500 µl RPE buffer was added to the spin column and centrifuged at 8000 x *g* for 15 seconds. The flow through was discarded and an additional 500 µl of RPE buffer was added. The spin column was centrifuged at 8000 x *g* for 2 minutes. The collection tube was discarded

and the spin column was placed in a new 2 ml collection tube. The spin column was centrifuged at 13 000 x *g* for 1 minute to remove residual RPE buffer on the membrane. The spin column was placed in a 1.5ml micro-centrifuge tube and 30 µl of RNA free water was pipetted onto the membrane for elution. The tube was centrifuged at 8000 x *g* for 1 minute. The eluted RNA was placed on ice and quantified using a Spectrophotometer ND1000 (NanoDrop Technologies). RNA samples were aliquoted and stored at -80^{o}C.

2.3.1. RNA Electrophoresis

The quality of the extracted RNA was evaluated by performing RNA gel electrophoresis. A 1.5% agarose, formaldehyde gel was prepared by dissolving 1.5g TopVision™ agarose (Fermentas) in 72ml of DEPC-treated water (Appendix B.4). 20 µl of 0.05 mg/ml ethidium bromide (Merck) (Appendix B.5) was added to the cooled agarose solution. In a fume hood, 10 ml of 10x MOPS buffer (Appendix B.6) (Sigma) and 18 ml of formaldehyde (Merck) were added to the agarose solution prior to pouring the gel into the mould. All gel electrophoresis apparatuses and glassware were soaked overnight in hydrogen peroxide to inactivate RNAses.

Two micrograms of RNA was added to 2 volumes of RNA loading buffer (Sigma) in a microcentrifuge tube and incubated at 65^{o}C for 10 minutes in a dry bath incubator (MRC). RNA samples were loaded onto the gel with an O'GeneRuler™ DNA ladder mix molecular marker (range 100-10 000 base pairs) (Fermentas). The gel was run for 75 minutes at 85V using a Bio-Rad Powerpac. A 1x MOPS buffer was used for the running buffer (Appendix B.6). The gel was imaged using a ChemiDoc XRS+ imaging system (Bio-Rad) and Image Lab software package (Bio-Rad).

2.4. cDNA Synthesis

cDNA was synthesised from RNA samples using the High Capacity RNA to cDNA Mastermix (Applied Biosystems). Midway through this project, this mastermix was discontinued by the manufacturer so subsequent cDNA was synthesised using the Tetro cDNA Synthesis Kit (Bioline). For all reactions, RNA samples were thawed on ice and 2 µg of RNA was used for synthesis.

2.4.1. High Capacity RNA to cDNA Mastermix

Two microgram of RNA was transferred to a PCR tube (Star Lab) and 4 µl of the mastermix was added. Nuclease free water (Invitrogen) was added for a total volume of 20 µl. The PCR tubes were placed in a Bio-Rad MyCycler thermal cycler. Tubes were incubated at 25^{o}C for 5 minutes, 42^{o}C for an hour and 85^{o}C for 5 minutes. Once incubation was over, tubes were immediately placed on ice and centrifuged in a Hermle Z100M mini centrifuge. The samples were diluted with 20 µl of nuclease free water and aliquoted. cDNA aliquots were stored at -20^{o}C.

2.4.2. Tetro cDNA Synthesis Kit

All buffers and solutions were allowed to thaw, vortexed and centrifuged. A priming premix was prepared on ice in a PCR tube. Two micrograms of RNA, 1 µl of Oligo $(dT)_{18}$ primer (uses poly-A-tail principle) and 1 µl of 10mM dNTP mix was added to the tube. DEPC-treated water was added for a final volume of 10 µl. The tubes were incubated at 70^{o}C in the Bio-Rad MyCycler for 5 minutes and chilled on ice for 1 minute.

A 10 µl reaction premix for each tube was prepared during incubation. Four microlitres of 5x RT buffer, 1 µl of Ribosafe RNase inhibitor, 1 µl Tetro reverse transcriptase (200 units/µl) and 4 µl of DEPC-treated water was used per premix. The reaction premix was added to the tubes post-incubation and mixed gently by pipetting. The tubes were incubated for 45^{o}C for an hour and the reaction was terminated by incubating samples for 5 minutes at 80^{o}C. Tubes were chilled on ice and 20 µl of RNase free water (QIAGEN) was added. cDNA aliquots were stored at -20^{o}C.

2.5 Conventional PCR

Conventional PCR was performed to identify the GR promoters expressed in the different cell lines. A 60 mm dish was used for the adherent cells (A549 and HEK) while the DMS79 cells were grown in a 25 cm^3 tissue culture flask (T25). The GR promoter primers and the reference gene, β-actin were sourced from Alt *et al.* (2010) (Table 2.1). All primers were synthesized by

Inqaba biotech. A 20 µl reaction consisted of 1 µl of cDNA, 2 µl of 10x *Taq* $(NH4)_2SO_4$ buffer, 1.8 µl 25mM $MgCl_2$, 1 µl of (10mM) forward and (10mM) reverse primer (Appendix B.7), 2 µl of 2mM dNTP (Appendix B.8), 0.2 µl of *Taq* recombinant DNA polymerase (5 units/µl) and 11 µl of nuclease free water was performed for each promoter. All PCR reagents were purchased from Fermentas. The incubation and amplification steps for conventional PCR reactions were performed in a Bio-Rad thermocycler with denaturation at 95^{o}C for 4 minutes, 35 cycles of 95^{o}C for 30 seconds, 60^{o}C for 1 minute and 72^{o}C for 1 minute and a final elongation period for 7 minutes at 72^{o}C. When amplification was completed, PCR products were centrifuged and stored at 4^{o}C.

Table 2.1: Primer sequences of the various promoter regions in GR and β-actin (Alt *et al*., 2010)

Forward Primer	**Sequence** **5'** **3'**
Promoter 1B	GCCGGCACGCGACTCC
Promoter 1C	GCTCCTCTGCCAGAGTTGAT
Promoter 1D	ACAACCTTTCCCAGAGTC
Promoter 1E	CGTGCAACTTCCTTCGAGT
Promoter 1F	GTAGCGAGAAAAGAAACTGG
Promoter 1H	CTGACAGCCCGCAACTTGGA
Promoter 1J	CCGGGGTGGAAGAAGAG
β-actin	GGCCACGGCTGCTTC
Reverse Primer	**Sequence** **5'** **3'**
GR Exon 2	CAGTGGATGCTGAACTCTTGG
β-actin	GTTGGCGTACAGGTCTTTGC

2.5.1. Agarose Gel Electrophoresis

To identify the promoters present in HEK, A549 and DMS79 cell lines, agarose gel electrophoresis was used to visualise the PCR products. A 1% agarose gel was used where 1g of TopVision™ agarose (Fermentas) was dissolved in 100 ml of 1 x TBE buffer (Appendix B.9). 5 µl of 0.05 mg/ml ethidium bromide (Merck) was added to the solution. The agarose gel was run at 80V with a Bio-Rad Powerpac for one and half hours. An O'GeneRuler™ DNA ladder mix molecular marker (Fermentas) was used to derive the size of the bands. The gel was imaged using a ChemiDoc XRS+ imaging system (Bio-Rad) and Image Lab software package (Bio-Rad).

2.6. Mapping of CpG Islands in Exon 1

To evaluate whether CpG islands are housed within the GR promoter region, the GR gene sequence was entered into CpG island identifying software. The GR gene sequence was obtained from the UCSC genome browser site (genome.ucsc.edu/) with reference number uc0031my.2; range=chr5: 142656497-142787254. The 5'-UTR was 5000 base pairs long. The input sequence, ranging from the 5'-UTR to the end of exon 2, was entered into a CpG Plot searcher software. The site utilised was EBI, an outstation of European Molecular Biology Laboratory website (www.ebi.ac.uk/Tools/emboss/cpgplot/) (Figure 2.1). The parameters used to analyse the GR sequence were as follows: the ratio of observed to expected of CpG islands was set to 0.60, the percentage of cytosines and guanine must be equal to or more than 50 and CpG island length must be equal to or greater than 200. When the CpG islands were identified, they were cross checked to the sequence region of the promoters selected for qPCR experiments.

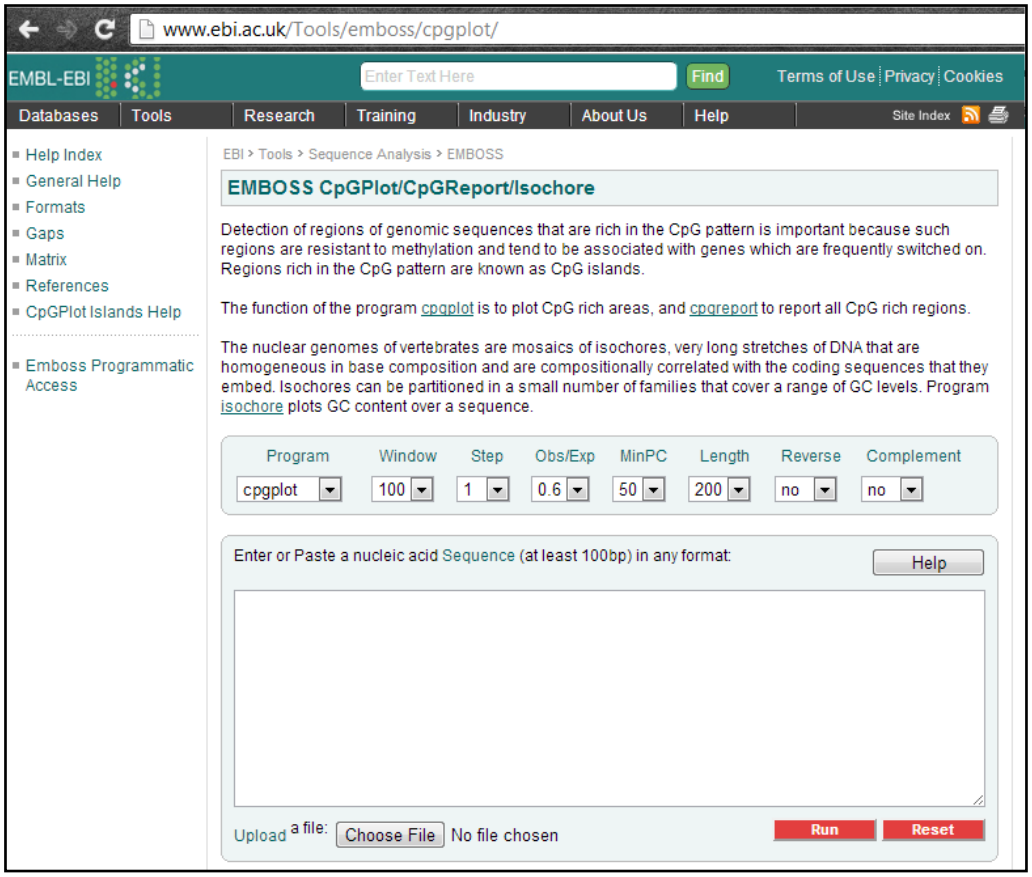

Figure 2.1: Image of the EBI site used to identify CpG Plots in gene sequences (www.ebi.ac.uk/Tools/emboss/cpgplot/)

2.7. Real Time Quantitative PCR (qPCR)

Once the promoters expressed by each cell line were identified by conventional PCR, qPCR was used to determine their relative expression. Two biological repeats were performed per cell line. Each biological repeat had 3 technical repeats and within each technical repeat, triplicates were run per cDNA type per primer set. Each run comprised of the reference gene, β-actin, and either promoter 1B or 1C. Each replicate was a master mix of 20 µl reactions using 2 µl of 5x HOT FIREPol® Evagreen® qPCR Mix Plus (Solis BioDyne), 1 µl cDNA, 0.5 µl of (10mM) forward and (10mM) reverse primer and 16 µl of nuclease free water. qPCR was performed in BIORAD MJ Mini Opticon Thermal Cycler with initial activation of polymerase at 95°C for 15 minutes followed by 40 cycles of 95°C for 15 seconds, 60°C for 30 seconds and 72°C for 1 minute with a plate read step and a final elongation step of 72°C for 10 minutes. The melt curve analysis ranged from 50 – 90°C with increments of 1°C and a plate read step for 5 seconds after every temperature change.

qPCR experimental design, procedures and analyses were adhered to the Minimum Information for Publication of Quantitative Real-Time PCR (MIQE) guidelines. The purpose of MIQE guidelines was to create a standard with which scientists were allowed to present, evaluate and report qPCR data that would be interpreted in an accurate manner (Bustin *et al*., 2009). All details of experiments satisfying the MIQE guidelines are presented in Appendix A.

2.7.1. The $2^{-\Delta\Delta Ct}$ Method of qPCR and Statistical Analysis

Results from qPCR reactions were observed using CFX manager software package (Bio-Rad) and the genetic-specific threshold cycles (Ct values) generated were used for semi-quantitative analysis of GR promoter 1B and 1C expression. This Ct value indicates the fractional cycle when the amplified target gene reaches a fixed threshold. The $2^{-\Delta\Delta Ct}$ method is used to analyse the relative changes in gene expression (Livak and Schmittgen, 2001). Validation of the use of the $2^{-\Delta\Delta Ct}$ method was performed in accordance of the MIQE guidelines. The reaction efficiency of each primer set was quantified by analysing the Ct values of a dilution series of cDNA. All reaction efficiencies were between 90-110% and the R^2 value was close to 1. The parameters were satisfied for reaction efficiencies therefore comparison of the data could be performed (Appendix A.6.1). No reverse transcription and template controls were performed for each primer set to verify amplification was specific (Appendix A.7).

In this study, the promoter expression was normalized to the reference gene β-actin. Analysis of $2^{-\Delta\Delta Ct}$ method and graphic illustration of analysis was performed in Microsoft Excel 2007. Differences between treatments were analysed using one way analysis of variance (ANOVA) and Tukey HSD post-hoc test performed on (IBM) SPSS Version 21 statistical software. All tests for normality were satisfied.

2.8. Glucocorticoid Receptor and Mutant Glucocorticoid Receptor Constructs

2.8.1. Plasmid Elution

Plasmid constructs labelled with a yellow fluorescent protein (eYFP) blotted on filter paper were received from Manchester University. These included the empty plasmid pFUNC1-eYFP, a wild type GR plasmid pFUNC1-GR-eYFP, a DNA binding mutant pFUNC1-GRA458T-

eYFP, a transactivation mutant pFUNC1-GRΔAF1-eYFP, a ligand binding mutant pFUNC1-GRC736S-eYFP and pVPack Vectors *Env*-expressing vector and gag-pol, pVPack-VSV-G and pVPack-GP respectively. The area where each plasmid was blotted on the filter paper was cut out and placed in a 1.5 ml microcentrifuge tube (Star Lab). Fifty microlitres of TE buffer (Appendix B.10) was pipetted onto the filter paper and the microcentrifuge tube was placed on an IKA® KS 130 basic shaker overnight for elution. Post-elution, the microcentrifuge tubes were centrifuged and the eluate was transferred into a new 1.5 ml microcentrifuge tube. The plasmids' DNA was quantified using a nanodrop spectrophotometer and stored at -20^{o}C.

2.8.2. Transformation of Competent Cells

Subcloning efficiency™ DH5α™ competent cells (Invitrogen) were thawed on ice and a 1.5 ml microcentrifuge tube was placed on ice to chill. The thawed competent cells were mixed gently with a pipette tip and 50 µl of the cells was transferred to the chilled microcentrifuge tube. Ten nanograms of plasmid DNA was added to the cells and mixed with a pipette tip. The tube was incubated on ice for 30 minutes and heat shocked for 20 seconds at 42^{o}C in a MRC dry bath incubator (Polychem Supplies Ltd.). The tube was immediately placed on ice for 2 minutes. Nine hundred and fifty microlitres of pre-warmed LB broth (Appendix B.11) was added to the microcentrifuge tube and incubated at 37^{o}C for one and half hours at 225 rpm in Environmental Incubator Shaker (New Brunswic Scientific Co. Inc.). The competent cells were centrifuged at 1500 x *g* in an Eppendorf 5418 centrifuge for 5 minutes. Eight hundred microlitres of the supernatant was discarded and the pellet of cells was re-suspended in the remaining 200 µl of LB broth. The 200 µl cell suspension was spread on a pre-warmed LB agar plate (Appendix B.12). The plate was incubated overnight at 37^{o}C.

2.8.3. Purification of Plasmids

2.8.3.1. Growth of Bacterial Colonies

Three colonies were picked from each plate for each plasmid using a 0.5 µl-20 µl pipette tip (Whitehead Scientific). Each pipette tip was placed in 5ml of LB broth containing 5µl of ampicillin (100 µg/ml) in a 15 ml centrifuge tube. The tubes were incubated overnight at 37^{o}C in a shaking incubator (225 rpm).

2.8.3.2. Mini-prep of Plasmid

The 15 ml centrifuge tubes were removed from the shaking incubator. The tubes were centrifuged at 1000 x *g* for 10 minutes in an Eppendorf 5180R centrifuge at 4^{o}C to pellet cells. The supernatant was discarded and the plasmid was purified using QIAprep Spin mini-prep kit (QIAGEN). The pellet was re-suspended in 250 µl of Buffer P1 containing RNase A and Lyse Blue and transferred into a 1.5 ml microcentrifuge tube. Tubes were vortexed to ensure complete re-suspension of pellet. 250 µl of Buffer P2 was added and mixed thoroughly by inverting the tube between four to six times. The solution was a uniform blue colour indicating that complete cell lysis had occurred. Three hundred and fifty microlitres of Buffer N3 was added to the tubes and mixed thoroughly by inverting the tube between four to six times until the solution turned white. The white solution indicates that the SDS had been effectively precipitated. The microcentrifuge tubes were centrifuged at 17900 x *g* for 10 minutes to pellet cell debris. The supernatant was carefully transferred to a QIAprep spin column (QIAGEN) and centrifuged for 60 seconds at 17900 x *g* and the flow through were discarded. The spin column was washed with 500 µl of Buffer PE and centrifuged for 60 seconds at 17900 x *g*. The flow through was discarded and the spin column was washed with an additional 750 µl of Buffer PE. The spin column was centrifuged at 17900 x *g* for 60 seconds. The flow through was discarded and the spin column was centrifuged at 17900 x *g* for 1 minute to remove residual Buffer PE from the membrane. The collection tube was discarded and the spin column was placed in a 1.5 ml microcentrifuge tube. The purified plasmid DNA was eluted by adding 50 µl of TE buffer onto the membrane of the spin column. The spin column was allowed to stand for 1 minute and centrifuged for 1 minute at 17900 x *g*. The spin column was discarded, the tubes were placed on ice and DNA was quantified using NanoDrop Spectrophotometer ND1000 and stored at -20^{o}C. One millilitre glycerol stocks of each colony was prepared and stored at -80^{o}C (Appendix B.13).

2.8.3.3. Digestion of Purified Plasmid DNA

The purified plasmid DNA was digested to verify that the colonies contained the plasmid insert. Each plasmid DNA sample was prepared as follows; approximately 1 µg of plasmid DNA, 1 µl of BglII restriction enzyme (Fermentas), 1 µl of Tango buffer (Fermentas) and nuclease free water to give a total volume of 20 µl was added into a 1.5 ml microcentrifuge tube. The microcentrifuge tubes were incubated in a dry bath incubator at 37^{o}C for 2 hours to facilitate restriction digest. Post-incubation, tubes were centrifuged and restriction products were

separated by agarose gel electrophoresis as described in section 2.5.1. Samples that contained the inserts were subjected to midi-prep purification.

2.8.3.4. Midi-prep of Plasmid

A starter culture of 10ml LB broth with 10 µl of ampicillin (100 µg/µl) was transferred into a 50ml centrifuge tube (Corning). Ten microlitres of the plasmid from glycerol stock was added to the culture. The starter culture was incubated for 8 hours at 37^{o}C at a rotation of 225 rpm in a shaking incubator and transferred into a 100 ml culture of LB broth for overnight growth.

The centrifuge tubes were centrifuged at 1000 x *g* for 10 minutes at 4^{o}C to pellet the cells. The supernatant was discarded and the pellet underwent purification using QIAGEN midi-prep kit. The pellet was re-suspended in 8 ml of Buffer P1 containing RNase A and LyseBlue and vortexed for complete re-suspension. The cell lysate was transferred to a 50 ml centrifuge tube. Eight millilitres of Buffer P2 was added to the tube and vigorously inverted between four to six times creating a blue solution. The solution was incubated at room temperature for 5 minutes. Eight millilitres of chilled Buffer N3 was added to the tube and vigorously inverted between four to six times until solution was white. The tube was placed in ice for 15 minutes. After incubation the tube was centrifuged at 1000 x *g* for 30 minutes at 4^{o}C to pellet all cell debris. The layer of cell debris above the supernatant was carefully removed and the supernatant was transferred to a new 50 ml centrifuge tube. The solution was centrifuged for an additional 15 minutes at 1000 x *g* at 4^{o}C to remove residual cell debris. A QIAGEN-tip 100 was equilibrated with 4 ml of Buffer QBT and the supernatant from the 50 ml tubes were transferred into the QIAGEN-tip and allowed gravity to filter the supernatant through the membrane. The membrane was washed twice with 10 ml Buffer QC. The DNA was eluted from the membrane by adding 5 ml of Buffer QF and collected in a 15 ml centrifuge tube. DNA was precipitated by adding 3.5 ml of room temperature isopropanol (Merck) and centrifuged at 1000 x *g* for 30 minutes at 4^{o}C. The supernatant was carefully decanted. Two millilitres of 70% ethanol (Merck) (Appendix B.14) was added and the pellet was washed by centrifugation at 1000 x *g* for 10 minutes at 4^{o}C. The supernatant was carefully decanted and the pellet was allowed to air dry. The pellet was dissolved in 30 µl of TE buffer and quantified by nanodrop spectrophotometer. Plasmids were stored at -20^{o}C.

2.9. Plasmid Transfection

A confluent 10cm dish of $7x10^6$ HEK cells was grown, trypsinised and transferred into a 1.5 ml microcentrifuge tube. The tube was centrifuged at 1500 x *g* for 5 minutes. The supernatant was discarded and the pellet of cells was re-suspended in 1 ml of DMEM medium. 12mm coverslips (Marienfeld GmbH and Co.) were sterilised in 100% ethanol and placed under the UV light for 30 minutes in laminar flow to dry. The coverslips were then placed in a 24-well tissue culture plate (Corning). Thirty microlitres of the suspended cells were pipetted onto the coverslips and 1ml of medium was added to each well. The HEK cells were allowed to grow until 70% confluent on the coverslips.

The pFUNC1-eYFP or pFUNC1-GR-eYFP plasmids were transfected into these cells using X-tremeGENE HP DNA transfection reagent (Roche). The transfection reagent was allowed to reach room temperature and vortexed for a second. One microgram of plasmid DNA was diluted in 100 µl of serum free medium in a 1.5 ml microcentrifuge tube. Three microlitres of XtremeGENE was added to the DNA complex and gently mixed by tapping the tube. The DNA-reagent complex was incubated at room temperature for 30 minutes. The 24-well plate was removed from the incubator and 500 µl of DMEM medium was added. Twenty microlitres of the DNA-reagent complex was added dropwise to each coverslip. One coverslip of HEK cells served as a control. The 24-well plate was gently swirled and placed in the incubator for 24 hours.

2.10. Microscopy

After 24 hours following transfection the 24-well plate was removed from the incubator and the medium was removed. The cells were washed twice with 200 µl of 1x PBS solution. The cells were fixed with 4% paraformaldehyde (Merck) containing 0.15% Triton X-100 (Sigma-Aldrich) (Appendix B.15) for 15 minutes at 4^oC to allow for permeablisation. The fixative was removed and the cells were washed thrice with 200 µl of 1x PBS solution. Cells were incubated with 1:50 dilution of DAPI (50ng/µl) in 1x PBS solution at room temperature for 10 minutes. Cells were washed once with 200 µl of 1x PBS solution. Coverslips were removed from the wells using a needle and forceps and dabbed on tissue paper to remove excess PBS solution. The coverslips were mounted on glass slides using a single drop of Mowiol with DABCO (Sigma) (Appendix B.16).

Slides were analysed using Nikon Eclipse 80i fluorescent microscope using the FITC range filter for eYFP and UV filter for DAPI staining of nuclei. Images were captured using Digital Sight DS-Fi1 digital camera and NIS Elements D software (Nikon). Fluorescent microscope and software was available at the UKZN Microscopy Microanalysis Unit (Westville campus).

2.11. Retrovirus Construction

Five 60 mm dishes of HEK cells were grown until 70% confluent. Each dish was transfected with three 250 µl of DNA-reagent complexes. These included a plasmid complex (control, wild-type or GR mutant), a pVPack-VSV-G complex and a pVPack-GP complex. Each 250 µl complex was prepared with 2.5 µg of DNA, 7.5 µl of XtremeGENE reagent and serum free medium. Complexes were prepared as described in 2.6.4. The dishes were incubated for 24 hours at 37^{o}C in the incubator. After 24 hours each dish was treated with 100 µmol/l sodium butyrate (Sigma-Aldrich) (Appendix B.17) and incubated for another 24 hours. This allowed for the production and secretion of replication incompetent retroviruses carrying pFUNC1-eYFP, pFUNC1-GR-eYFP, pFUNC1-GRA458T-eYFP, pFUNC1-GRΔAF1-eYFP or pFUNC1-GRC736S-eYFP into the supernatant.

2.12. Retroviral Infection

2.12.1. Adherent Cell Lines

For HEK cell line, six 60 mm dishes were grown until 70% confluent, one dish for each plasmid and one dish served as a control. The medium was removed from the five dishes and the supernatant containing the retroviruses was added dropwise onto the cells. To increase infection efficiency, polybrene (Hexadimethrine bromide) (Sigma) (Appendix B.18) was added to each dish to a final concentration of 8µg/ml. The plates were placed in the incubator for 72 hours at 37^{o}C.

2.12.2. Suspension Cell Line

Six T25 flasks of DMS79 were grown until 70% confluent. Five of the T25 flasks were spin-infected with one of the five retroviral supernatants (pFUNC1-eYFP, pFUNC1-GR-eYFP, pFUNC1-GRA458T-eYFP, pFUNC1-GRΔAF1-eYFP or pFUNC1-GRC736S-eYFP). The DMS79 cells were pippetted into a 15 ml centrifuge tube and centrifuge at 1000 x *g* for 5 minutes. The supernatant was removed and the pellet of cells was re-suspended in retroviral supernatant. To increase infection efficiency, hexadimethrine bromide was added to each centrifuge tube to a final concentration of 8μg/ml. The cells were centrifuged at 800 g for 2 hours at 37^{o}C. After spin-infection, the supernatant was discarded and the pellet of cells was re-suspended in 1 ml of RPMI 1640 medium. The cells were transferred to a T25 flask containing 9 ml RPMI 1640 medium. The cells were incubated for 72 hours at 37^{o}C.

2.13. Spin-infection Efficiency

To evaluate the spin-infection efficiency of DMS79 cells, qPCR analyses were performed on cells transfected, infected and spin-infected with the viruses. Post 72 hour incubation of cells, the cells were harvested for RNA extraction as described in section 2.3 above. cDNA was synthesised using the Tetro cDNA Synthesis kit as described in section 2.4.2 above. β-actin was used as the reference gene for qPCR analyses and eYFP primers were used for the target gene. eYFP is not endogenously expressed in the cell and therefore indicative of viral infection. eYFP primers were as follows: forward primer: 5'-TGCTTCAGCCGCTACCCCGACC-3' and reverse primer 5'-CGCCGATGGGGGTGTTCTGCTG-3'. The efficiency of spin-infection and infection was evaluated relative to transfected HEK cells where 100% of the cells were shown by microscopy to express eYFP 24 hours post transfection.

Amplification was verified as being eYFP specific by performing a NTC (Appendix A.7) and analysing the melt analysis performed during qPCR (Appendix A.6.2). The $2^{-\Delta\Delta Ct}$ method was used to analyses qPCR data.

2.14 Apoptosis Induction

To identify the component of the GR receptor responsible for inducing apoptosis, cell lines were infected with retroviruses containing either the control virus; pFUNC1-eYFP; the wild-type GR expressing virus; pFUNC1-GR-eYFP; the DNA binding mutant virus; pFUNC1-GRA458T-

eYFP; the transactivation mutant virus; pFUNC1-GRΔAF1-eYFP or the ligand binding mutant virus; pFUNC1-GRC736S-eYFP. The DNA binding mutant virus, pFUNC1-GRA458T-eYFP, has a point mutation of adenine to thymine at position 458. The transactivation mutant, pFUNC1-GRΔAF1-eYFP, has a 555bp deletion of the AF1 region (amino acid 77 to 262) in the NTD of the GR gene. The ligand binding mutant, pFUNC1-GRC736S-eYFP, has a point mutation of cysteine to serine at position 736 in the sequence. These point mutations and deletion render the GR protein dysfunctional in the respective domains.

2.14.1. Microscopic Analysis of Apoptosis and Cell Death

DMS79 cells and HEK cells were spin-infected and infected, respectively, with retroviral supernatant containing plasmid as described in section 2.12. After 72 hours, DMS79 cells were collected from T25 flasks into 15ml centrifuge tubes and centrifuged at 1000 x *g* for 5 minutes to pellet the cells. Culture dishes containing infected HEK cells were removed from the incubator and the retroviral supernatant was carefully removed and discarded. Each dish was washed with 1ml of sterile 1x PBS solution to remove residual retroviral supernatant. HEK cells were washed off culture dishes using sterile 1x PBS and pipetted into 15 ml centrifuge tubes. The tubes were centrifuged at 1000 x *g* for 5 minutes to pellet the cells. The supernatant was removed and the pellet was washed with 200 µl of 1x PBS and transferred to a 1.5 ml microcentrifuge tubes. The tubes were centrifuged at 1500 x *g* for 5 minutes. The supernatant was discarded and the pellet was re-suspended in 500 µl of 4% paraformaldehyde containing 0.15% Triton X-100 and cells were fixed at 4^{o}C for 15 minutes. The tubes were centrifuged at 1000 x *g* for 5 minutes. The pellet of cells were washed twice with 200 µl of 1x PBS. After each wash cells were centrifuged at 1000 x *g* for 5 minutes.

After the second wash, the supernatant was discarded and the pellet of cells was re-suspended in 100 µl of Annexin V binding buffer. Five microlitres of Annexin V APC (10Mm HEPES, 10mM NaOH, 140mM NaCl, 2.5mM $CaCl_2$) (Appendix B.19) and 5 µl of PI (Appendix B.20) was added to each tube and incubated at room temperature in the dark for 20 minutes. Tubes were centrifuged and the pellet was washed with 200 µl of 1x PBS. The tubes were centrifuged and the pellet was re-suspended in 50 µl of 1:50 dilution of DAPI. The tubes were incubated at room temperature in the dark for 10 minutes. The tubes were centrifuged at 1000 x *g* for 5 minutes and the pellet of cells were washed with 1x PBS. The cells were centrifuged and the supernatant was discarded and the pellet was re-suspended in minimal 1x PBS. Cells were

transferred to slides by pipetting with a 20-200 µl yellow tip (Star lab) and covered with a 16mm coverslip (Marienfeld) containing a single drop of MOWIOL with DABCO.

Slides were analysed by confocal microscopy using a LSM 710 microscope (Zeiss) at the UKZN Centre for electron microscopy (Pietermaritzburg campus). Images were obtained using the software program ZEN Efficient Navigation 2010 (Zeiss). Four channels were analysed; FITC using 488nm laser (to detect eYFP), DAPI using 405 nm laser (nuclei detection), APC using 633 nm laser (Annexin V APC stain apoptotic cells) and PI using 488nm laser (detect cell death). In the acquisition mode of the Zen 2010 software, the pin hole was set at 160.4 with diameter at 1 airy unit and the speed of capturing images was 4 frames. The frame size of images captured was 1024 by 1024 pixels.

2.14.2. Statistical Analysis

A population of 200 cells was selected for each treatment. In this population cells were counted for Annexin V APC, PI, DAPI and eYFP positive cells. The number of positive cells were converted to a percentage and expressed on a graph with standard error of mean. A one-way ANOVA with a Tukey HSD post-hoc test was performed using IBM SPSS Version 21 statistical software. All tests for normality were satisfied for each data set.

3. Results

3.1. Evaluation of RNA extraction

Prior to cDNA synthesis, the quality of all RNA samples was validated by RNA gel electrophoresis. One microgram of RNA extracted using the QIAGEN RNeasy method was run on a 1.5% agarose-formaldehyde gel. Each gel was run with an O'GeneRuler™ DNA ladder mix molecular marker (range 100-10 000 base pairs). Good quality RNA is denoted by the presence of two distinct bands on the gel representing the 28S rRNA and 18S rRNA subunits (Figure 3.1).

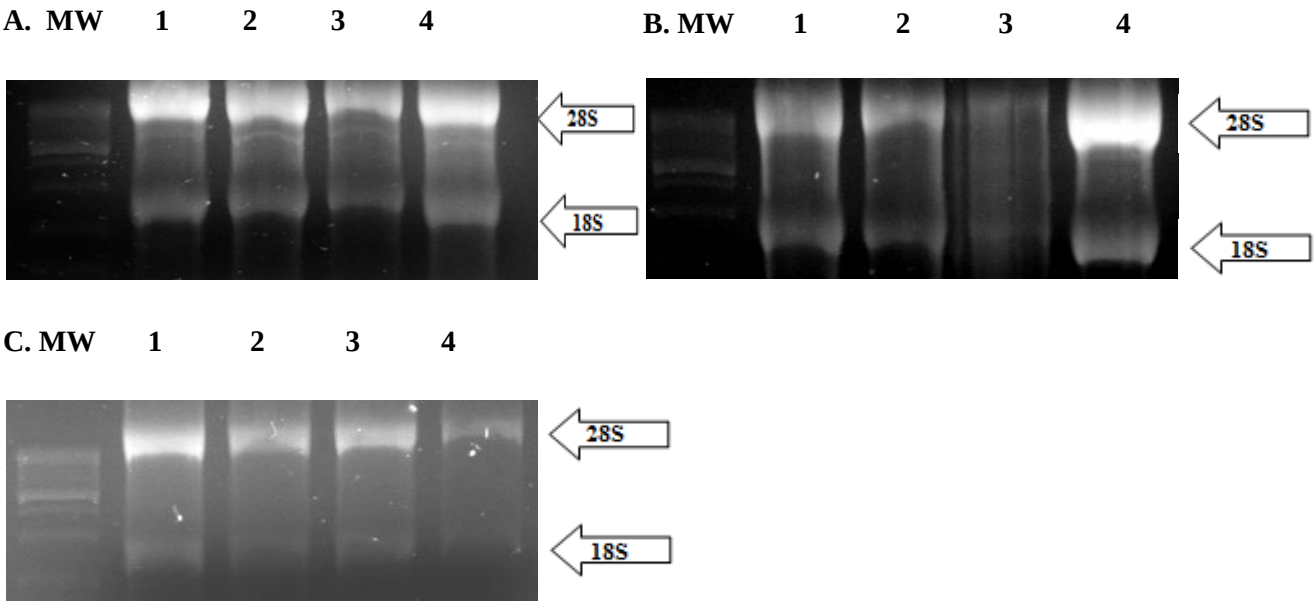

Figure 3.1: RNA gel images displaying the RNA integrity of cell lines treated with 5-aza. MW – Molecular weight marker; 1 – Control; 2 – 0.5 µmol/l 5-aza; 3 – 1 µmol/l 5-aza; 4 – 5 µmol/l 5-aza (A) A549 cell line; (B) HEK cell line; (C) DMS79 cell line. 28S and 18S RNA subunits

Glucocorticoid Receptor Promoter Usage in SCLC and Control Cell Lines

The GR is a complex gene with many different promoters. The reason for so many different promoters is unknown but thought to be tissue-specific. In this section, we investigate which promoters are utilised by the different cell lines for GR expression and which of these are possibly methylated.

3.2. Identification of promoters utilised by A549, HEK and DMS79 cell lines

The GR has 8 identified promoters (1A – 1J). Promoter 1A was excluded as it is only present in T-cells (Alt *et al*., 2010). To identify which GR promoters are utilised by A549, HEK and DMS79 cells, conventional PCR was performed using primers for promoters 1B – 1J. The reference gene used for conventional PCR reactions was β-actin. The PCR products for each cell line were run on 1% agarose gel electrophoresis with O'GeneRuler™ DNA ladder mix molecular marker.

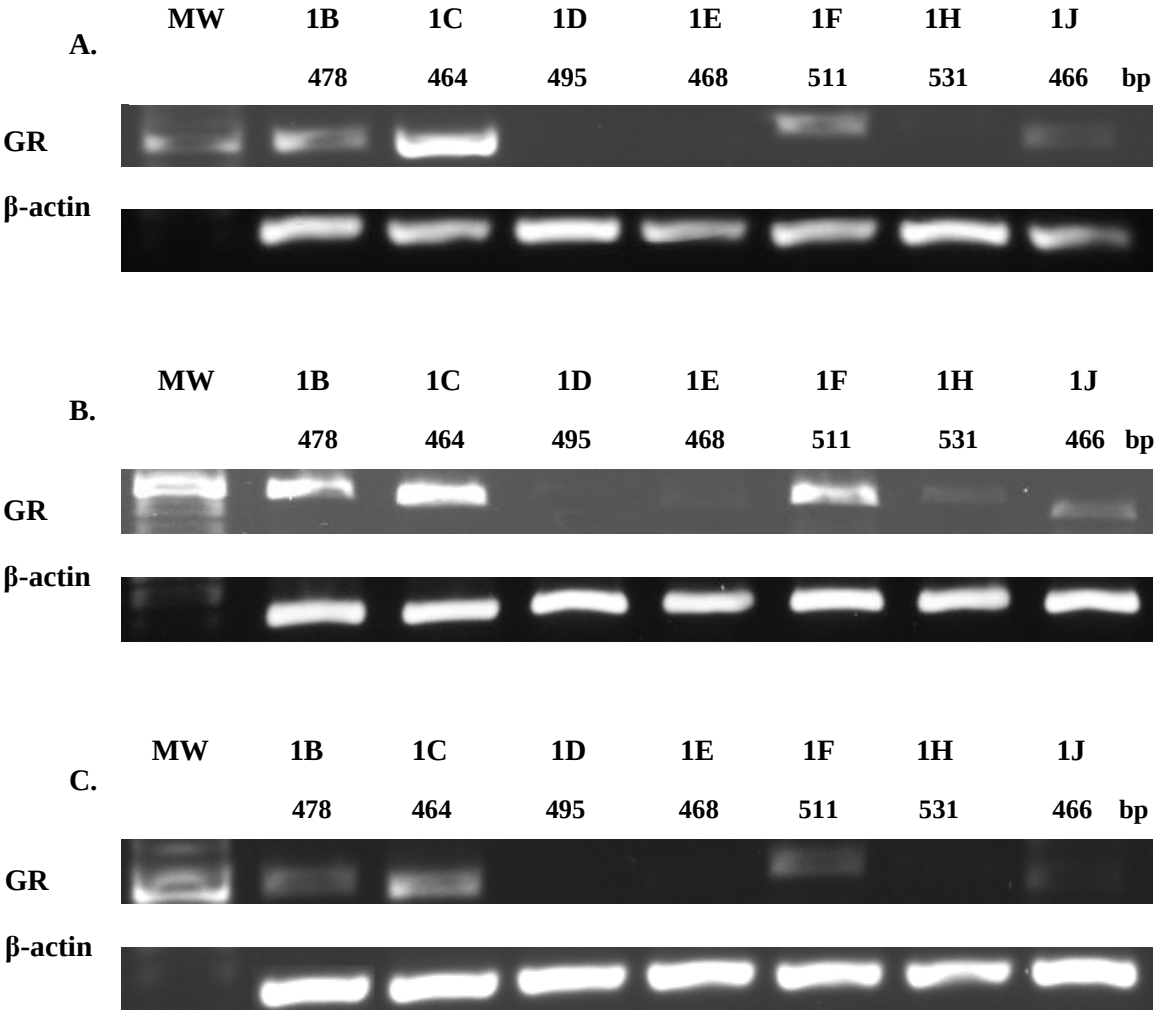

Figure 3.2: Agarose gel image of GR promoter expression in (A) A549, (B) HEK and (C) DMS79 cell lines. MW – O'GeneRuler™ DNA Ladder molecular marker; 1B-1J: GR promoters; bp – base pairs of the product size

A549 cells expressed high levels of promoters 1B and 1C and low levels of promoters 1F and 1J. Promoters 1D, 1E and 1H were not amplified in A549 cells indicating that these promoters are not involved in transcription of the GR in these cells. In HEK cells, promoters 1B, 1C and 1F were present at high levels and 1E, 1H and 1J were expressed at low levels. Promoter 1D utilisation was absent in HEK cells. DMS79 cells had high levels of promoters 1B and 1C present while promoters 1F and 1J were present at low levels. Usage of promoters 1D, 1E and 1H was absent in DMS79 cells (Figure 3.2). Since promoters 1B and 1C were transcribed commonly in all three cell lines, it was decided that these promoters were suitable target genes for qPCR analyses. Prior to qPCR analyses, the presence of CpG islands within or near promoters 1B and 1C was determined by bioinformatic analysis.

3.3. CpG Island Identification

In order to identify the CpG islands present within the promoter region of GR, the GR sequence was entered into the EBI CpG plot finder software. From the output, it was determined that there were putative CpG islands between base numbers 246 to 530, 1141 to 2395 and 2501 to 3192 (Figure 3.3). The promoter 1B region is found between base numbers 934 to 1199 and the promoter 1C region is found between base numbers 1926 to 2787. Thus it was concluded that promoters 1B and 1C contain CpG islands. It is known that DMS79 cells express very low levels of the normally ubiquitous GR. This silencing of the GR may be due to methylation of these CpG islands. De-methylation by treatment with 5-aza could lead to re-expression of the GR.

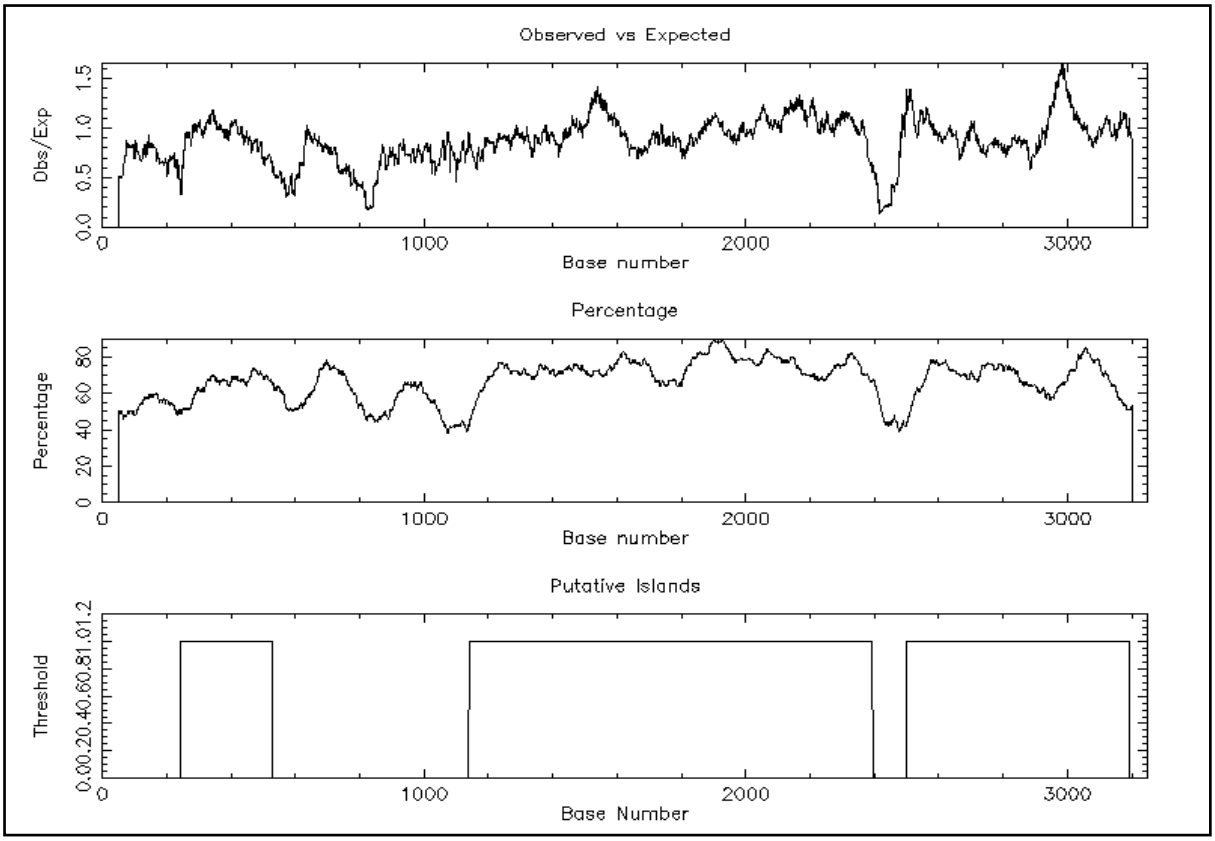

Figure 3.3: Image of predicted CpG island plots identified in the GR gene (http://www.ebi.ac.uk/Tools/es/cgi-bin/jobresults.cgi/cpgplot/cpgplot-20121203-0635285558.html)

3.4. Relative level of Promoter 1B and 1C expression in A549, DMS79 and HEK cell lines after 5-aza treatment.

Once it was confirmed that promoters 1B and 1C contained possible CpG islands, cell lines were treated with 0.5, 1 and 5 μmol/l of the de-methylating agent, 5-aza, for 72 hours. The control was treated with the vehicle, glacial acetic acid, for 72 hours. qPCR analyses were performed with all data normalised to the reference gene β-actin.

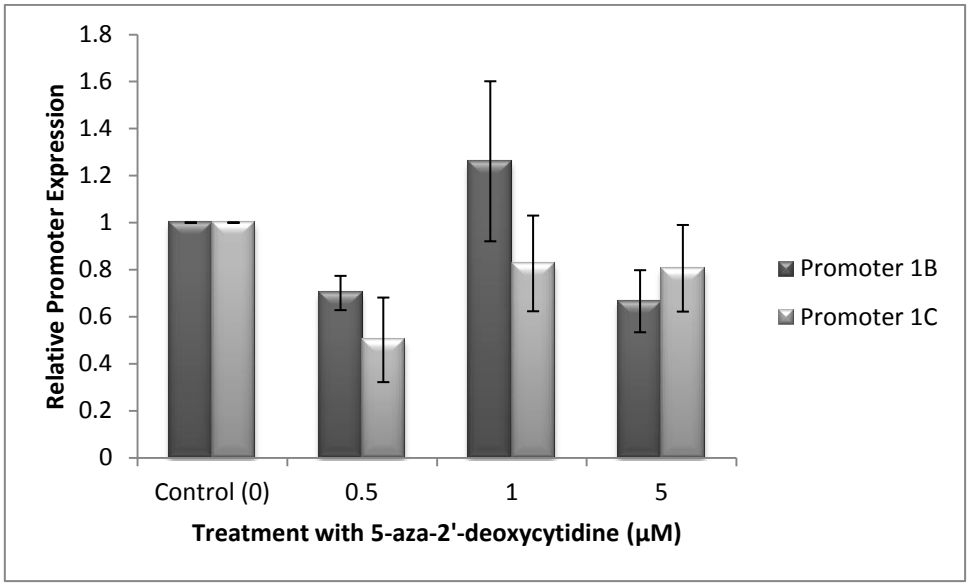

Figure 3.4: Relative promoter 1B and 1C expression in A549 cells treated with varying concentrations of 5-aza and control cells with mean ± standard error (n=6; Promoter 1B and 1C expression: $p>0.05$)

In A549 cells, treatment with 5-aza appeared to have little or no effect on promoter expression. Cells treated with 1 µmol/l 5-aza showed a slight increase in promoter 1B expression however this expression was not statistically significant ($F = 2.882$; $p>0.05$). Promoter 1C expression in 5-aza treated cells appeared diminished compared to the control cells but not statistical significantly so ($F = 1.715$; $p>0.05$) (Figure 3.4).

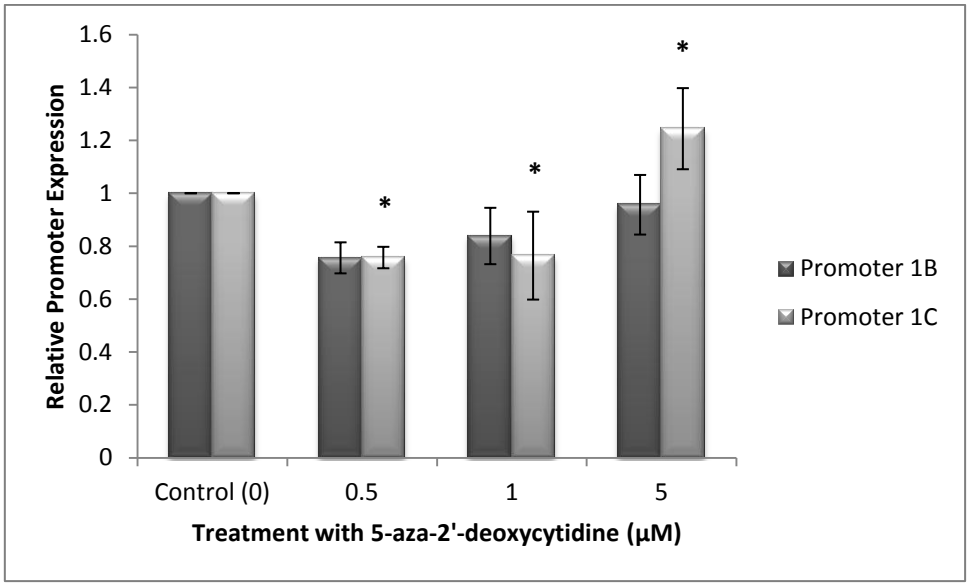

Figure 3.5: Relative promoter 1B and 1C expression in HEK control cells and cells treated with varying concentrations of 5-aza with mean ± standard error (n=6; promoter 1B expression: $p>0.05$; significant promoter 1C expression: $p<0.05$; *promoter 1C expression was significant between 5-aza treatments: $p<0.05$)

Promoter 1B transcript expression in all 5-aza treated HEK cells showed a slight reduction when compared to the control cells however this difference did not reach significance(F = 2.264, $p>0.05$). Promoter 1C transcript expression was significantly affected by 5-aza exposure (F = 3.983, $p<0.05$) where treatment with 0.5 and 1 µmol/l 5-aza decreased promoter 1C transcripts in HEK cells while 5 µmol/l 5-aza treated cells displayed a slight increase in promoter 1C transcript expression when compared to control (*$p<0.05$) (Figure 3.5).

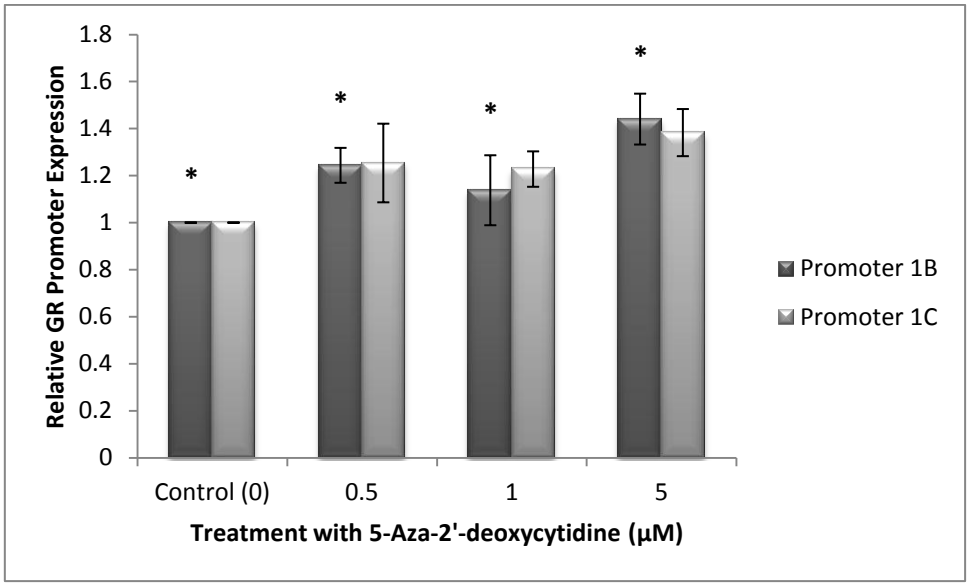

Figure 3.6: Relative promoter 1B and 1C expression in DMS79 control and 5-aza treated cells with mean ± standard error (n=6; promoter 1B expression: *p<0.05; promoter 1C expression: p >0.05)

Treatment of DMS79 cells with all concentrations of 5-aza appeared to increase the level of promoter 1B and 1C transcripts. While the level of promoter 1C was not significantly different from the control (F = 2.219, p>0.05), all 5-aza concentrations significantly increased expression of promoter 1B transcripts (F = 4.763, p<0.05). These data suggest that promoter 1B is responsive to the de-methylation agent and that promoter 1B may be methylated in DMS79 cells (Figure 3.6).

Identification of the Glucocorticoid Receptor component able to induce apoptosis in SCLC and control cell lines

Over-expression of the GR both *in vitro* and *in vivo* has been shown to induce apoptosis of DMS79 but not HEK cells (Sommer *et al.,* 2007). In this section, we attempt to determine which domain of the GR is necessary for apoptotic induction.

3.5. Digestion of Plasmids

Five plasmids were eluted representing wild-type and different GR mutants as well as a control plasmid (pFUNC1-eYFP, pFUNC1-GR-eYFP, pFUNC1-GRA458T-eYFP, pFUNC1-GRΔAF1-

eYFP and pFUNC1-GRC736S-eYFP). The plasmids were transformed into DH5α competent cells. Clones were picked and allowed to grow in LB broth and the plasmid DNA was extracted using QIAGEN mini-prep kit. To verify that the selected clones contained the specific insert, 1μg of purified DNA was digested with BglII restriction enzyme. Digestion with BglII would yield a 555bp fragment that was representative of the AF1 transactivation domain of the GR gene. The pFUNC1-GRΔAF1-eYFP is a mutant plasmid that has the AF1 region already deleted therefore verification of the insert being present was the evidence of all other fragments besides the 555bp fragment being present. The digested samples were run on a 1% agarose gel.

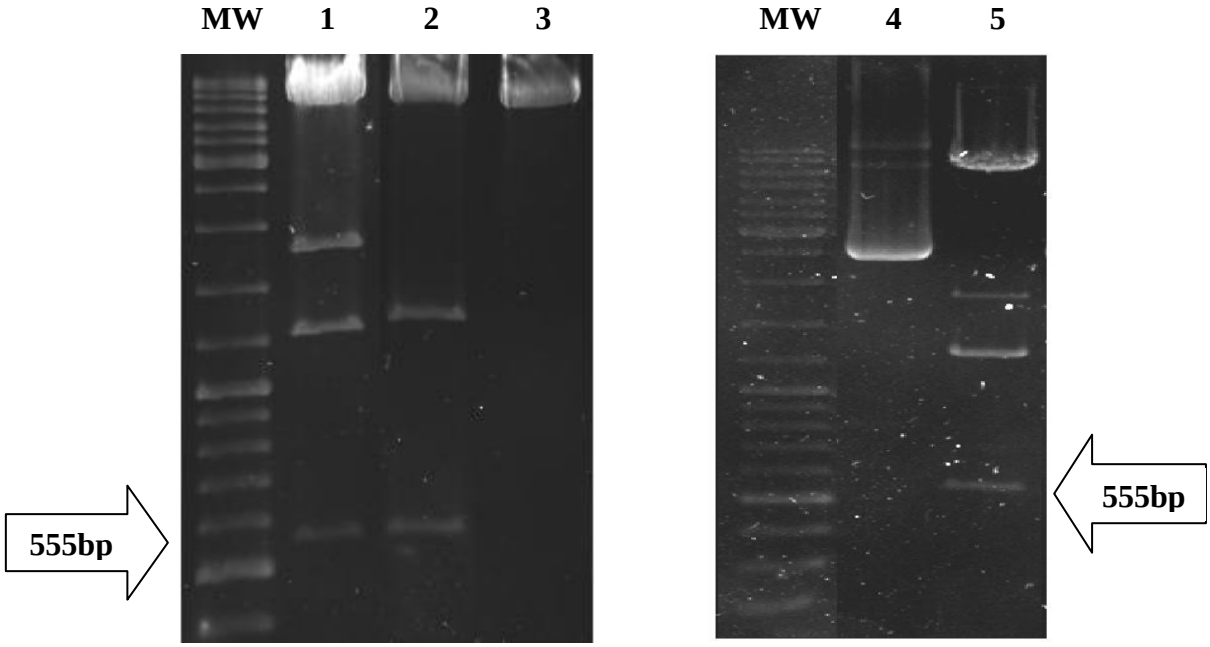

Figure 3.7: Agarose gel image of restriction digest of pFUNC1-GRC736S-eYFP, pFUNC1-GRA458T-eYFP, pFUNC1-eYFP, pFUNC1-GRΔAF1-eYFP and pFUNC1-GR-eYFP plasmids with BglII restriction enzyme. MW – O'GeneRuler™ DNA Ladder molecular marker; 1 - pFUNC1-GRC736S-eYFP; 2 - pFUNC1-GRA458T-eYFP; 3 - pFUNC1-eYFP; 4 – pFUNC1-GRΔAF1-eYFP; 5 – pFUNC1-GR-eYFP

The pFUNC1-eYFP plasmid has only 1 BglII restriction site which cuts the circular plasmid into a linear plasmid therefore a single band is present (lane 3; Figure 3.7). Plasmid constructs of pFUNC1-GRC736S-eYFP, pFUNC1-GRA458T-eYFP and pFUNC1-GR-eYFP had the 555bp fragment which codes for the AF1 region of the NTD. The first fragment at the top

indicates the total linear plasmid construct. For these plasmids there are three BglII restriction sites which create three possible combinations of BglII restriction sites for digestion of the plasmid DNA. This would result in the other bands present for pFUNC1-GRC736S-eYFP, pFUNC1-GRA458T-eYFP and pFUNC1-GR-eYFP digested products (lane 1, 2 and 5 respectively; Figure 3.7). Digestion of pFUNC1-GRΔAF1 DNA produced three fragments, whole linear plasmid and products of combination of two BglII restriction sites.

3.6. Transfection of HEK cells

To transfer of plasmids containing the different GR constructs into cells, transfection of cells with the plasmid-transfection reagent complex can be performed. HEK cells grow in a monolayer which allows for a dropwise addition of plasmid-transfection reagent complex to the culture. DMS79 cells, however, grow in suspension which makes them impossible to transfect. In order to transfer the plasmids into DMS79 cells, the plasmids must be assembled, using host cells and gag-pol and env vectors, into a retrovirus, to infect the cells. It is known that HEK cells transfect easily. Therefore, in order to test the plasmid vectors, HEK cells were transfected with plasmids using XtremeGENE transfection reagent for 24 hours. After infection cells were prepped for microscopy.

A **B**

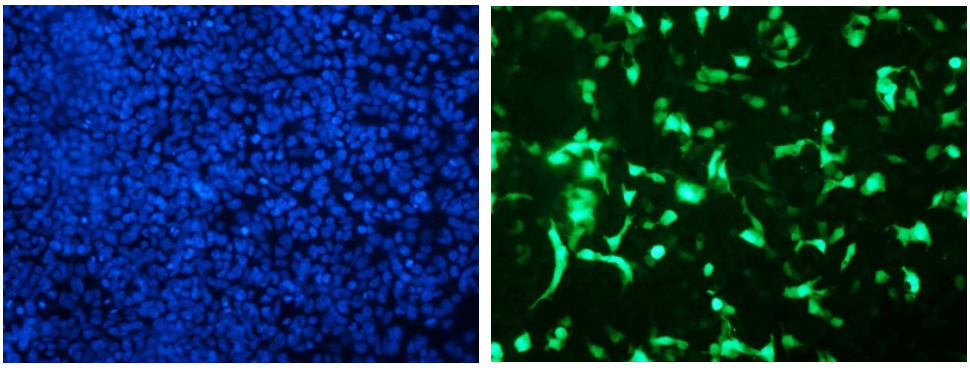

Figure 3.8: Fluorescent images of HEK cells transfected with plasmid, pFUNC1-eYFP, viewed at 20x magnification. (A) HEK cells stained with DAPI and (B) HEK cells expressing eYFP

A successfully transfected cell was indicated by the fluorescence of eYFP. In Figure 3.8, the nuclei of all cells in the field are stained with DAPI stain (A). eYFP fluorescence is shown in B where highly eYFP expressing cells are seen. Under the microscope, all cells were seen to express the eYFP marker. This is not particularly evident in the printed Figure 3.8 therefore the original images are supplied on the attached CD. Thus, transfection of HEK cells with plasmid yielded 100% efficiency; this was evident by the presence of eYFP fluorescence using the FITC filter. The transfected HEK cells served as a control to determine infection and spin-infection efficiency.

A **B**

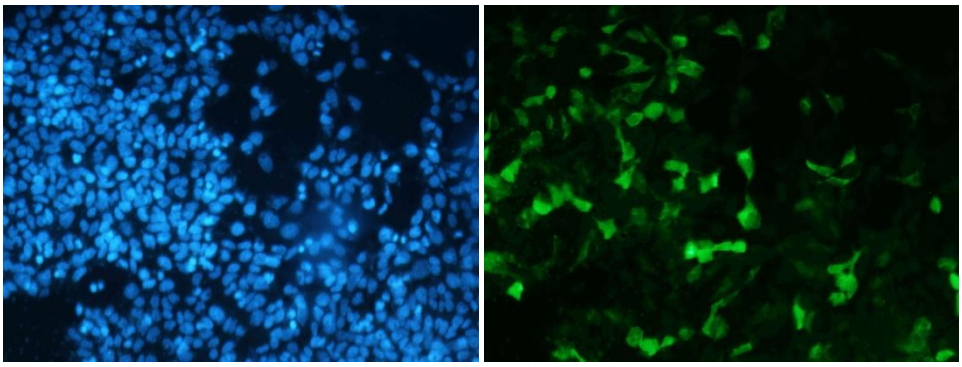

Figure 3.9: Fluorescent images of HEK cells transfected with pFUNC1-GR-eYFP viewed at 20x magnification. (A) HEK cells stained with DAPI and (B) HEK cells expressing eYFP

In Figure 3.9, cells were transfected with the pFUNC1-GR-eYFP fusion construct. Nuclei stained with DAPI are seen in A while the expression of pFUNC1-GR-eYFP is seen in B. Overall fluorescence is lower than the eYFP alone (Figure 3.8) as the pFUNC1-GR-eYFP is a large fusion protein. Once again, all cells expressed pFUNC1-GR-eYFP as evident by eYFP fluorescence (original images are supplied on the attached CD).

3.7. Retroviral Infection

HEK cells were infected with retroviral supernatant as described in section 2.12.1. The HEK cells were prepared for microscopy and viewed using the FITC channel for eYFP positive cells (Figure 3.10). This was performed to check whether cells can be infected with retroviral

supernatant containing eYFP plasmid. The pFUNC1-eYFP plasmid was used as it was the smallest of the five plamid constructs.

Transfection efficiency (Figure 3.8) was very high and it was estimated that all cells were transfected. Infection of cells with plasmid constructs was significantly less successful. After infection, very few cells exhibited eYFP fluorescence upon microscopic analysis (Figure 3.10). This could have been further compounded by the absence of hexadimethrine bromide (polybrene). Polybrene is a polycation used to transfect mammalian cells with DNA, increasing the efficiency of infections or transfection (Sigma-Aldrich product information sheet) and was used in all further infection experiments.

A **B**

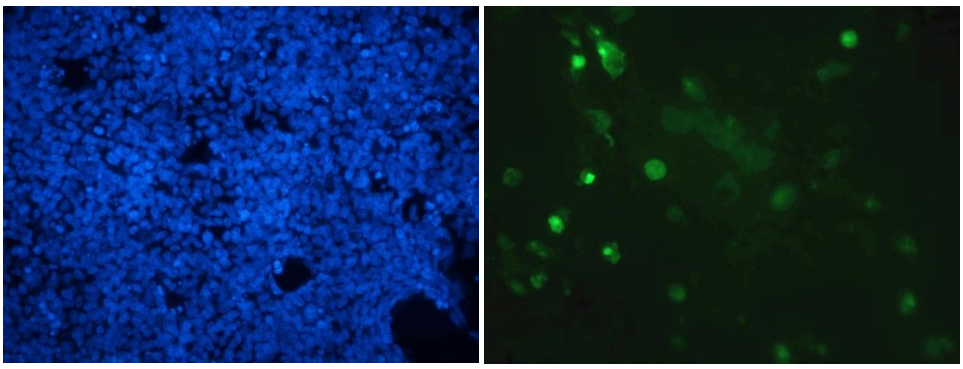

Figure 3.10: Fluorescent images of HEK cells infected with retroviral supernatant containing pFUNC1-eYFP viewed at 20x magnification. (A) HEK cells stained with DAPI (B) HEK cells expression pFUNC1-eYFP construct (Original image on attached CD)

3.8. Spin-infection Efficiency

As infections were less successful than transfections, we determined the infection efficiency. To do this, it was assumed that transfection resulted in 100% success. The control HEK cells were transfected with the five plasmids and infected with retroviral supernatant while DMS79 cells were spin-infected with retroviral supernatant in the presence of hexadimethrine bromide for 72 hours. qPCR analyses were performed to quantify the relative eYFP expression in transfected, infected and spin-infected cells.

Transfected, infected and spin-infected qPCR data were normalised to the reference gene β-actin. For qPCR analyses, transfected HEK cells served as the control with the fold expression values set to 100%. Infected HEK cells had a very low eYFP expression when compared to the control. DMS79 cells spin-infected with retroviral constructs had minimal expression of eYFP when compared to the control (Table 3.1).

Table 3.1: Relative eYFP expression in transfected and infected HEK cells and spin-infected DMS79 cells.

GR Constructs	eYFP Expression (%)		
	Transfected HEK	**Infected HEK**	**Spin-infected DMS79**
pFUNC1-eYFP	100	54	0.6
pFUNC1-GR-eYFP	100	1.7	0.7
pFUNC1-GRA458T-eYFP	100	1.5	0.2
pFUNC1-GRC736S-eYFP	100	0.6	0.3
pFUNC1-GRΔAF1-eYFP	100	130	6.6

eYFP expression was seen in infected HEK and spin-infected DMS79 cells expressing pFUNC1-eYFP, pFUNC1-GR-eYFP, pFUNC1-GRA458T-eYFP and pFUNC1-GRC736S-eYFP (Table 3.1). The best infection efficiencies were observed in HEK cells infected with pFUNC1-eYFP (54%) and pFUNC1-GRΔAF1 (130%) (Table 3.1).

DMS79 cells spin-infected with pFUNC1-eYFP, pFUNC1-GR-eYFP, pFUNC1-GRA458T-eYFP and pFUNC1-GRC736S-eYFP retroviral constructs had extremely low spin-infection efficiencies, less than 1%. pFUNC1-GRΔAF1-eYFP expression in DMS79 cells showed the highest spin-infection efficiency with 6.6% (Table 3.1).

3.9. Microscopic Analysis of Apoptosis and Cell Death

To determine the ability of these different GR constructs to induce apoptosis in DMS79 cells, the cells were spin-infected with the different constructs. HEK cells were infected with retroviral supernatant and served as the control. Cells were prepared for microscopic analysis.

The cells were stained with DAPI; which has an affinity for nuclear material; PI; stains dead cells; and Annexin V APC; stains apoptotic cells. As infection rates were shown to be low, cells were checked for eYFP fluorescence indicating the presence of virus constructs. Cells were counted for Annexin V APC, PI, DAPI and eYFP fluorescence (Figure 3.11 and Figure 3.16).

This experiment consisted of two biological repeats for each cell line with sample size of 200 cells. There were five treatments and a control for each cell line. The control comprised untreated cells while the treatments comprised of the control virus; pFUNC1-eYFP; the wild-type GR expressing virus; pFUNC1-GR-eYFP; the DNA binding mutant virus; pFUNC1-GRA458T-eYFP; the transactivation mutant virus; pFUNC1-GRΔAF1-eYFP or the ligand binding mutant virus; pFUNC1-GRC736S-eYFP.

In Figure 3.11, HEK cells expressing the pFUNC1-GRC736S-eYFP virus were used as a representative image of confocal microscopic analysis while Figure 3.16 shows DMS79 cells infected with pFUNC1-GR-eYFP as a representative image.

3.9.1 Microscopic analysis of apoptosis and cell death in HEK cells

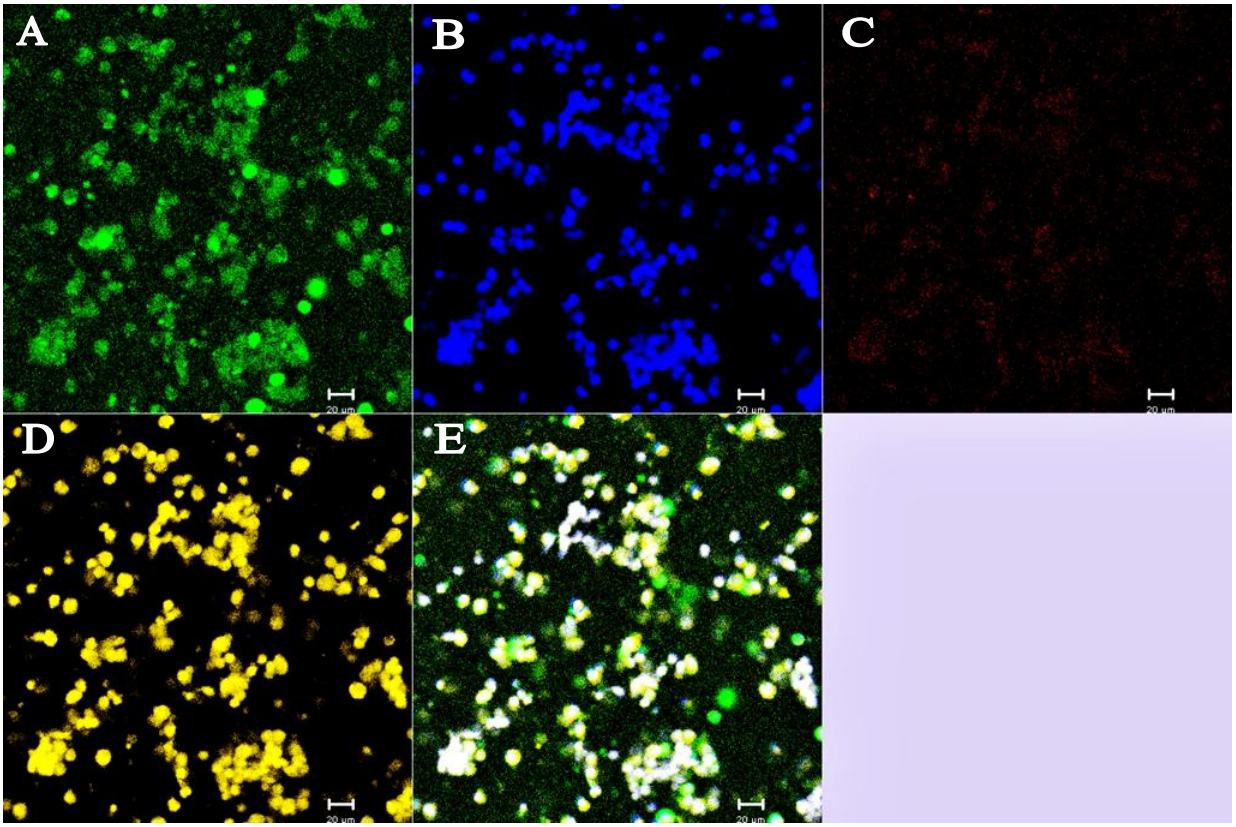

Figure 3.11: Confocal image of HEK cells infected with pFUNC1-GRC736S-eYFP viewed at 25x magnification. A – eYFP fluorescence; B – DAPI fluorescence; C – Annexin V APC; D – PI; E – Merged image of A, B, C and D (Original image on supplied CD).

Panel A – E is a representative image of the field of view used to count 200 cells per treatment (Figure 3.11); images were captured and merged using Zen 2010 imaging software. In panel A cells were viewed using FITC channel (488nm) that fluoresces cells expressing eYFP. Fluorescence of eYFP indicated a positive cell uptake of retrovirus containing construct. Panel B was viewed with a UV channel (405nm) for fluorescence of the DAPI stain enabling visualisation of all cells in the field of view. Cells that had undergone apoptosis would have taken up the Annexin V APC stain. Positive APC cells would fluoresce when the red laser (633nm) was used (Panel C). At the time of fixing, any cells that were dead would have taken up the PI stain (488nm) (Panel D). Panel E is a merged image of all five panels. This image is included on the attached CD.

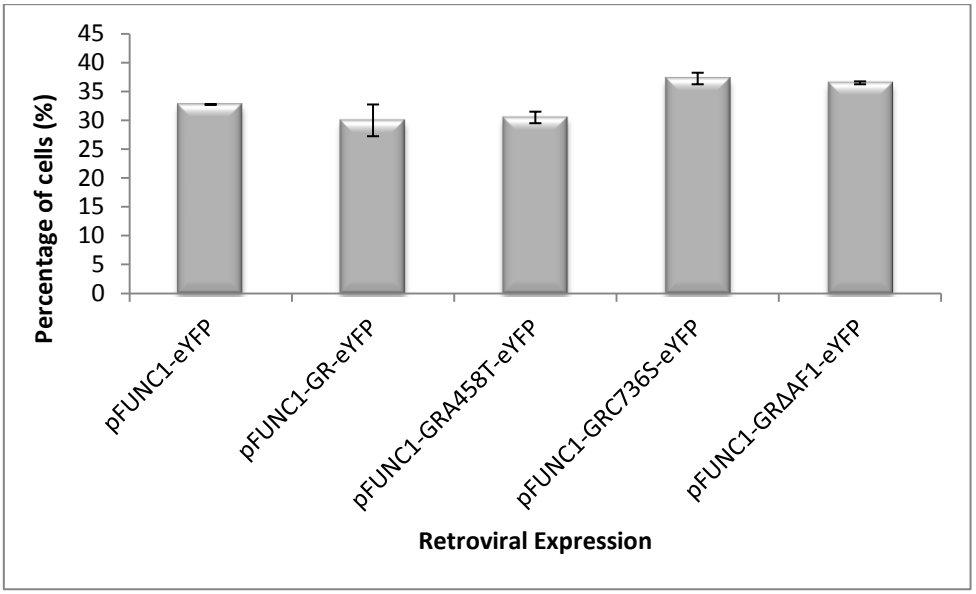

Figure 3.12: Percentage of HEK cells expressing eYFP fluorescence (mean ± standard error)

HEK cells expressing the different retroviral constructs will express the eYFP, the control cells were not infected with plasmid therefore had zero percent of eYFP fluorescence and were excluded from the graph (Figure 3.12). When eYFP expression was compared between treatments there was no statistical significance as the percentage of positive infected cells ranged between 30 to 37%. These infection rates were higher than previously shown (Table 3.1). This may be due to the increased efficiency of the technique after repetition or the different method of assessing infection. Since eYFP expression was similar across the treatments, comparison between treatments were possible.

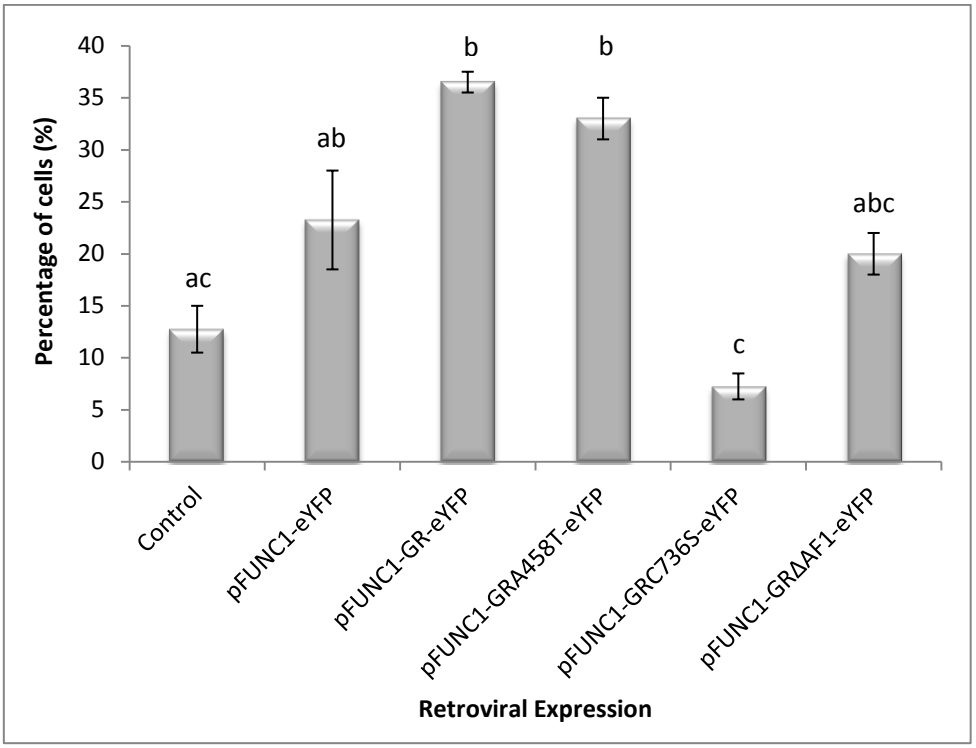

Figure 3.13: Percentage of HEK cells stained with Annexin V APC with mean ± standard error (Dissimilar characters denote statistical significance between treatment) (ANOVA: $p < 0.05$; $F = 20.106$)

Twelve percent of untreated, control cells were undergoing apoptosis as indicated by Annexin V APC staining. The empty virus, pFUNC1-eYFP, had 22% positive Annexin V APC stained cells. Thirty seven percent of pFUNC1-GR-eYFP virus expressing cells were undergoing apoptosis as evidenced by the Annexin V APC stain. pFUNC1-GRA458T-eYFP virus expressing cells had 32% Annexin V APC positive cells. The ligand binding mutant, pFUNC1-GRC736S-eYFP had 7% Annexin V APC positive cells. The percentage of Annexin V APC positive cells in pFUNC1-GR-eYFP and pFUNC1-GRA458T-eYFP was statistically significant when compared to the control (Figure 3.13). The low percentage of apoptotic pFUNC1-GRC736S-eYFP cells was statistically significant when compared to pFUNC1-eYFP, pFUNC1-GR-eYFP and pFUNC1-GRA458T-eYFP. The number of pFUNC1-GRΔAF1-eYFP apoptotic positive cells was not statistically significant when compared to the control and other treatments. In terms of apoptotic cells, cells infected with pFUNC1-GRC736S-eYFP exhibited significantly low levels of apoptosis while those infected with pFUNC1-GR-eYFP showed the highest levels of apoptosis.

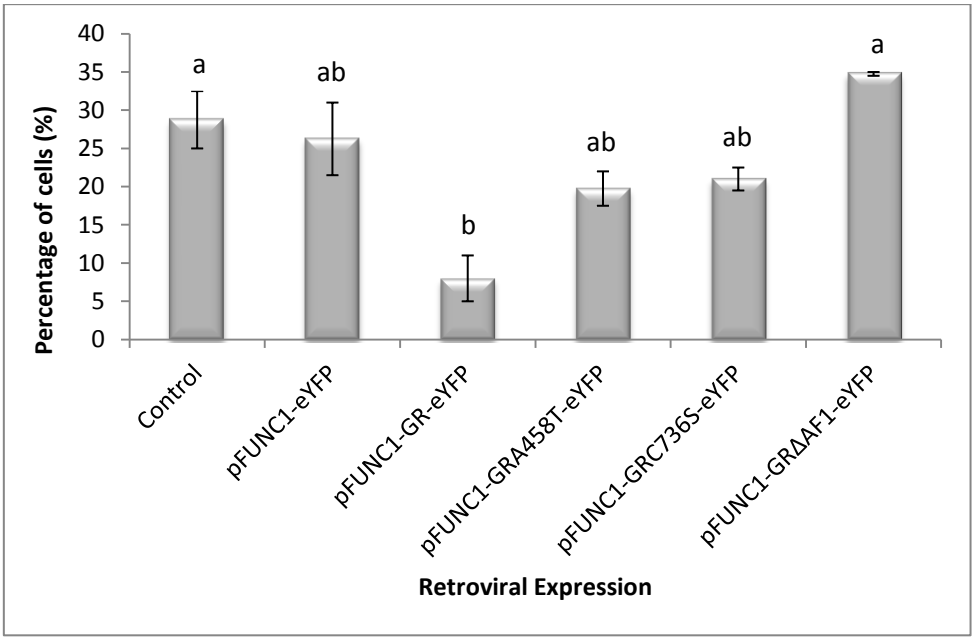

Figure 3.14: Percentage of HEK cells stained with PI with mean ± standard error (Dissimilar characters denote statistical significance between treatments) (ANOVA: $p<0.05$; $F = 9.537$)

Cells stained with PI indicate any dead cells (Figure 3.14). The untreated, control cells had 29% PI positive cells. The pFUNC1-eYFP expressing cells had 25% PI positive cells. 8% of pFUNC1-GR-eYFP cells were positive for PI. pFUNC1-GRA458T-eYFP and pFUNC1-GRC736S-eYFP had 20% dead cells evident by the PI stain. pFUNC1-GRΔAF1-eYFP virus expressing cells had 35% PI positive cells indicating the treatment with the highest percentage of dead cells. pFUNC1-GR-eYFP virus expressing cells had the least percentage of dead cells and was statistically significant when compared to the control and pFUNC1-GRΔAF1-eYFP treatment.

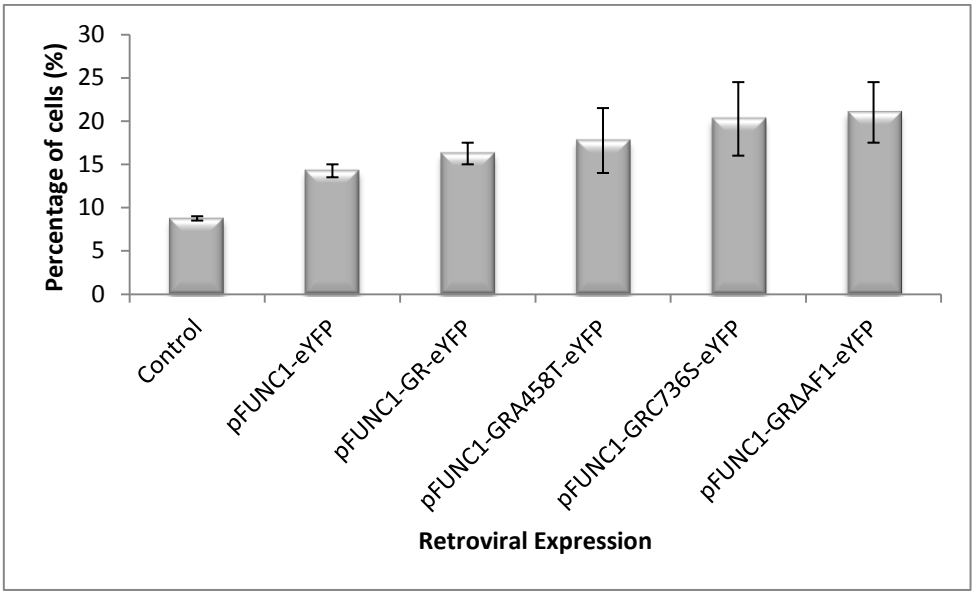

Figure 3.15: Percentage of HEK cells displaying chromatin condensation with mean ± standard error ($p>0.05$; $F = 2.602$)

Using panel B (Figure 3.11), HEK cells were analysed for chromatin condensation, as this is one of the indicators of apoptosis, where the chromatin starts to condense. Any cell that had unusual nuclear staining or fragmented nuclei was considered positive. Chromatin condensation was not statistically significant ($p>0.05$) among treatments and the control however a trend of increased chromatin condensation from the control to the various treatments was noticed. Control cells had the least percentage of chromatin condensation (8%), pFUNC1-eYFP virus expressing cells contained 5% more cells with condensed chromatin than the control. pFUNC1-GRΔAF1-eYFP had the highest percentage of chromatin condensation of 20% (Figure 3.15).

3.9.2. Microscopic analysis of apoptosis and cell death in DMS79 cells

In Figure 3.16, pFUNC1-GR-eYFP was used as a representative image of the field of view used to count 200 cells per treatment. Panel A shows cells that express eYFP protein. Panel B shows cells that are stained with DAPI. DAPI stains the chromatin material of the cells. Cells undergoing apoptosis would take up the Annexin V APC stain as shown in panel C. Dead cells take up the PI stain and were counted using panel D. Panel E is a merged image of panels A to D.

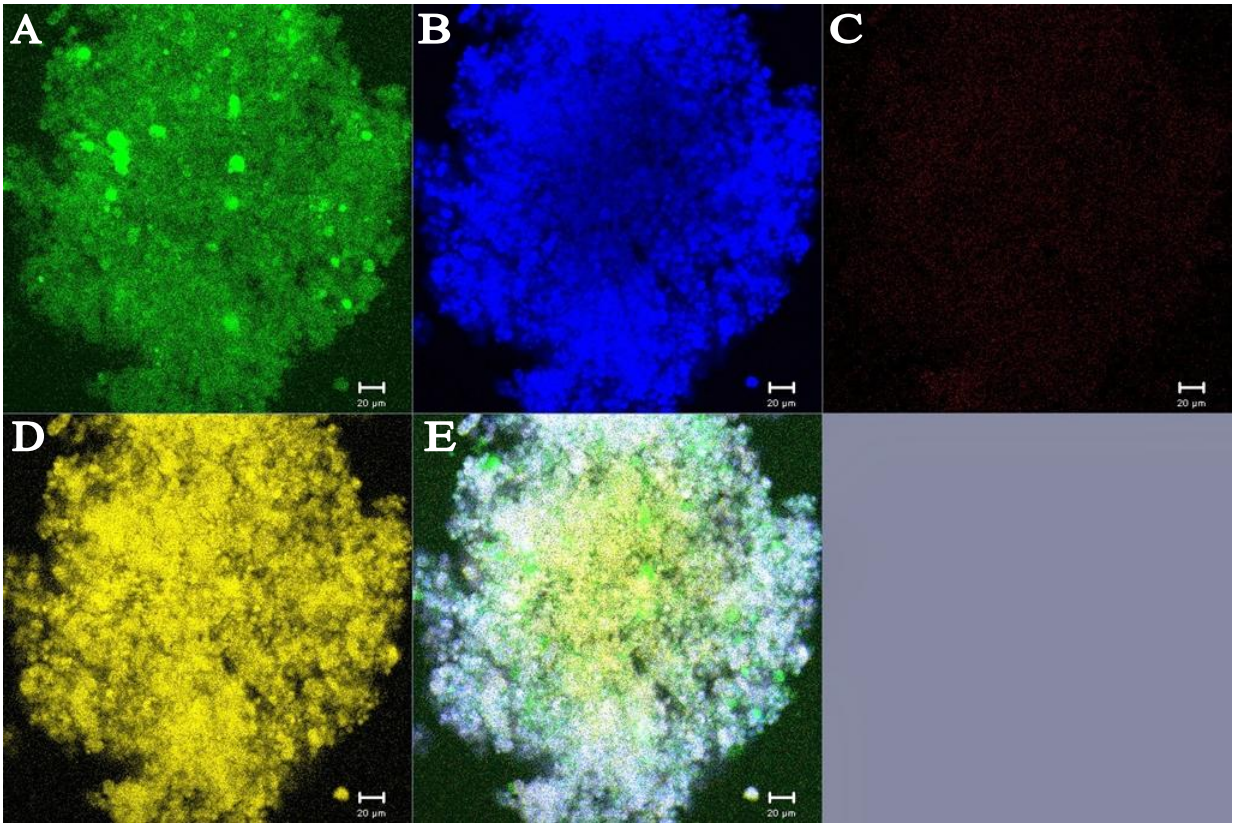

Figure 3.16: Confocal image of DMS79 cells infected with pFUNC1-GR-eYFP viewed at 25x magnification. A – eYFP fluorescence; B – DAPI fluorescence; C – Annexin V APC; D – PI; E – Merged image of A, B, C and D (Original image on supplied CD).

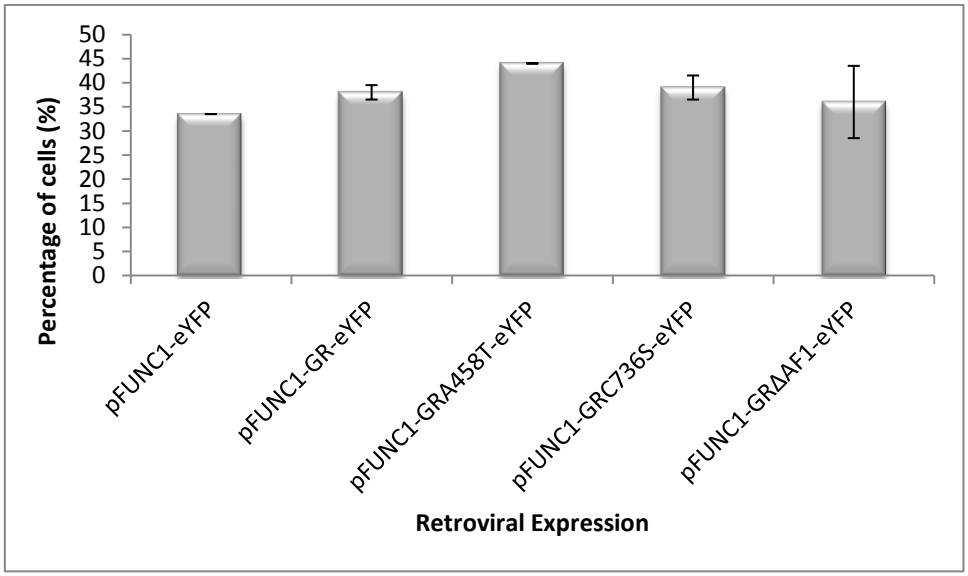

Figure 3.17: Percentage of DMS79 cells expressing eYFP fluorescence with mean ± standard error ($p>0.05$; $F = 0.759$)

The DMS79 untreated control cells were not spin-infected with a construct containing eYFP, therefore was excluded from the graph (Figure 3.17). eYFP expression is an indicator of the retroviral incorporation into the cells. The spin-infection of the retroviral constructs into DMS79 cells was similar among treatments therefore comparisons could be made between treatments. The percentage of eYFP positive cells ranged from 33% to 44% among treatments. The pFUNC1-GRA458T-eYFP infected cells contained the highest percentage of eYFP positive cells (44%). The least expressing eYFP treatment was the empty virus, pFUNC1-eYFP, at 33%. These infection rates are also comparable to the HEK cells.

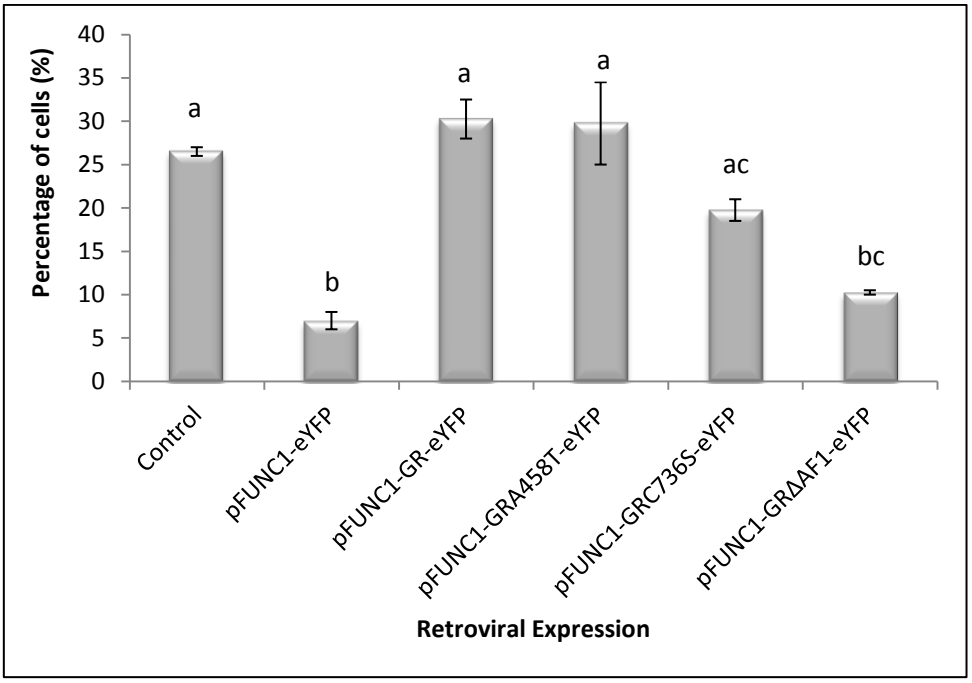

Figure 3.18: Percentage of DMS79 cells stained with Annexin V APC (mean with standard error (Dissimilar characters denote statistical significance between treatments; ANOVA: $p<0.05$, $F = 19.848$)

Surprisingly, 27% of DMS79 untreated, control cells were Annexin V APC positive. Cells expressing the control construct, the pFUNC1-eYFP virus only had 7% of infected cells positive for Annexin V APC. These results are contradictory and may be due to counting errors or errors in preparation of the control cells. Thirty percent of pFUNC1-GR-eYFP virus expressing cells was apoptotic while cells infected with pFUNC1-GRA458T-eYFP exhibited 29% apoptotic cells. pFUNC1-GRC736S-eYFP treatment had 20% Annexin V APC positive cells. Twelve percent of pFUNC1-GRΔAF1-eYFP virus expressing cells was apoptotic indicated by APC fluorescence (Panel C) (Figure 3.18 and Figure 3.16 respectively). The pFUNC1-eYFP treatment had the least percentage of apoptotic cells (7%) and was statistically significant when compared to the control, pFUNC1-GR-eYFP, pFUNC1GRA458T-eYFP and pFUNC1-GRC736S-eYFP. pFUNC1-GRΔAF1-eYFP treatment had the second lowest apoptotic population of cells (10%) and was statistically significant from the control, pFUNC1-GR-eYFP and pFUNC1-GRA458T-eYFP. The highest apoptotic population viewed was in cells expressing pFUNC1-GR-eYFP virus (30%).

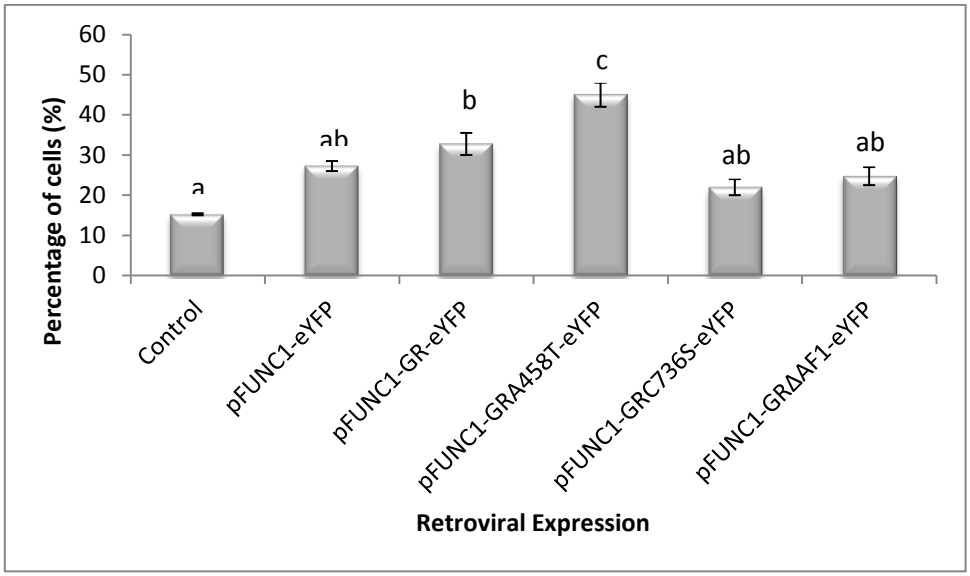

Figure 3.19: Percentage of DMS79 cells stained with PI with mean ± standard error (Dissimilar characters denote statistical significance between treatments) (ANOVA: $p<0.05$, $F = 22.947$)

Untreated DMS79 cells (control) had a percentage of 15 for PI stain uptake indicating dead cells. pFUNC1-eYFP virus expressing cells exhibited 28% cell death. pFUNC1-GR-eYFP virus expressing cells had 32% PI positive cells while 45% of the pFUNC1-GRA458T-eYFP population was positive for PI and 25% of pFUNC1-GRC736S-eYFP cells were dead. pFUNC1-GRΔAF1-eYFP virus expressing cells contained 27% PI positive cells. pFUNC1-GRA458T-eYFP had the highest population of dead cells and was statistically significant when compared to percentage of PI positive cells in control and other treatments ($p<0.05$). PI positive cells in pFUNC1-GR-eYFP treatment were statistically significant from percentage of PI positive cells in control, DMS79 cells. As expected, the control had the lowest percentage of dead cells (Figure 3.19).

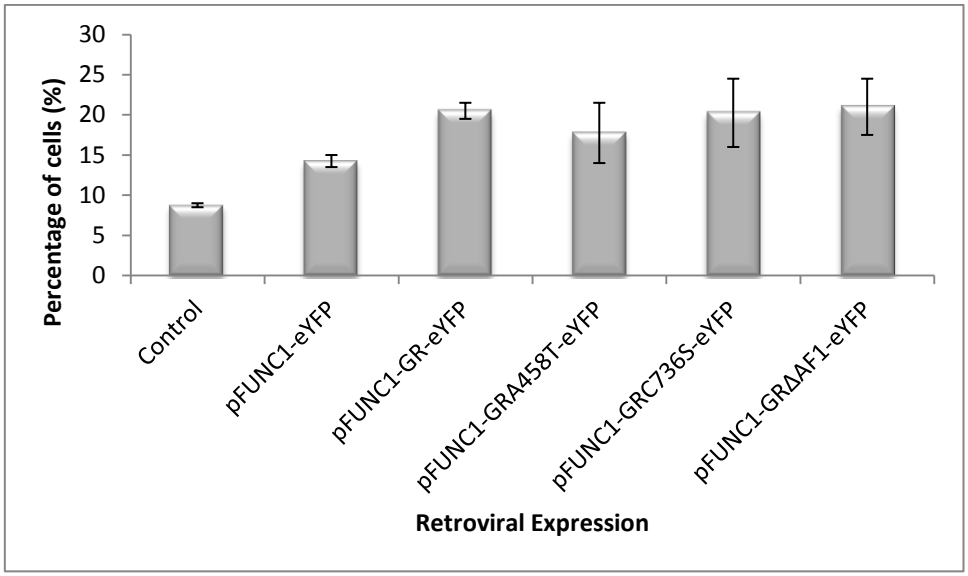

Figure 3.20: Percentage of DMS79 cells displaying chromatin condensation (mean ± standard error) ($p>0.05$; $F = 2.999$)

The percentage of chromatin condensation among the treatments and control was not statistically significant ($p>0.05$). Control cells had the least percentage of noticeable chromatin condensation (8%). The highest percentage of chromatin condensation was recorded in pFUNC1-GRA458T-eYFP virus expressing cells with 22%. There is a general though non-significant thread of increased condensation in spin-infection with all constructs (Figure 3.20).

4. Discussion

Lung cancer is considered the most common cancer worldwide (Panani and Roussous, 2006) and the second most common cause of death in the western world (Hopkins-Donaldson *et al*., 2003). It can be categorised into two types; non-SCLC and SCLC. SCLC cancer comprises 20% of all lung cancer cases and is an aggressive tumour (Simon and Wagner, 2003; Jackman and Johnson, 2005; Panani and Roussous, 2006). SCLC cells are derived from neuro-endocrine cells present in the bronchoepithelium (Hopkins and Donaldson *et al*., 2003) and produce the neuropeptide, POMC, a precursor of ACTH (Ray *et al*., 1994; 1996; Jackman and Johnson, 2005). ACTH is responsible for the production of the steroid hormone, GC. The secreted GC hormone then inhibits the production of ACTH by the HPA axis through a negative feedback system (Munck *et al*., 1984; Ray *et al*., 1994; 1996). The ectopic secretion of ACTH by SCLC cells creates an ACTH syndrome that does not respond to the negative feedback system of the HPA axis (Ray *et al*., 1994; 1996). However, SCLC cells are insensitive to the GC stimulus to halt ACTH production (Ray *et al*., 1994; 1996). The GC hormone's action is mediated through the GR (Munck *et al*., 1984; Duma *et al*., 2006; O'Connor *et al*., 2000; Tsigos and Chrousos, 2002; Nicolaides *et al*., 2010; Kassi and Moutsatsou, 2011).

In 2007, a study by Sommer and colleagues showed that SCLC cells express negligible levels of GR, conferring GC insensitivity to the cells. This led to the investigation of the effects of restoration of GR expression by inducing an over-expression of the GR through retroviral infection of SCLC cells (Sommer *et al*., 2007). Restoration of exogenous GR expression in SCLC cells allowed for restored GC sensitivity in SCLC cells and resulted in apoptosis of the cells. According to Sommer *et al*. (2007) it was believed that SCLC cells choose to have a reduced expression of the GR to ensure their immortality.

The mechanism utilised by SCLC cells for the reduction of GR expression is not known. Cancer cells usually alter/silence the expression of tumour suppressor genes to favour their longevity (Jones and Laird, 1999; Baylin *et al*., 2004). It can be postulated that SCLC cells deem the GR to possess tumour suppressor behaviour as its expression results in cell death. Therefore, the cancer would prefer to silence or reduce GR expression. Many cancer cells choose to silence unfavourable genes by an epigenetic mechanism known as methylation (Jones and Laird, 1999;

Baylin *et al*., 2004; Turner *et al*., 2010). Methylation occurs when a methyl group is added to a cytosine present in a region of high guanine-cytosine content (CpG islands) (Baylin *et al*., 2004). The GR gene has a 5'UTR that contains a host of alternative first exons that serve as promoter regions (Turner *et al*., 2006; 2010; Alt *et al*., 2010, Kassi and Moutsatsou, 2011). These promoter regions house CpG islands which have the potential to be methylated (Cao-Lei *et al*., 2011). A recent study by Kay *et al*. (2011) has shown that the GR in SCLC cells is methylated and treatment with a de-methylating agent resulted in re-expression of the GR.

The first aim of this study was to determine the GR promoter/s utilised by SCLC cells when re-expression was induced using a de-methylating agent (5-aza).

4.1. Glucocorticoid Promoter Usage in SCLC cells and Control Cells

4.1.1. Identification of promoters utilised by A549, HEK and DMS79 cells

Conventional PCR was performed to determine the promoters usually utilised by the A549, HEK and DMS79 cell lines. The A549 cell line was derived from a human lung adenocarcinoma (Foster *et al*., 1998) and the DMS79 cell line was derived from lung carcinoma. The HEK cell line was derived from human embryonic kidney epithelial cells. It was determined that all three cell lines contained promoter 1B and 1C transcripts (Figure 3.2). A study by Nunez and Vedeckis (2002) showed that promoter 1B and 1C expression was essential for the ubiquitous expression of the human GR receptor. Promoters 1B and 1C transcripts have been shown to be co-expressed in many tissues including the brain, cerebellum, spinal cord, heart, trachea, lung, kidney and placenta (Nunez and Vedeckis, 2002). A study by Turner and Muller (2005) had shown that lung tissue only expressed promoters 1B and 1C; however, in this study in addition to these promoters, transcripts of promoters 1F and 1J were also present. Promoter 1F has been shown to be only expressed in the hippocampus and immune system while promoter 1E was absent in all three cell lines and according to Turner *et al*. (2005; 2006), its expression is specific for hippocampus and immune system. Promoter 1D expression is also thought to be specific for the hippocampus (Turner *et al*., 2005; 2006) which supports the absence of promoter 1D transcript in the three cell lines. The HEK cell line was the only cell line to express the 1H transcript which has been previously shown to be present in the mouse

kidney, validating these results (Bockmühl *et al*., 2011). Promoter 1H is highly conserved between rat, mouse and human (Bockmühl *et al*., 2011).

4.1.2. Relative level of Promoter 1B and 1C expression in A549, DMS79 and HEK cell lines after 5-aza treatment

Since promoters 1B and 1C were the most abundant transcripts present in the three cell lines, bioinformatic analysis was performed to determine whether these promoters contain possible CpG islands (Figure 3.3). Bioinformatic analysis produced three potential CpG islands. Two of these CpG islands were identified in the region coding for promoter 1B and promoter 1C. The identification of the potential CpG islands suggested that the promoters had the potential to be methylated; this could be confirmed by the use of a de-meythlating treatment, 5-aza.

In the A549 cell line there was a noticeable, but not significant, decrease in transcript levels of both promoter 1B and 1C (except for 1 μmol/l treatment of promoter 1B) (Figure 3.4.). In a study by Yuan *et al*. (2004) has shown A549 cells to be responsive to 1 μmol/l 5-aza treatment but to only have a marginal increase in the target gene, tyrosine protein kinase ABL2 expression. The relative, but not significant, decrease in promoter transcripts for the three 5-aza treatments could possibly be due to the cytotoxicity of the de-methylating agent. 5-Aza treatment has been known to inhibit cell growth, cell cycle arrest and apoptosis during treatment (Yuan *et al*., 2004; Palii *et al*., 2008). 5-Aza-containing DNA forms covalent DNMT-DNA adducts that lead to DNA damage and cytotoxicty where activation of G_1 checkpoint regulator p53 inhibits cell proliferation (Palii *et al*., 2008). This cytotoxic effect could result in reduced cell population and result in decreased promoter transcripts as observed in A549 treated cells (Figure 3.4). It was concluded that the GR promoters are not methylated in A549 cells and this was expected as A549 cells express abundant GR protein (Greenberg *et al*., 2002). Since the GR is highly expressed there should be no or little methylation markers present in the GR gene and Kay *et al*. (2011) showed that A549 cells had only two methylated CpG dinucleotides in promoter 1C region. Therefore treatment of A549 cells with 5-aza does not govern drastic increase in promoter transcript expression as there is very little methylation within the GR gene in these cells. De-methylation of these CpG dinucleotides has no effect on transcriptional activity of the GR in A549 cells. Thus, the A549 cells are appropriate controls for this study.

HEK cells showed a significant increase in promoter 1C transcripts when treated with 5 μmol/l 5-aza (Figure 3.5). This indicates that promoter 1C may be methylated in HEK cells. Promoter 1C alone may be considered as constitutive in GR expression (Cao-Lei *et al*., 2011) and perhaps is the main promoter used for GR expression in HEK cells. According to the study by Kay *et al*. (2011), the HEK cell line possessed seven methylated CpG dinucleotides in the promoter 1C region. However, in the Kay *et al*. (2011) study, when HEK cells were treated with 5 μmol/l 5-aza there was no drastic increase in total GR expression. However, Kay *et al*. (2011) did not look at relative promoter usage and only looked at total GR expression. Promoter 1B expression decreased upon 5-aza treatment however 5 μmol/l 5-aza expression was similar to the control. It may be possible that promoter 1B alone is not able to constitutively regulate GR expression (Nunez and Vedeckis, 2002) which would support the notion of promoter 1B not being methylated at the basal state. The reduced expression of promoter transcripts in 0.5 and 1 μmol/l 5-aza treatments might be due to the cytotoxic effects of DMNT-DNA adducts which results in DNA damage, therefore, resulting in fewer promoter 1B and 1C transcripts being present (Palii *et al*., 2008).

When promoter 1B and promoter 1C transcripts are compared in untreated cells (Figure 3.2.B), it appears the level of promoter 1B and promoter 1C transcripts are relatively the same which could indicate that HEK uses a co-expression of both promoters for GR expression. Nunez and Vedeckis (2002) investigated promoter utilisation of promoter 1B and promoter 1C in several cultured human cell lines. Cells were transiently infected with luciferase reporter constructs of promoter 1B and 1C together, promoter 1B and promoter 1Cm33. It was shown that differences in transcriptional activity from promoters 1B and 1C depended on the type of cell. Some cell types tended to use both promoters for a significant transcriptional activity while other cell types appeared to favour one promoter for transcriptional activity (Nunez and Vedeckis, 2002). In our study, only promoter 1C appears to be methylated in HEK cells. Kay *et al*. (2011) showed that 5-aza has no effect on overall GR expression. While we have shown that promoter 1C in HEK cells is sensitive to 5-aza and thus methylated, the expression of unmethylated promoter 1B may render total GR re-expression insensitive to 5-aza effects.

The DMS79 cells showed an increased in both promoter 1B and promoter 1C transcripts with increasing 5-aza concentrations (Figure 3.6). Promoter 1B transcript levels were significantly greater when compared to the control, with 5 μmol/l 5-aza treated DMS79 cells having the most

promoter 1B transcripts. It appears that promoter 1B may be methylated in DMS79 cells however when Kay and colleagues (2011) determined the methylation status of promoter 1B and promoter 1C in DMS79 cells, no methylation of promoter 1B was detected in DMS79 cells. However, the promoter 1B region analysed by Kay *et al*. (2011) does not correlate with the map of the promoter 1B region used in the Turner and Muller (2005) and this study and considering that the bioinformatic analysis suggests the presence of a CpG island in the promoter 1B region, methylation is possible. Promoter 1C transcript levels increased with increasing 5-aza concentration however were not statistically significant from the control (Figure 3.6). According to Kay *et al*. (2011) promoter 1C possessed 12 methylated CpG dinucleotides. Since both promoter 1B and promoter 1C transcript levels increased with de-methylation treatment, it would suggest that co-expression of these promoters is required to enhance GR transcriptional activity (Nunez and Vedeckis, 2002). When a comparison is made between the qPCR results (Figure 3.6) and normal promoter expression in DMS79 cells (Figure 3.2.C), there were relatively low levels of promoter 1B and 1C transcripts. This supports the hypothesis that both promoters appear to be methylated resulting in low levels of transcripts and upon de-methylation there appears to be an increase in transcript levels. Kay *et al*. (2011) showed that the GR protein expression was correlated with the percentage of methylation where with increasing percentage of methylation, there was decreased expression of the GR protein. Thus it could be concluded that the reduced GR expression exhibited by DMS79 cells maybe due to the methylation of its promoter region. Kay *et al*. (2011) did show re-expression of the GR following 5-aza treatment and they did show methylation in promoter 1C however they did not explicitly show that promoter 1C is responsible for the re-expression. This study reported here suggests that promoter 1B is potentially methylated in regions not analysed by Kay *et al*. (2011) and that promoter 1B and possibly promoter 1C are responsible for GR re-expression following 5-aza treatment. Retrospective analysis of these data (and others), in this study, revealed that the 5-aza used in these experiments had defrosted due to breakdown of the -80^{o}C freezer. 5-Aza is an unstable compound and it is probable that the aliquots used for these experiments had reduced activity. Repetition of this work with fresh 5-aza may reveal more significant difference in GR re-expression and promoter 1C re-expression levels may reach significance.

4.2. Apoptosis Induction

The GR protein structure is divided into three domains; the DNA binding domain (DBD), ligand binding domain (LBD) and N-terminal domain (NTD) (Figure 1.5). Each domain is responsible for a specific function during transcription (Kassi and Moutsatsou, 2011; Nicolaides *et al*., 2010). The DBD binds to specific palindromic DNA sequences, known as GREs, on genes that can either result in transactivation or transrepression of transcription process (Chen *et al*., 2008; Chivers *et al*., 2006; Hittelman *et al*., 1999; Vandevyver *et al*., 2012). The LBD is responsible for binding the GC ligand and mediating the GCs mode of action for transcription (Kumar and Thompson, 2005; Nicolaides *et al*., 2010). The NTD houses one of the major transactivation factors (AF1) that is responsible for binding of transcription factors and the transcription machinery and recruit either positive or negative GREs for the initiation transcription to occur (Kumar and Thompson, 2005; Hittelman *et al*., 1999; Duma *et al*., 2006; Garza *et al*., 2010; Schaaf and Cidlowski, 2003). Each of these domains contributes an important role that regulates the transcription factor behaviour of the GR.

A study by Sommer and colleagues (2007) showed that over-expression of the GR in SCLC cells restored GC sensitivity. This over-expression of the GR was shown to elicit apoptotic cell death in SCLC cells (Sommer *et al*., 2007). The addition of the GR ligand, the synthetic GC dexamethasone, did not appear to affect apoptotic cell death. However, the mechanism utilised by the GR protein to induce apoptosis in SCLC cells is still unknown. The second aim of this study was to identify which component of the GR is necessary to cause GC-induced apoptosis of the SCLC cells. SCLC cells (DMS79) were infected with retroviral supernatant containing an empty plasmid (pFUNC1-eYFP), wild-type GR (pFUNC1-GR-eYFP), a transactivation mutant (pFUNC1-GRΔAF1-eYFP), DNA binding mutant (pFUNC1-GRA458T-eYFP) and a ligand binging mutant (pFUNC1-GRC736S-eYFP) and the virus expressing cells were quantified for apoptosis and cell death by microscopic analysis.

4.2.1. Spin-infection efficiency of SCLC cells

DMS79 cells grow in suspension which makes it impossible to transfect them with plasmid constructs therefore retroviral constructs containing the genes of interest were required. HEK cells, in contrast, grow as a monolayer and transfect easily. Transfection of HEK cells yielded

100% expression of plasmid indicated by the presence of eYFP (Figures 3.8 and 3.9) and thus served as a control to quantify the efficiency of spin-infection in DMS79 cells. The infection efficiency of HEK cells was also compared to transfected HEK cells. In Table 3.1 it is noted that infection and spin-infection efficiencies were relatively low in both HEK and DMS79 cells, respectively, when compared to the transfected control. HEK cells infected with the retroviruses carrying the eYFP construct alone had 50% infection efficiency. This eYFP construct is a small construct which would be expressed by the cells. However the rest of the GR and mutant GR constructs yielded low infection efficiencies. This could be due to the larger sizes of the construct (~10 kb). DMS79 cells yielded a spin-infection efficiency of less than 1% which is close to the spin-infection efficiency observed by Sommer *et al*. (2010) of 2%. This indicates that retroviral spin-infection yields low expression of virus-encoded proteins. It was noted that the transactivation mutant (pFUNC1-GRΔAF1-eYFP) was taken up very well by the cells. HEK infected cells yielded 130% infection efficiency and DMS79 cells had a spin-infection efficiency of 6.6%. The pFUNC1-GRΔAF1-eYFP construct has a 555bp deletion of the AF1 region of the NTD of the GR. This decrease in size might have allowed for increased uptake of the retroviral construct. Even though infection efficiencies were low, all constructs contain the eYFP marker, allowing visual identification of infected cells.

4.2.2. Microscopic Analysis of Apoptosis and Cell Death

HEK and DMS79 cells were infected with retroviral constructs for 72 hours and prepared for microscopic analysis. The cells were stained with DAPI (to stain the nuclei), Annexin V APC (to stain the apoptotic cells), and PI (to stain dead cells) and checked for eYFP expression. The presence of eYFP indicated positive uptake of retroviral constructs. Untreated cells were used as a control for each cell line. For both cell lines, about 30% of the cells were infected with all the constructs allowing comparison between the cell lines and between treatments. This infection efficiency is higher than described earlier and may be due to improved investigative technique after repetitive runs or due to the use of a different assessment method.

Apoptotic cell death is characterised by DNA fragmentation, plasma membrane blebbing, nuclear and cytoplasmic condensation and margination of chromosomes into distinct masses. These cells will stain with Annexin V APC. PI stains dead cells but does not distinguish between cells that have died from necrosis or apoptosis. As there was no significant differences

in infection efficiency between constructs for both cell lines, comparisons could be made between treatments.

The HEK untreated control cells had a low percentage of apoptotic cells (Figure 3.13) but a high percentage of dead cells indicated by the positive PI staining (Figure 3.14). The empty virus, pFUNC1-eYFP, had a PI positive population was lower than the control but a higher percentage of apoptotic cells. The pFUNC1-GR-eYFP expressing cells had the highest population of apoptotic cells in the HEK cells. This indicates at the time of microscopic preparation, a large population of cells were undergoing apoptosis and had not yet transitioned to cell death. The DNA binding mutant (pFUNC1-GRA458T-eYFP) had a very high percentage of apoptotic cells and the transactivation mutant (pFUNC1-GRΔAF1-eYFP) had the highest dead cell population and a low apoptotic population. It appears that both the wild-type GR and the DNA binding mutant are capable of inducing apoptosis and that the NTD (containing the transactivation domain (AF1)) and LBD do not induce apoptosis. Studies have shown that when these mutant constructs are transfected into GC-resistant cells, they restore GC sensitivity allowing for GC-mediated apoptosis in CEM and S49 cell lines (Dieken and Miesfeld, 1992; Tao *et al*., 2001). The ligand binding mutant (pFUNC1-GRC736S-eYFP) had the lowest apoptotic population (not significantly different from the control). This indicates that the ligand binding mutant population exhibited the lowest death as a consequence of infection. These data suggest that the LBD is necessary for apoptosis to occur in HEK cells. This is in contrast to Sommer *et al*. (2007) who showed that HEK cells do not undergo apoptosis when the GR expression is restored to the cells. The differing results may be due to different modes of analysis. Sommer *et al*. (2007) analysed apoptosis and cell death by flow cytometry, as this method analyses 100 000 cells. Microscopic analysis had a small sample size of 200 cells which can attribute to the differing percentages, in respect to apoptosis and cell death. Flow cytometric analysis was attempted for this study but could not be repeated due to restricted access to the flow cytometer. Thus, the samples were analysed by microscopy.

The control, uninfected DMS79 cells showed 27% apoptotic cells while cells infected with viruses carrying the control construct, eYFP alone, exhibited 7% apoptotic cells (Figure 3.18). This discrepancy is surprising and may be due to an investigative error in treatment or methodology when preparing these cells. Infection with pFUNC1-GR-eYFP yielded significantly more apoptotic cells than infection with pFUNC1-eYFP alone. These findings are

similar to Sommer *et al*. (2007) who showed that DMS79 cells expressing pFUNC1-eYFP comprised of 30% dead cells while cells expressing pFUNC1-GR-eYFP had double the cell death population. The pFUNC1-GRA458T-eYFP expressing cells had similar results to HEK cells, having the second highest apoptotic population, while pFUNC1-GRC736S-eYFP expressing cells had only 20% apoptotic positive cells. The pFUNC1-GRΔAF1-eYFP expressing cells had even fewer apoptotic positive cells. With regards to cell death, the relative percentage of PI positive cells produced similar results to the apoptotic positive cells which indicate this domain plays a role. The pFUNC1-GRA458T-eYFP and pFUNC1-GR-eYFP treatments had the highest percentage of dead cells. The ligand binding mutant and the transactivation mutant had the lowest percentage of dead cells (Figure 3.19). It can therefore be postulated that the transactivation domain is important to induce apoptosis in DMS79 cells. Ligand binding of the GR may play a role but its ability to induce apoptosis did not reach significance when compared to the effect of wild-type GR.

GCs have been known to elicit apoptosis in lymphocytes (Dieken and Miesfeld, 1992; Distelhorst, 2002). This has led to numerous studies to investigate the mechanism used by cells to mediate GC-induced apoptosis (Distelhorst, 2002). Reichardt and colleagues (1998) designed a DNA binding mutant by introducing a point mutation A458T into the DBD. This created a mutation in the D-loop of the DBD that prevents GR dimerization from occurring (Reichardt *et al*., 1998; Tao *et al*., 2001). It was shown that, due to an impairment of dimerization, the GR could not perform GRE dependent transactivation but was still able to elicit transrepression of transcription factors (Reichardt *et al*., 1998). Tao *et al*. (2001) performed a study where they used the A458T mutant to investigate transrepression of the transcription factors AP-1 and NF-κB. AP-1 and NF-κB are involved in genes responsible for immunosuppression and inflammation (Tao *et al*., 2001; Distelhorst, 2002). They showed that the mutant construct could not repress NF-κB expression but did repress AP-1 expression. The GR A458T mutant was capable of transrepressing AP-1 transcription factor as a monomer and expression of the A458T mutant was sufficient to confer GC sensitivity in resistant cell lines which allowed for the induction of apoptosis (Tao *et al*., 2001). This could possibly explain the results obtained for HEK and DMS79 cells expressing pFUNC1-GRA458T-eYFP virus having high levels of apoptotic positive cells.

A study by Dieken and Miesfeld (1992) showed in lymphocytes that an intact functional GR is required for apoptosis induction. They showed that removal of the NTD of the GR prevented apoptosis in the GR-deficient S49 murine cell line. However, they noticed that NTD mutant GR expression in cells resulted in GC sensitivity in conjunction with wild-type GR expressed by the cells. Their data suggested that heterodimers were formed between the NTD mutant GR and endogenously expressed GR which allowed for transcriptional activity, indicating one functional transactivation domain is sufficient to elicit hormonal responses (Dieken and Miesfeld, 1992). This could have occurred in HEK cells expressing the transactivation domain mutant (pFUNC1-GRΔAF1-eYFP) where a significant percentage of cells were dead (Figure 3.14). In another study by Rogatsky *et al*. (2003) focused on all three domains of the GR where the AF1 region of the NTD contained 3 point mutations (E219K/F220L/W234R). This silenced the AF1 region but did not affect conformational structure of the GR protein. Silencing of the AF1 region resulted in abolishment of the induction of human inhibitor of apoptosis 2 gene (hIAP2) (Rogatsky *et al*., 2003). The mutant used in this study had the entire AF1 region deleted from the GR construct. If the entire AF1 region is absent the conformational structure of the GR protein would be compromised. This would prevent the induction of hIAP2 gene, therefore possibly allowing apoptosis to occur in HEK cells.

Over-expression of full length GR, the DNA binding mutant and ligand binding mutant induced apoptosis of DMS79 cells to varying degrees. In DMS79 cells, expression of the pFUNC1-GRΔAF1-eYFP virus did not result in significant apoptosis induction, this could be attributed to absence of the AF1 region. Phosphorylation of serine residues present in AF1 region are necessary for nuclear translocation of the GR protein for GC-induced transcriptional activity to occur (Kumar and Thompson, 2005; Chen *et al*., 2008). Serine 211 of the AF1 region is an important residue for phosphorylation. Its phosphorylation by p38 MAPK creates a substrate for GC-induced apoptosis in lymphoid cells (Miller *et al*., 2005; Garza *et al*., 2010). A study by Miller *et al*. (2005) showed that mutagenesis of serine 211 resulted in diminished transcriptional activity and apoptosis induction in lymphoid cells. Since the pFUNC1-GRΔAF1-eYFP construct has the AF1 region deleted, there is no serine 211 residue to phosphorylate resulting in inhibition of p38 MAPK induced apoptosis. Inhibition of the p38 MAPK activity by pharmacological blockade resulted in protection from GC-induced apoptosis in mouse and human lymphoid cells (Miller *et al*., 2005). In order for apoptosis to occur in cells through the p38 MAPK signalling pathway, functional GR is required. Restoration of the GR protein by transfection restored apoptotic activity in cells (Miller *et al*., 2005). The deletion of the AF1

region in the GR has been shown to be unable to inhibit the pro-survival activity of NF-κB (Scheinman *et al*., 1995). It appears that, due to the loss of the transactivation domain, the GR cannot interact with the p65 subunit (Scheinman *et al*., 1995). The p65 subunit of NF-κB is required to be in physical contact with the GR to repress NF-κB (Garside *et al*., 2004). NF-κB is a transcription factor and the GR interacts with transcription factors through the AF1 region (Kumar and Thompson, 2005). The inability of the transactivation mutant to repress NF-κB activity may have resulted in the low apoptotic and dead cells percentages seen in DMS79 cells. The study by Rogatsky *et al*. (2003) showed that silencing of the AF1 region had no effect on serum-glucocorticoid regulated kinase (SGK). SGK has been known to be expressed at high levels in breast cancer cells as it protects tumours from apoptosis (Beck *et al*., 2009). SGK has been considered as an oncogene that upregulated NF-κB transcription which leads to pro-survival of the cells (Beck *et al*., 2009). It may be possible that SCLC cells may utilise the kinase for survival. SGK expression has been known to be influenced by GCs (Beck *et al*., 2009).

The HEK cells expressing the ligand binding mutant virus (pFUNC1-GRC736S-eYFP) showed a marked decrease in apoptosis when compared to the wild-type GR virus. The ligand binding mutant was designed by Lind and colleagues in 1996. Cysteine 736 was chosen as it lies in close proximity to the bound GC hormone molecule. By oligonucleotide-directed mutagenesis, two functional substitutions was identified, serine and threonine. This gave rise to the C736S and C736T mutants (Lind *et al*., 1996). The C736S mutant showed the most reduced sensitivity to all steroid hormones in transactivation assays and reduced binding affinity of steroid hormone (Lind *et al*., 1996). Most studies show that the GC hormone is necessary for GC-induced apoptosis as the single point mutation compromised the binding affinity of the GR to the ligand (Schaaf and Cidlowski, 2003) and decrease transcriptional activity (Kauppi *et al*., 2003). In the other GR constructs, the LBD was intact which would allow for GC-mediated apoptosis occurring through one of the several pathways GCs use to elicit apoptosis (Distelhorst, 2002). Both cell lines were incubated with medium containing foetal bovine serum and foetal bovine serum has GCs present. This may account for minimal apoptosis induction noted in the GR, NTD and DBD mutant construct expressing treatments. However, the study by Sommer *et al*. (2007) showed that GR-mediated apoptosis appeared to be ligand-independent in SCLC cells. Mathieu *et al*. (1999) showed HeLa cells were able to induce apoptosis while expressing ligand binding deficient GR construct. The ligand binding deficient cells were able to repress the proinflammatory transcription factors, AP-1 and NF-κB, and induce apoptosis (Mathieu *et al*.,

1999). A study by Doucas *et al*. (2000) also showed that over-expression of GR resulted in repression of NF-κB in a ligand dependent manner. Despite not adding a GC analog, dexamethasone, GC-mediated apoptosis occurred in the cell lines. These studies suggest that it is possible that GR-mediated apoptosis in SCLC cells may be ligand independent. The results of this study corroborate these findings.

5. Conclusion and Future Work

In summary, all cell lines contained promoter 1B and 1C transcripts suggesting that co-expression of these promoters is required for GR expression. The A549 cell line does not appear to have a methylated promoter region and this is supported by the natural abundant expression of the GR in the cells. Our data suggest that promoter 1C is methylated in HEK cells. While both promoter 1B and 1C expression in DMS79 cells increased after treatment with the de-methylating agent, although only promoter 1B increased significantly.

The hypothesis of both promoter 1B and 1C being methylated may play important role in GR expression in SCLC cells. This could lead to investigations of identifying which promoter contributes the most to transcription of the GR; that is either promoter 1B or promoter 1C or co-expression of both promoters result in GR expression. This could be achieved by using luciferase assays tagged to each promoter as mentioned in Nunez and Vedeckis (2002) or by silencing each promoter by siRNA and analysing how this affects GR expression. Promoters 1F and 1J were also expressed in DMS79 cells and de-methylation experiments could be performed to see if the transcripts increase indicating the presence of methylation. Since there is an indication of methylation of promoters in SCLC cells, this can lead to development of therapeutic treatments. 5-Aza has been used in clinical trials, known as decitabine, as an epigenetic drug to treat cancers however has been shown to have adverse effects, such as cytotoxicity, on non-target cells (Christman, 2002; Streseman and Lyko, 2008). Alternatively, natural de-methylating agents, such as genistein, can be identified and analysed for their effectiveness as use of a treatment regiment for cancer patients as there will be less side effects as compared to be treated with 5-aza.

Both HEK and DMS79 cells underwent apoptotic activity when exogenous GR was over-expressed in the cells. These results are in contrast to Sommer *et al*. (2007) study which showed that HEK cells do not undergo apoptosis when the GR is over-expressed. Apoptosis occurred in HEK cells expressing either wild-type GR or mutant DBD mutant. This could be due to the difference in experimental designs. With microscopics analysis, cell counting is more subjective than flow cytometry. Experiments will be repeated using flow cytometry. In DMS79 cells, a dysfunctional DBD and LBD were still able to induce apoptosis in cells. In the HEK cell line, a

defective LBD resulted in drastic decrease in apoptotic activity. DMS79 cells had low apoptotic cells when expressing a NTD mutant. It can be postulated that the LBD is necessary for apoptosis to occur in HEK cells and DMS79 cells require a functional NTD to elicit apoptosis. This experiment can be analysed using flow cytometry which analyses larger cell populations or by performing a sensitive PARP Eliza to determine apoptosis induction. Since medium containing foetal bovine serum was used for the experiment, the experiment could be repeated using stripped medium (which removes all GCs) to determine if this alters apoptotic activity. A synthetic GC hormone such as dexamethasone can be added to virus expressing cells and the effects of adding ligand on apoptosis can be observed. The effect of added ligand to cells over-expressing GR may be noted and compared to Sommer *et al*. (2007) and Kay *et al*. (2011) studies. If ligand treatment does have an effect on cells, then a GR agonist (such as RU486) could be added to see if this mirrors results that are produced to treatments with cells expressing GR and GR mutant constructs alone.

The GR is able to elicit its effects by interacting with proteins or by non-genomic actions. In particular the GR exerts non-genomic anti-inflammatory effects by interfering with the phosphotidylinositol-3 kinase (PI3K) and Akt signalling pathway (Moore *et al.,* 1998). The PI3K/Akt pathway has been found to upregulate the expression of anti-apoptotic proteins via phosphorylation of CREB which in turn activates the expression of anti-apoptotic genes, Bcl-2 and Mcl-1. Akt is an inhibitor of pro-apoptotic protein, Bad. In SCLC cells, the PI3K pathway is constitutively active which results in the repression of Bad expression and in turn Akt thereby allowing for tumourgenesis occurring (Moore *et al.,* 1998). Furthermore over expression of exogenous GR in SCLC resulted in apoptotic cell death with the up-regulation of the pro-apoptotic genes, Bad and Bax (Sommer *et al.,* 2007). The GR in SCLC cells can be over-expressed using the wild-type GR construct and the levels of PI3K, Akt and associated anti-apoptotic proteins can be observed. Cell proliferation may also be performed to see effects of PI3K and Akt and its inhibition when cells over-express GR protein.

In summary, we have determined the methylation status and GR promoter usage in SCLC cells and shown that the NTD (AF1) is responsible for GR-induced apoptosis in these cells. Understanding the details of this endogenous mechanism may contribute to the development of more effective therapies for this deadly disease. These results will be repeated to produce robust data for a publication.

6. References

Alberg, A.J., Ford, J.G. and Samet, J.M. 2007. Epidemiology of Lung Cancer ACCP Evidence-based clinical practice guidelines (2nd Edition). Chest. 132. 29S-55S.

Alt, S.R., Turner, J.D., Klok, M.D., Meijer, O.C., Lakke, E.A.J.F., DeRijk, R.H. and Muller, C.P. 2010. Differential expression of glucocorticoid receptor transcripts in major depressive disorder is not epigenetically programmed. Pyschoneuroendocrinology. 35. 544-556.

Baylin, S.B., Futscher, B.W. and Gore, S.D., 2004. Understanding DNA methylation and Epigenetic Gene Silencing in Cancer. Current Therapeutics Incorporated. Carden Jennings Publishing. 1-28.

Bello, B., Fadahun, O., Kielkowski, D. and Nelson, G. 2011. Trends in lung cancer mortality in South Africa: 1995-2006. BMC Public Health. 11. 209-213.

Beck, I.M.E., Berghe, W.V., Vermeulen, L., Yamamoto, K.R., Haegeman, G. and De Bosccher, K. 2009. Crosstalk in inflammation: The interplay of glucocorticoid receptor-based mechanisms and kinases and phosphatases. Endocrine Reviews. 30. 830-882.

Bhola, P.D. and Simon, S.M. 2009. Determinism and divergence of apoptosis susceptibility in mammalian cells. Journal of Cell Science. 122. 4296-4302.

Bockmühl, Y., Murgatroyd, C.A., Kuczynska, A., Adcock, I.M., Almeida, O.F.X. and Spengler, D. 2011. Differential regulation and function of 5'-untranslated GR-Exon 1 Transcripts. Molecular Endocrinology. 25. 1100-1110.

Bustin, S.A., Benes, V., Garson, J.A., Hellemans, J., Huggett, J., Kubista, M., Mueller, R., Nolan, T., Pfaffl, M.W., Shipley, G.L., Vandesompele, J. and Wittwer, C.T. 2009. The MIQE

guidelines: Minimum information for publication of quantitative real-time PCR experiments. Clinical Chemistry. 55. 611-622.

Cao-Lei, L., Leija, S.C., Kumsta, R., Wüst, S., Meyer, J., Turner, J.D. and Muller, C.P. 2011. Transcriptional control of the human glucocorticoid receptor: identification and analysis of alternative promoter regions. Human Genetics. 129. 533-543.

Chen, W., Dang, T., Blind, R.D., Wang, Z., Cavasotto, C.N., Hittelman, A.B., Rogatsky, I., Logan, S.K. and Garabedian, M.J. 2008. Glucocorticoid receptor phosphorylation differentially affects target gene expression. Molecular Endocrinology. 22. 1754-1766.

Chivers, J.E., Gong, W., King, E.M., Seybold, J., Mak, J.C., Donnelly, L.E., Holden, N.S. and Newton, R. 2006. Analysis of the dissociated steroid RU24858 does not exclude a role for inducible genes in the anti-inflammatory actions of glucocorticoids. Molecular Pharmacology. 70. 2084-2095.

Christman, J.K. 2002. 5-Azacytidine and 5-aza-2'-deoxycytidine as inhibitors of DNA methylation: mechanistic studies and their implications for cancer therapy. Oncogene. 21. 5483-5495.

Croxtall, J.D., van Hal, P.Th.W., Choudhury, Q., Gilroy, D.W. and Flower, R.J. 2002. Different glucocorticoids vary in their genomic and non-genomic mechanism of action in A549 cells. Nature. 135. 511-519.

Dieken, E.S. and Miesfeld, R.L. 1992. Transcriptional transactivation functions localized to the glucocorticoid receptor N terminus are necessary for steroid induction of lymphocyte apoptosis. Molecular and Cellular Biology. 12. 589-597.

Distelhorst, C.W. 2002. Recent insights into the mechanism of glucocorticosteroid-induced apoptosis. Cell Death and Differentiation. 9. 6-19.

Doucas, V., Shi, Y., Miyamoto, S., West, A., Verma, I. and Evans, R.M. 2000. Cytoplasmic catalytic subunit of protein kinase A mediates cross-repression by NF-κB and the glucocorticoid receptor. Proceedings of the National Academy of Sciences of the United States of America. 97. 11893-11898.

Dresler, C.M., Fratelli, C., Babb, J., Everley, L., Evans, A.A. and Clapper, M.L. 2000. Gender differences in genetic susceptibility for lung cancer. Lung Cancer. 30. 153-160.

Duma, D., Jewell, C.M. and Cidlowski, J.A. 2006. Multiple glucocorticoid receptor isoforms and mechanisms of post-translational modification. Steroid Biochemistry and Molecular Biology. 102. 11-21.

Elmore, S. 2007. Apoptosis: A review of programmed cell death. Toxicologic Pathology. 35. 495-516.

Foster, K.A., Oster, C.G., Mayer, M.M., Avery, M.L. and Audus, K.L. 1998. Characterization of the A549 cell line as a type II pulmonary epithelial cell model for drug metabolism. Experiment Cell Research. 243. 359-366.

Garside, H., Stevens, A., Farrows, S., Normand, C., Houle, B., Berry, A., Maschera, B. and Ray, D. 2004. Glucocorticoid ligands specify different interactions with NF-κB by allosteric effects on the glucocorticoid receptor DNA binding domain. The Journal of Biological Chemistry. 279. 50050-50059.

Garza, A.M.S., Khan, S.H. and Kumar, R. 2010. Site-specific phosphorylation induces functionally active conformation in intrinsically disordered N-terminal activation function (AF1) domain of the glucocorticoid receptor. Molecular and Cellular Biology. 30. 220-230.

Greenberg, A.K., Hu, J., Basu, S., Hay, J., Reibman, J., Yei, T., Tchou-Weng, K.M., Rom., W.M. and Lee, T.C. 2002. Glucocorticoids inhibit lung cancer cell growth through both the extracellular signal-related kinase pathway and cell cycle regulators. American Journal of Respiratory Cell and Molecular Biology. 27. 320-328.

Hirsch, F.R., Franklin, W.A., Gazdar, A.F. and Bunn, P.A. Jr. 2001. Early detection of lung cancer: Clinical perspective of recent advances in biology and radiology. Clinical Cancer Research. 7. 5-22.

Hittelman, A.B., Burakov, D., Iñiguez-Lluhí, J.A., Freedman, L.P. and Garabedian, M.J. 1999. Differential regulation of glucocorticoid receptor transcriptional activation via AF-1-associated proteins. The European Molecular Biology Organization Journal. 18. 5380-5388.

Hopkins-Donaldson, S., Ziegler, A., Kurtz, S., Bigosch, C., Kandioler, D., Ludwig, D., Zangemiester-Wittke, U. and Stahel, R. 2003. Silencing of death receptor and caspase-8 expression in small cell lung carcinoma cell lines and tumors by DNA methylation. Cell Death and Differentiation. 10. 356-364.

Ihde, D.C. 1995. Small cell lung cancer: State-of-the-art therapy 1994. Chest. 107. 243S-248S.

Jackman, D.M. and Johnson, B.E. 2005. Small-cell lung cancer. Lancet. 366. 1385-1396.

Johnstone, R.W., Ruefli, A.A. and Lowe, S.W. 2002. Apoptosis: A Link between Cancer Genetics and Chemotherapy. Cell. 108. 153-164.

Jones, P.A. and Laird, P.W. 1999. Cancer epigenetics comes of age. Nature Genetics. 21. 163-167.

Kassi, E. And Moutsatsou, P. 2011. Glucocorticoid receptor signalling and prostate cancer. Cancer Letters. 302. 1-10.

Kauppi, B., Jakob, C., Färnegårdh, M., Yang, J., Ahola, H., Alarcon, M., Calles, K., Engström, O., Harlan, J., Muchmore, S., Ramqvist, A., Thorell, S., Öhman, L., Greer, J., Gustafsson, J., Carlstedt-Duke, J. and Carlquist, M. 2003. The three-dimensional structures of antagonistic and agonistic forms of the glucocorticoid receptor ligand-binding domain. The Journal of Biological Chemistry. 278. 22748-22754.

Kay, P., Schlossmacher, G., Matthews, L., Sommer, P., Singh, D., White, A. and Ray, D. 2011. Loss of glucocorticoid receptor expression by DNA methylation prevents glucocorticoid induced apoptosis in human small cell lung cancer cells. PLoS ONE. 6. e24839. doi:10.1371/journal.pone.0024839.

Kumar, R. and Thompson, E.B. 2005. Gene regulation by the glucocorticoid receptor: Structure:function relationship. Journal of Steroid Biochemistry and Molecular Biology. 94. 383-394.

Lavery, D.N. and McEwan, I.J. 2005. Structure and function of the steroid receptor AF1 transactivation domains induction of active conformations. Biochemical Journal. 391. 449-464.

Lind, U., Carsltedt-Duke, J., Gustafsson, J.A. and Wright, A.P. 1996. Identification of single amino acid substitutions of Cys-736 that affect the steroid-binding affinity and specificity of the glucocorticoid receptor using phenotypic screening in yeast. Molecular Endocrinology. 10. 303-311.

Livak, K.J. and Schmittgen, T.D. 2001. Analysis of relative gene expression data using real-time quantitative PCR and the $2^{-\Delta\Delta CT}$ method. Methods. 25. 402-408.

Mathieu, M., Gougat, C., Jaffuel, D., Danielsen, M., Godard, P., Bousquet, J. and Demoly, P. 1999. The glucocorticoid receptor gene as a candidate for gene therapy in asthma. Gene Therapy. 6. 245-252.

Moore, S.M., Rintoul, R.C., Walker, T.R., Chilvers, E.R., Haslett, C. and Sethi, T. 1998. The presence of a constitutively active phosphoinositide 3-kinase in small cell lung cancer cells mediates anchorage-independent proliferation via a protein kinase B and p70s6k-dependent pathway. Cancer Research. 58. 5239-5247.

Mountain, C.F. 2000. The international system for staging lung cancer. Seminars in Surgical Oncology. 18. 106-115.

Munck, A., Guyre, P.M. and Holbrook, N.J. 1984. Physiological functions of glucocorticoids in stress and their relation to pharmacological actions. Endocrine Reviews. 5. 25-44.

Nicolaides, N.C., Galata, Z., Kino, T., Chrousos, G.P. and Charmandari, E. 2010. The human glucocorticoid receptor: Molecular basis of biologic function. Steroids. 75. 1 -12.

Nunez, B.S. and Vedeckis, W.V. 2002. Characterization of promoter 1B in the human glucocorticoid receptor gene. Molecular and Cellular Endocrinology. 189. 191-199.

O'Connor, T.M., Halloran, D.J. and Shanahan, F. 2000. The stress response and hypothalamic-pituitary-adenal axis: from molecule to melancholia. Quarterly Journal of Medicine. 93. 323-333.

Palii, S.S., Van Emburgh, B.O., Sankpal, U.T., Brown, K.D. and Robertson, K.D. 2008. DNA methylation inhibitor 5-aza-2'deoxycytidine induces reversible genome-wide DNA damage that is distinctly influenced by DNA methyltransferases 1 and 3B. Molecular and Cellular Biology. 28. 752-771.

Panani, A.D. and Roussos, C. 2006. Cytogenetic and molecular aspects of lung cancer. Cancer Letters. 239. 1-9.

Presul, E., Schmidt, S., Kofler, R. and Helmberg, A. 2007. Identification, tissue expression, and glucocorticoid responsiveness of alternative first exons of the human glucocorticoid receptor. Journal of Molecular Endocrinology. 38. 79-90.

Ray, D.W., Littlewood, A.C., Clark, A.J.L. and White, A. 1994. Human small cell lung cancer cell lines expressing the proopiomelanocortin gene have aberrant glucocorticoid receptor function. Journal of Clinical Investigations. 93. 1625-1630.

Ray, D.W., Davis, J.R.E., White, A. and Clark, A.J.L. 1996. Glucocorticoid receptor structure a function in glucocorticoid-resistant small cell lung carcinoma cells. Cancer Research. 56. 3276-3280.

Reichardt, H.M., Kaestner, K.H., Tuckerman, J., Kretz, O., Wessely, O., Bock, R., Gass, P., Schmid, W., Herrlich, P., Angel, P. and Schütz, G. 1998. DNA binding of the glucocorticoid receptor is not essential for survival. Cell. 93. 531-541.

Rogatsky, I., Weng, J., Derynck, M.K., Nonaka, D.F., Khodabakhsh, D.B., Haqq, C.M., Darimont, B.D., Garabedian, M.J. and Yamamoto, K.R. 2003. Target-specific utilization of transcriptional regulatory surfaces by the glucocorticoid receptor. Proceedings of the National Academy of Sciences of the United States of America. 100. 13845-13850.

Schaaf, M.J.M. and Cidlowski, J. 2003. Molecular mechanisms of glucocorticoid action and resistance. Journal of Steroid Biochemistry and Molecular Biology. 83. 37-48.

Scheinman, R.I., Gualberto, A., Jewell, C.M., Cidlowski, J.A. and Baldwin, A.S. Jr. 1995. Characterization of mechanisms involved in transrepression of NF-κB by activated glucocorticoid receptors. Molecular and Cellular Biology. 15. 943-953.

Simon, G.R. and Wagner, H. 2003. Small cell lung cancer. Chest. 123. 259S-271S.

Sommer, P., Le Rouzic, P., Gillingham, H., Berry, A., Kayahara, M., Huynh, T., White, A. and Ray, D.W. 2007. Glucocorticoid receptor overexpression exerts an antisurvival effect on human small cell lung cancer cells. Oncogene. 26. 1-11.

Sommer, P., Cowen, R.L., Berry, A., Cookson, A., Telfer, B.A., Williams, K.J., Stratford, I.J., Kay, P., White, A. and Ray, D.W. 2010. Glucocorticoid receptor over-expression promotes human small cell lung cancer apoptosis *in vivo* and thereby slows tumor growth. Endocrine-Related Cancer. 17. 203-213.

Streseman, C. and Lyko, F. 2008. Modes of action of the DNA methyltransferase inhibitors azacytidine and decitabine. International Journal of Cancer. 123. 8-13.

Tao, Y., Williams-Skipp, C. and Scheinman, R.I. 2001. Mapping of glucocorticoid receptor DNA binding domain surfaces contributing to transrepression of NF-κB and induction of apoptosis. The Journal of Biological Chemistry. 276. 2329-2332.

Tsigos, C. and Chrousos, G.P. 2002. Hypothalamic-pituitary-adrenal axis, neuroendocrine factors and stress. Journal of Psychosomatic Research. 53. 865-871.

Turner, J.D. and Muller, C.P. 2005. Structure of the glucocorticoid receptor (NR3C1) gene 5' untranslated region: identification and tissue distribution of multiple new human exon 1. Journal of Molecular Endocrinology. 35. 283-292.

Turner, J.D., Schote, A.B., Macedo, J.A., Pelascini, L.P.L. and Muller, C.P. 2006. Tissue specific glucocorticoid receptor expression, a role for alternative first exon usage? Biochemical Pharmacology. 72. 1529-1537.

Turner, J.D. Pelascini, L.P.L., Macedo, J.A and Muller, C.P. 2008. Highly individual methylation patterns of alternative glucocorticoid receptor promoters suggest individualized epigenetic regulatory mechanisms. Nucleic Acids Research. 36. 7207-7218.

Turner, J.D., Alt, S.R., Cao, L., Vernocchi, S., Trifonova, S., Battello, N. and Muller, C.P. 2010. Transcriptional control of the glucocorticoid receptor: CpG islands, epigenetics, and more. Biochemical Pharmacology. 80. 1860-1868.

Vandevyver, S., Dejager, L. and Libert C. 2012. On the trail of the glucocorticoid receptor: Into the nucleus and back. Traffic. 13. 364-374.

Yuan, B., Jefferson, A.M., Popescu, N.C. and Reynolds, S.H. 2004. Aberrant gene expression in human non small cell lung carcinoma cells exposed to demethylating agent 5-aza-2'-deoxycytidine. Neoplasia. 6. 412-419.

Zhou, J. and Cidlowski, J.A. 2005. The human glucocorticoid receptor: One gene, multiple proteins and diverse responses. Steroids. 70. 407-417.

7. Appendix

A. MIQE Guidelines

All qPCR experimental designs, procedures and analyses were performed in accordance to the Minimum Information for Publication of Quantitative Real-Time PCR Experiments (MIQE) guidelines (Bustin *et al*., 2009). The MIQE guidelines were designed to create a standard with which scientists were allowed to present, evaluate and report qPCR data that would be interpreted in an accurate manner (Bustin *et al*., 2009).

A.1. Experimental Design

Three human-derived cell lines (A549, DMS79 and HEK) were used to evaluate the effects of demethylating agent, 5-aza, on GR promoter expression. qPCR analyses were focused on promoters 1B and 1C of the GR. A549 and HEK cell lines served as controls with abundant GR expression and GR deficient expression, respectively. The control cell lines were grown in 10cm culture dishes (Corning) and the DMS79 cells were grown in T75 flasks (Corning). Cells were treated with 0.5, 1 and 5 μmol/l of 5-aza and vehicle control of glacial acetic acid for 72 hours. RNA was isolated using QIAGEN RNeasy kit. cDNA was synthesized using High Capacity RNA-to-cDNA Mastermix (Applied Biosystems) and Tetro cDNA synthesis kit (Bioline) when Applied Biosystems discontinued the kit. Two biological repeats were performed and within each repeat three technical repeats were performed. Triplicate of each sample was run for each technical repeat.

DMS79 cells were spin-infected with retroviral constructs containing pFUNC1-eYFP, pFUNC1-GR-eYFP, pFUNC1-GRA458T-eYFP, pFUNC1-GRΔAF1-eYFP and pFUNC1-GRC736S-eYFP and incubated for 72 hours. DMS79 cells were grown in T25 flasks (Corning). Post-infection, RNA was extracted using the QIAGEN kit and cDNA was synthesized with the Tetro cDNA synthesis kit. qPCR was performed to evaluate the infection efficiency of the retroviral constructs. HEK cells transfected with the plasmids using XtremeGene transfection

reagent for 24 hours. The transfected HEK cells served as a control. The HEK cells were grown in 60mm culture dishes (Corning).

All qPCR analyses were performed by Nimisha Singh at the research lab of Dr. Paula Sommer at the School of Life Sciences, Biological and Conservation Sciences building, University of KwaZulu-Natal, Durban, South Africa.

A.2. Sample Information

HEK and A549 cell stocks of confluent 10 cm culture dishes were stored in 1 ml of DMEM medium containing 10% dimethyl sulfoxide (DMSO) in 1.5ml cryovials (Corning). DMS79 cell stocks of confluent T75 or T25 flasks were stored in 1 ml of RPMI 1640 medium containing 5% DMSO in 1.5 ml cryovials. Cells were stored in liquid nitrogen at -196^{o}C and -80^{o}C freezer.

HEK and A549 cell lines were cultured in DMEM medium (PAA) containing 10% inactivated FBS (PAA) and 100 units/ml penicillin/streptomycin (PAA). DMS79 cells were cultures in RPMI 1640 medium (PAA) containing 10% FBS and 100 units/ml of penicillin/streptomycin. Cells were incubated at 37^{o}C with 5% CO_2 in a Shel Lab 3552 high heat decontamination CO_2 incubator.

A.3. Nucleic Acid Extraction

RNA was isolated using QIAGEN RNeasy kit as discussed in section 2.3.1 of materials and methods. RNA samples were quantified using Nanodrop technology (ND1000) with samples having a purity between 1.8 and 2 as per the 260/280 absorbance ratio. RNA samples were aliquoted and stored at -80^{o}C.

The integrity of RNA samples were evaluated by running 1.5% agarose MOPS/formaldehyde gels as described in section 2.3.2 in materials and methods section. An O'GeneRuler Ladder Mix molecular marker was run with the RNA samples. The presence of two distinct bands of

28S rRNA and 18S rRNA subunits indicated good quality of RNA. Gels were imaged using a ChemiDoc™ XRS+ imaging system and Image Lab™ software (Bio-Rad).

A.4. qPCR primer and target gene information

Primers for alternative promoters in exon 1 of GR were sourced from Alt *et al*. (2010). Sequences are presented in Table 1 of the materials and methods section. For infection efficiency qPCR reactions, an eYFP primer set sourced from Sommer *et al*. (2010) was used. The primer stocks had a concentration of 100 μmol/l and were stored at -20^{o}C. Working solutions of primers for qPCR reactions were at a concentration of 10 μmol/l and aliquoted and stored at -20^{o}C (Appendix B.19).

A.5. qPCR Protocol

One protocol was used for amplification of target genes. A standard reaction volume of 20μl was used that consisted of 1 μl cDNA, 0.5 μl of forward primer, 0.5 μl reverse primer, 2 μl of 5x HOT FIREPol® EvaGreen® qPCR Mix Plus (Solis BioDyne: catalogue number 08-25-00001) and 16 μl of nuclease free water (Invitrogen). The 5x HOT FIREPol® EvaGreen® qPCR Mix Plus composition contains HOT FIREPol® DNA Polymerase, 5x EvaGreen® qPCR buffer, 12.5 mM $MgCl_2$, dNTPs (including dTTP to improve reaction sensitivity and efficiency), EvaGreen® dye and no ROX dye. qPCR consumables consisted of 0.2 ml white strip tubes (Bio-Rad: catalogue number: TLS-0851) and optical flat cap strips (Bio-Rad: TCS-0803). The same set of Gilson Pipetman® starter kit micropipettes were used for manual set up of all qPCR reactions. Reaction preparation was set up on ice throughout the duration of procedure.

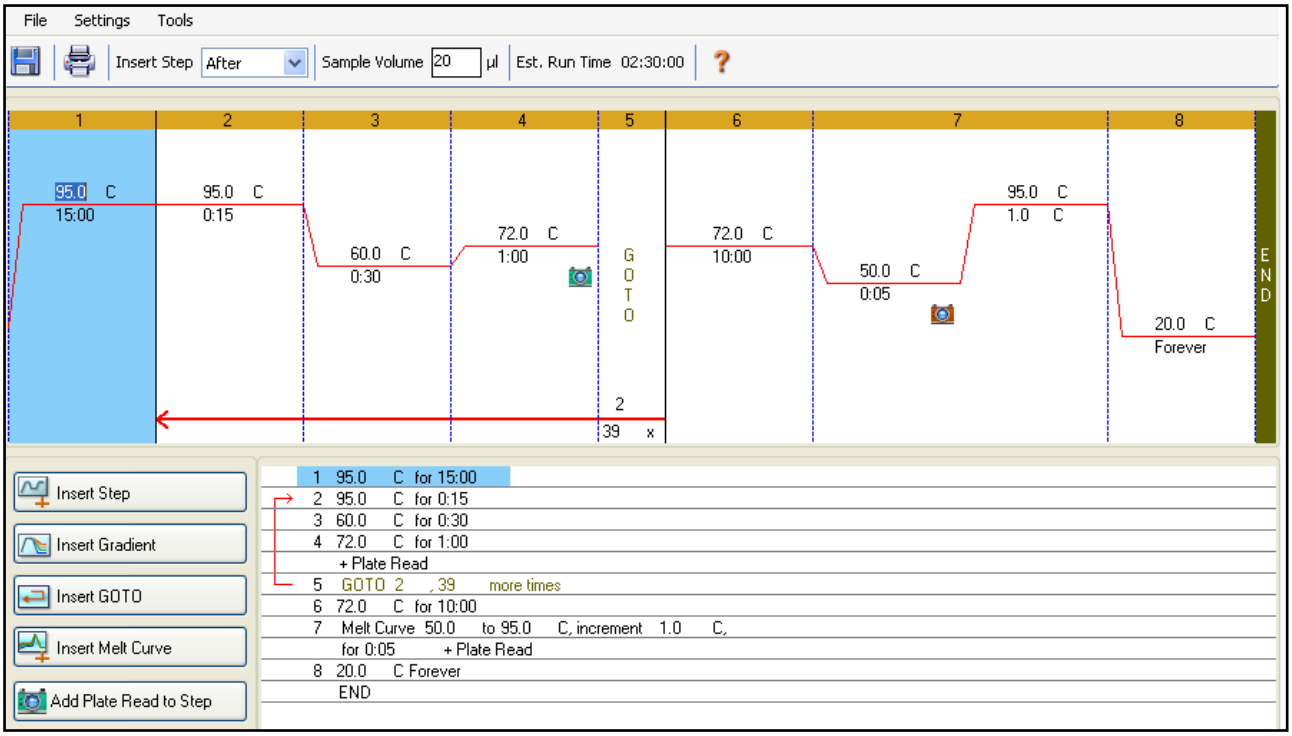

Figure 7.1: The qPCR protocol used in all qPCR experiments using the Bio-Rad CFX Manager Software

qPCR analyses were carried out in an MJ Mini Opticon thermal cycler (Bio-Rad) with software package CFX Manager version 5 (Bio-Rad) to set up qPCR reaction parameters. The CFX Manager was used to analyse amplification readings with C_q values being determined at a single baseline threshold of 0.05 RFU. Fluorescence was read with FAM channel.

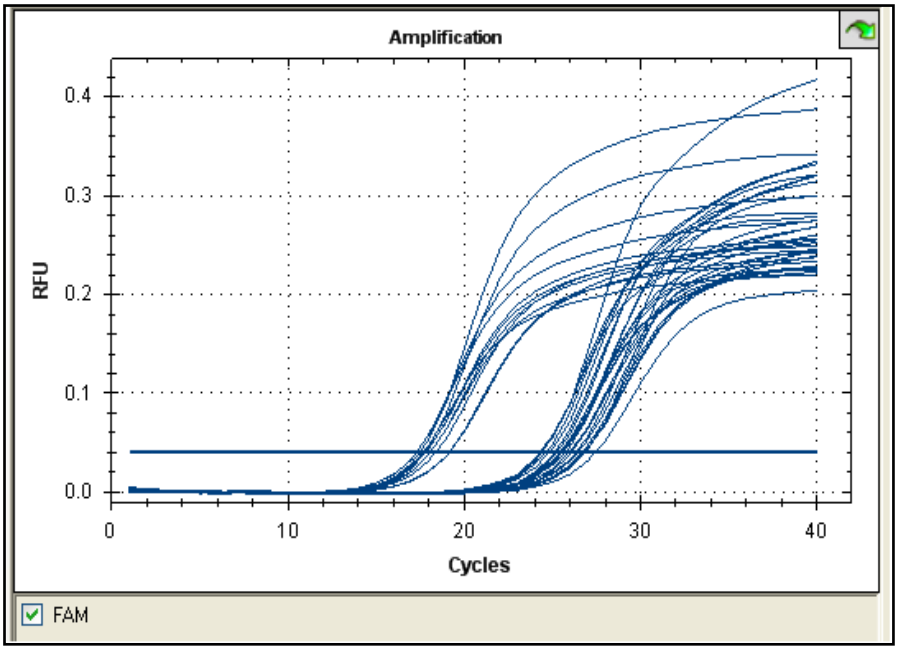

Figure 7.2: Amplification of qPCR reactions using FAM fluorescence channel at RFU baseline of 0.05

A.6. qPCR Validation

A.6.1. Evaluation of qPCR reaction efficiency

Analysis of qPCR data by the $2^{-\Delta\Delta Ct}$ method could only be performed if the reaction efficiencies of the target genes are equal to that of the reference gene, β-actin (Livak and Schmittgen, 2001). This $2^{-\Delta\Delta Ct}$ calculation was validated by a serial dilution of cDNA template of a 100-fold range. Amplification of target genes was performed as per section 2.5.2.1 of materials and methods chapter. The Ct values are averaged for target and reference genes and the ΔCt value was calculated ($Ct_{\text{target gene}} - Ct_{\text{reference gene}}$). The ΔCt values were plotted against the cDNA dilution range with standard deviation. The slope value of the resultant regression line had to be close to zero for the $2^{-\Delta\Delta Ct}$ method to be applicable (Livak and Schmittgen, 2001). Reaction efficiencies were calculated using QPCR Standard Curve Slope to Efficiency Calculator website software (http://www.genomics.agilent.com/CalculatorPopupWindow.aspx?CalID=8). Reaction efficiencies between 90% and 110% and R^2 values close to 1 were acceptable.

A.

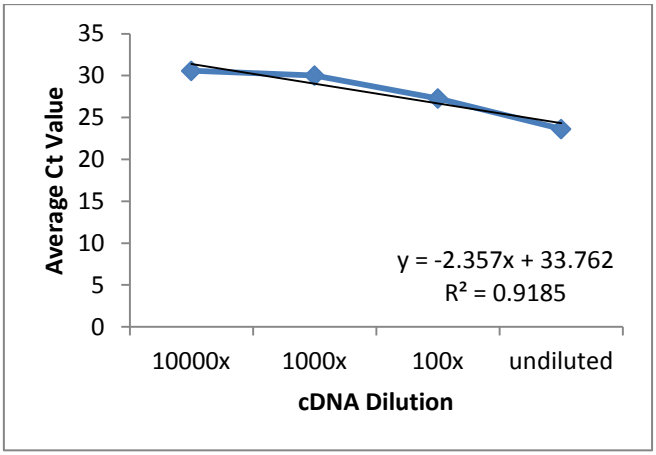

Reaction Efficiency: 90.80%

B.

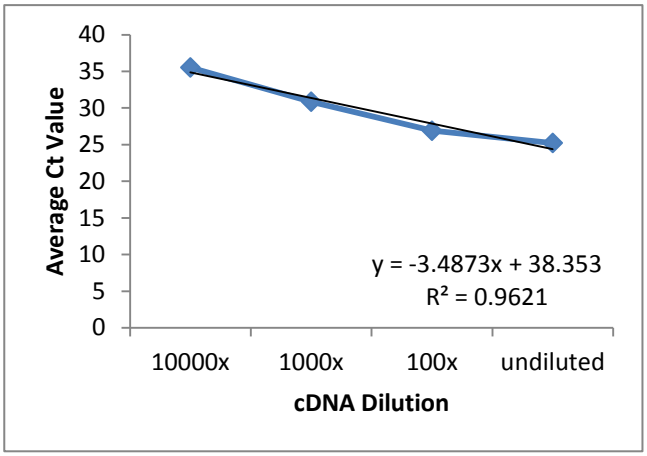

Reaction Efficiency: 165%

C.

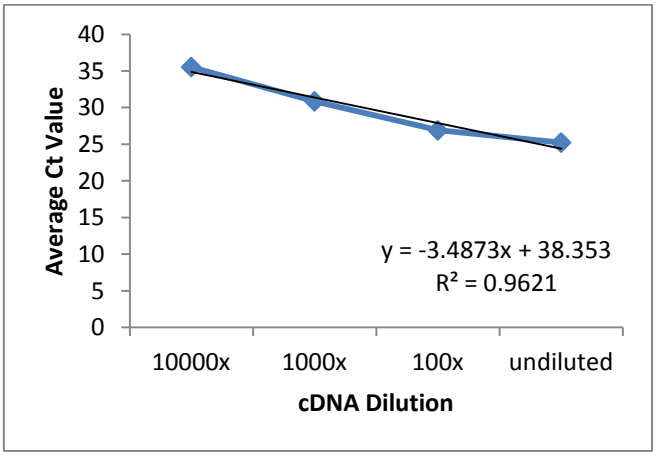

Reaction Efficiency: 93.52%

Figure 7.3: Line graphs with standard deviation of qPCR reaction efficiency of 100-fold serial dilution of cDNA using primer sets (A) β-actin, (B) Promoter 1B and (C) Promoter 1C. All averages are expressed with standard deviation

A.6.2. qPCR Melt Analysis Verification

A melt curve analysis was performed for each qPCR run for each target gene and cDNA sample. A single melt temperature corresponded to each target gene yielding a single product that was verified by agarose gel electrophoresis. A 1% agarose gel was prepared as described in

section 2.5.1. of materials and methods section. Agarose gels were run with an O'GeneRuler™ DNA ladder mix molecular marker (range: 100 bp-10 000 bp) (Fermentas) to confirm band size for each target gene.

β-actin

A **B**

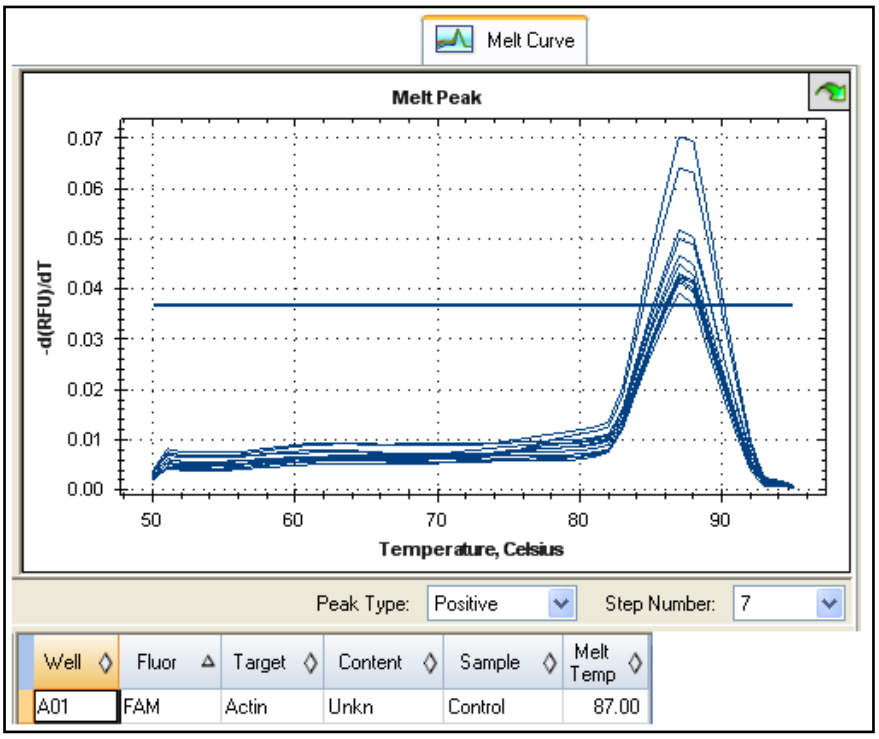

Figure 7.4: A. Melt Curve analysis of β-actin primer set with a melt temperature of 87°C

B. Agarose gel electrophoresis confirmation of β-actin amplification (size: 208 bp)

Promoter 1B

A **B**

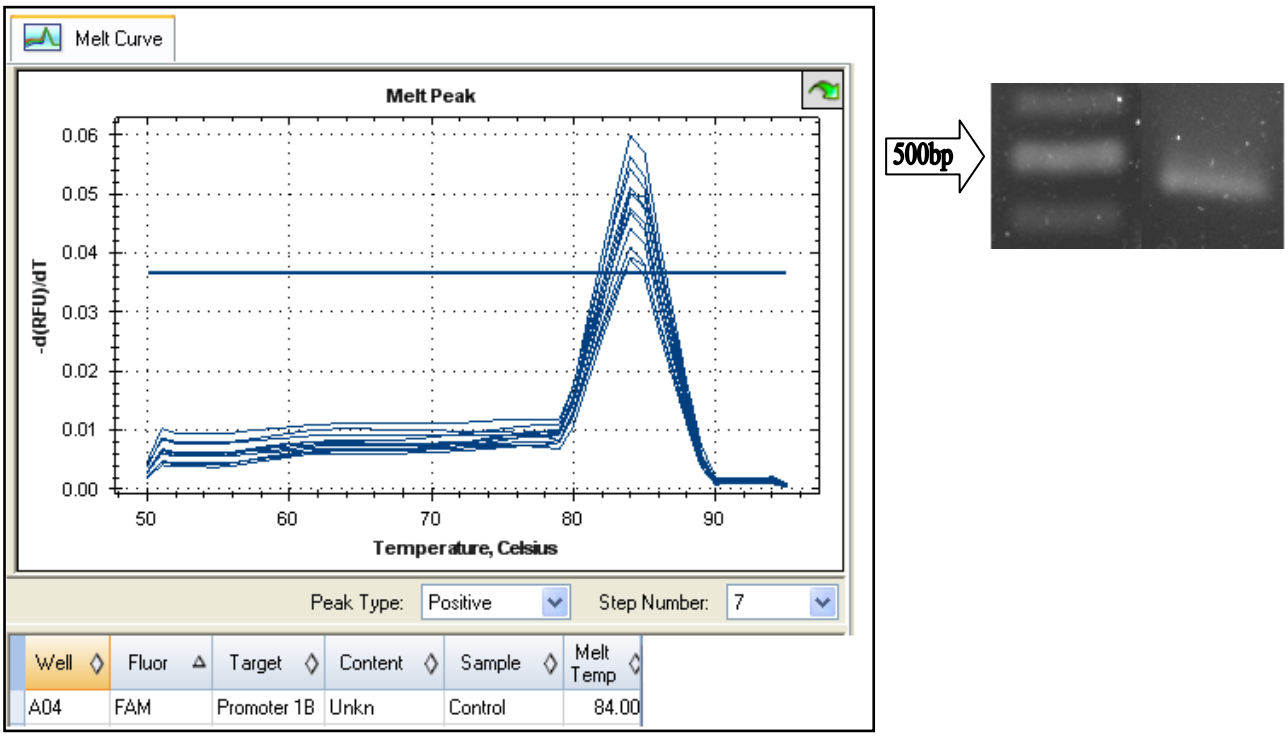

Figure 7.5: A. Melt Curve analysis of Promoter 1B primer set with a melt temperature of 84^{o}C

B. Agarose gel electrophoresis confirmation of Promoter 1B amplification (size: 478 bp)

Promoter 1C

A **B**

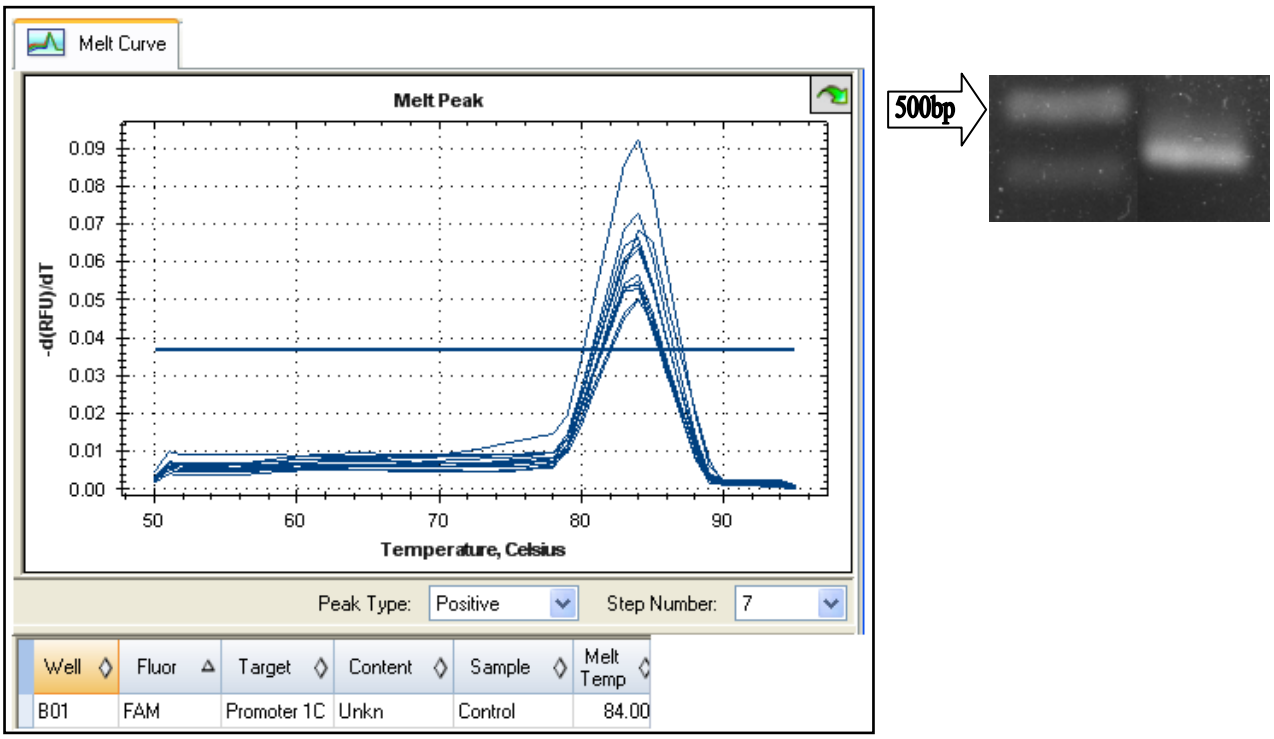

Figure 7.6: A. Melt Curve analysis of Promoter 1C primer set with a melt temperature of 84^{o}C

B. Agarose gel electrophoresis confirmation of Promoter 1C amplification (size: 464 bp)

eYFP

A **B**

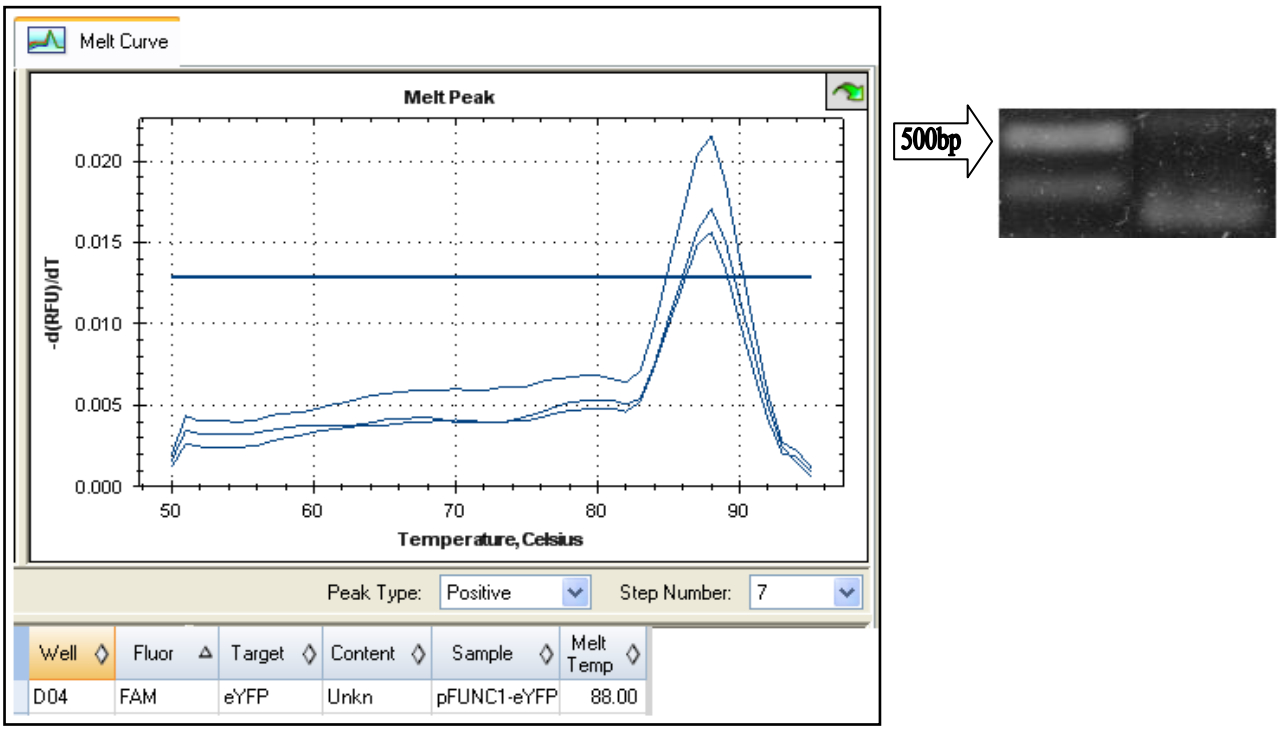

Figure 7.7: A. Melt Curve analysis of eYFP primer set with a melt temperature of 88°C B. Agarose gel electrophoresis confirmation of eYFP amplification

A.7. Data Analysis

Ct values were determined using the CFX Manager v5 (Bio-Rad) at a baseline fluorescence reading of 0.05 RFU. Outliers that did not meet the parameters were excluded from analysis. The no template controls (NTC) and no reverse transcriptase controls (noRT) for each qPCR target gene were determined either by primer dimers or no product formation. This was verified by agarose gel electrophoresis.

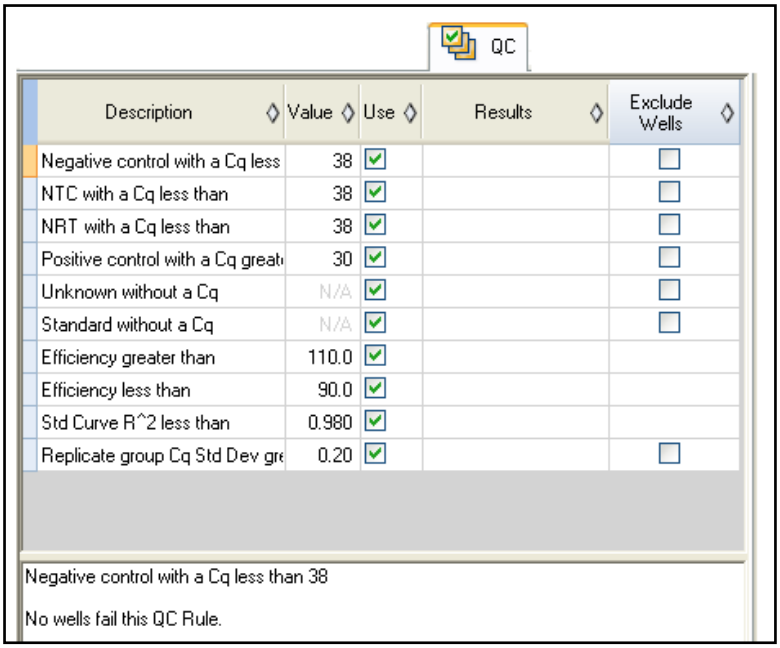

Figure 7.8: The parameters used to eliminate outlier wells from analyses using CFX software

β-actin

The reference gene used was β-actin sourced from Alt *et al*. (2010). One reference gene was used as GAPDH did not produce reputable qPCR data.

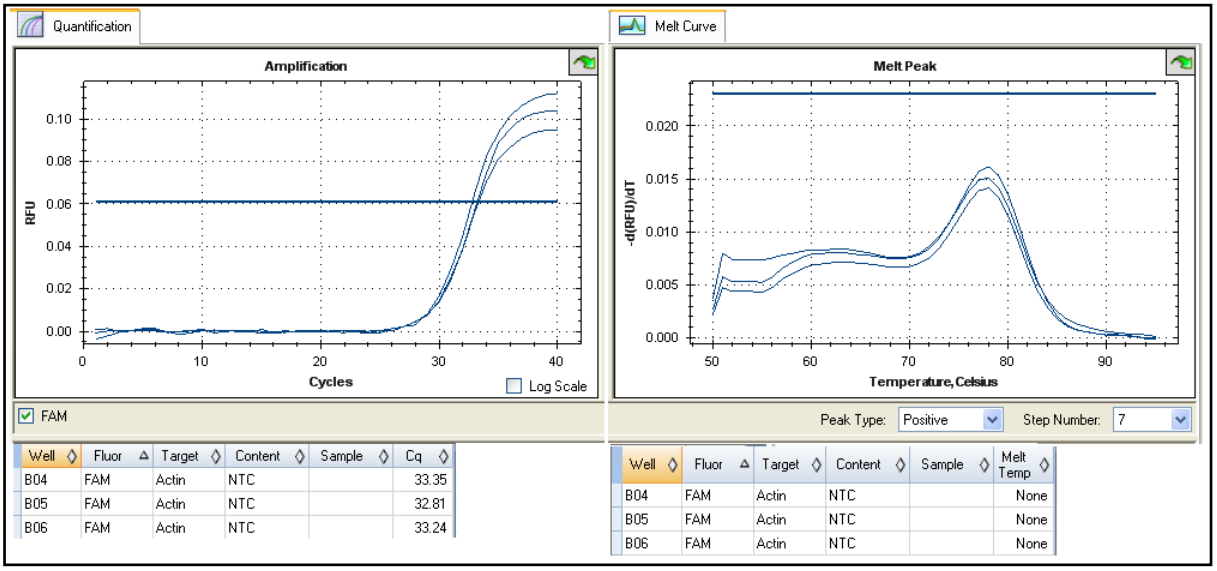

Figure 7.9: Amplification and Melt Curve analyses of β-actin primer NTC

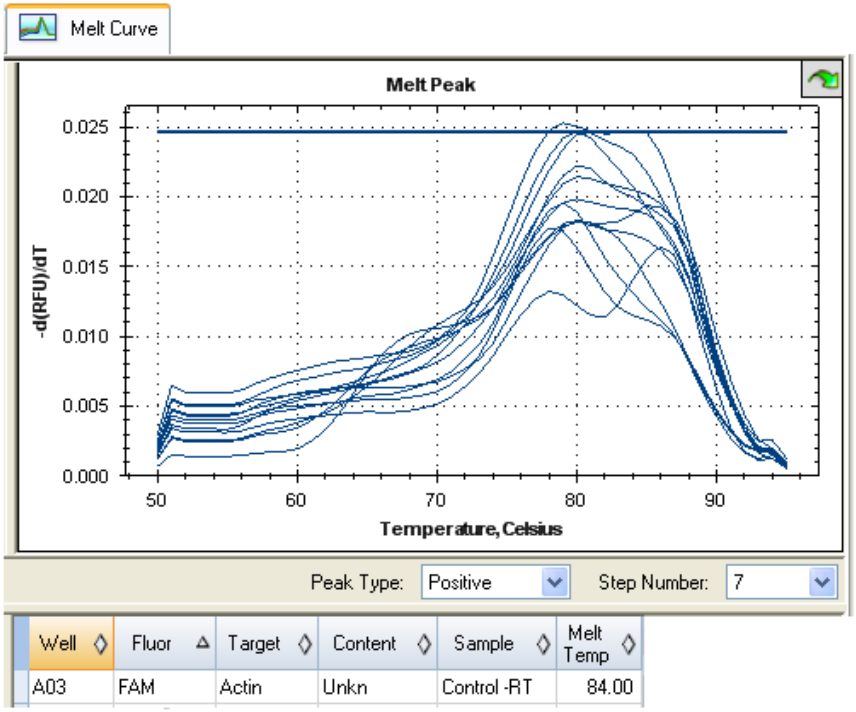

Figure 7.10: Melt Curve Analysis of β-actin primer noRT

Promoter 1B

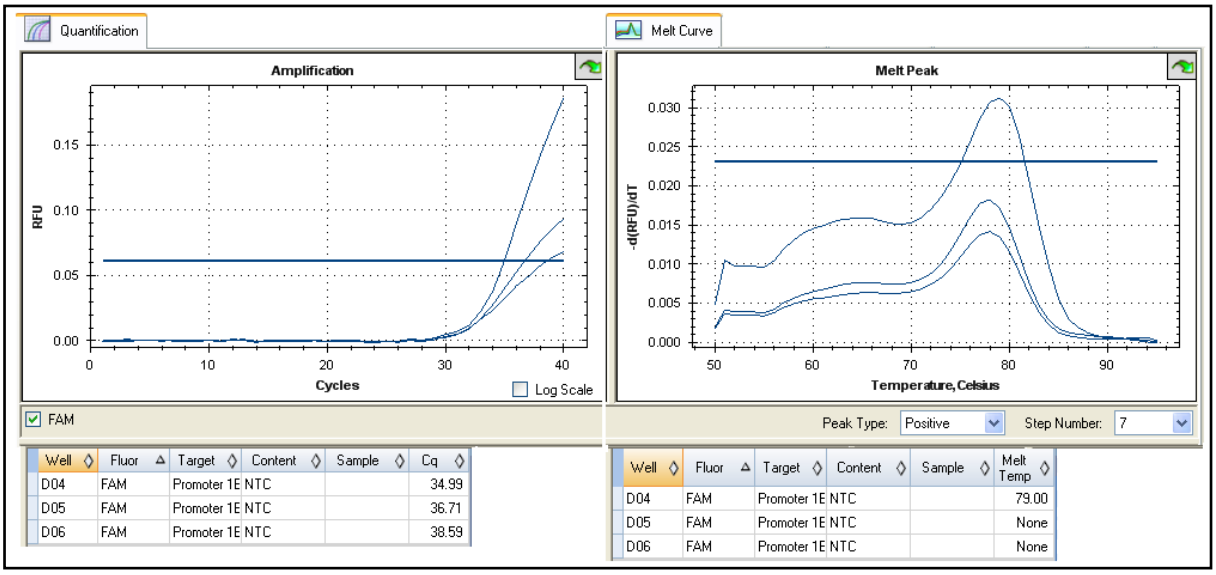

Figure 7.11: Amplification and Melt Curve Analysis of Promoter 1B primer NTC

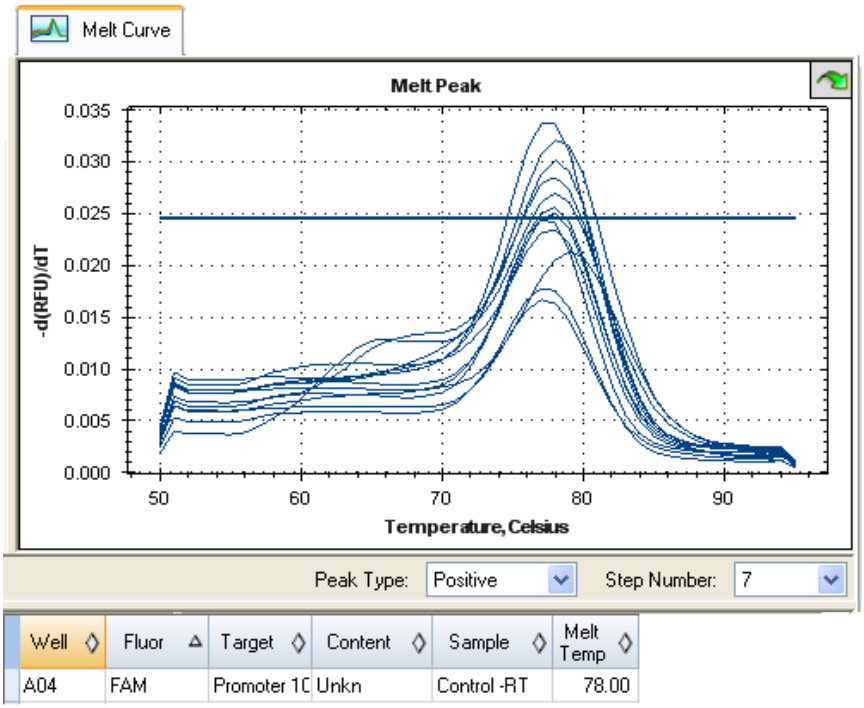

Figure 7.12: Melt Curve analysis of Promoter 1B primer noRT

Promoter 1C

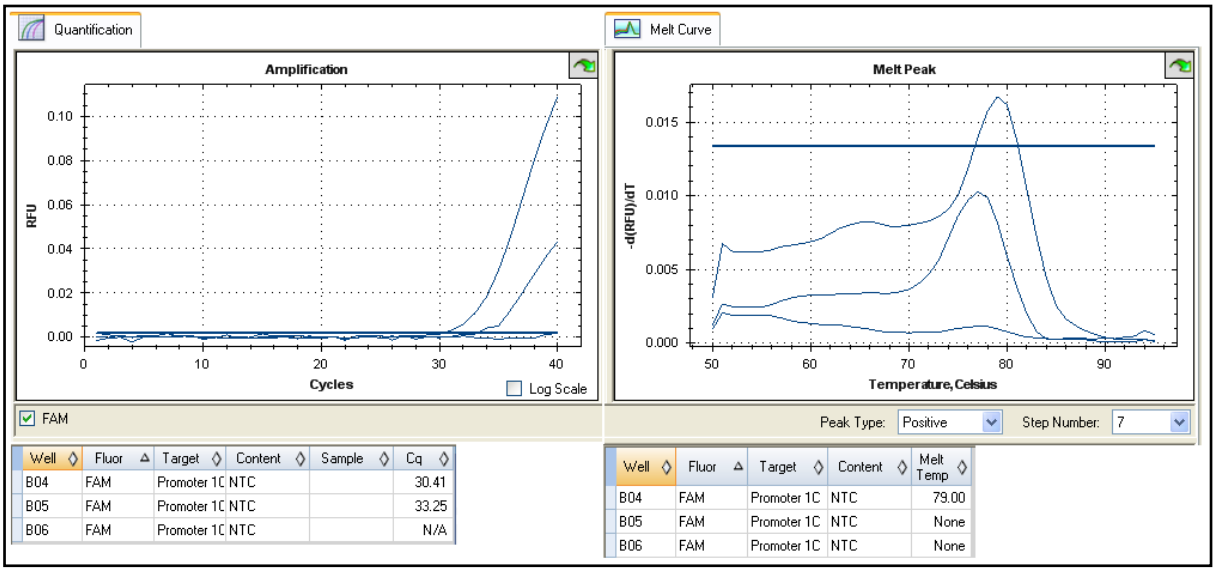

Figure 7.13: Amplification and Melt Curve analysis of Promoter 1C primer NTC

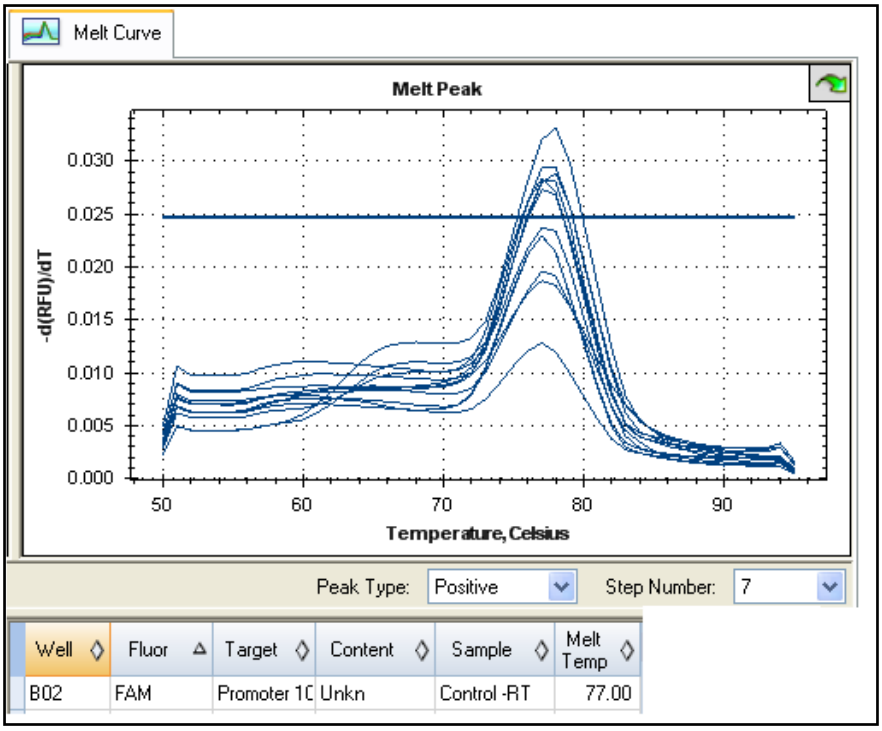

Figure 7.14: Melt Curve Analysis of Promoter 1C primer noRT

eYFP

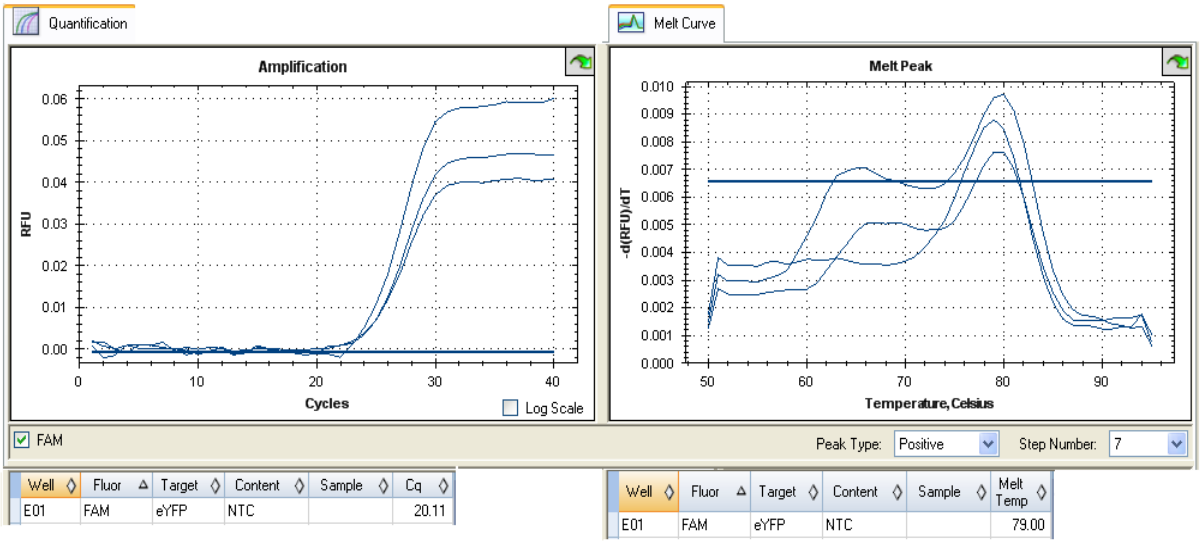

Figure 7.15: Amplification and Melt Curve analysis of eYFP primer NTC

The relative fold change of the target gene in relation to the reference gene was tested for statistical significance by a one-way ANOVA or one sample t-test depending on the number of factors being analysed. Statistical analyses were performed using the SPSS software package version 21 (IBM®). The mean relative fold changes for each target gene were represented as bar graphs with standard errors using Microsoft Office Excel 2007 software.

B. Recipes

1. 1x Trypsin-EDTA

One millilitre of 10x Trypsin (PAA) was dissolved in 9 ml of sodium EDTA solution and stored at -20^{o}C.

2. 5-Aza-2'-deoxcytidine stock solution

Reagent	Manufacturer	Amount
5-Aza	Sigma-Aldrich	50 mg
Glacial Acetic Acid	Saarchem	500 µl
Distilled Water		500 µl

Fifty milligrams of 5-Aza was dissolved in 500 µl of filter sterilised glacial acetic acid and distilled water. The total volume of the stock was 1ml and was aliquoted at a volume of 100 µl into PCR tubes. Aliquots were stored at -80^{o}C.

3. 10x Phosphate Buffer Saline (PBS)

Reagent	Manufacturer	Amount
$Na_2H_2PO_4$	Merck	2.28 g
Na_2HPO_4	Merck	11.5 g
NaCl	Merck	43.84 g
Distilled water		450 ml

The above reagents were dissolved in 450ml of distilled water. The pH of the solution was adjusted to 7.4 and 50 ml of distilled water was added with a final volume of 500 ml. PBS solution was stored at room temperature.

1x PBS solution

Five millilitres of 10x PBS was dissolved in 45 ml of sterile distilled water.

4. DEPC-treated Water

Hundred microlitres of DEPC (Sigma) was dissolved in 1 L of de-ionised water. The water was incubated for 2 hours at 37^{o}C and autoclaved.

5. Ethidium Bromide Stock Solution

Ten milligrams of ethidium bromide was dissolved in 1 ml of distilled water.

Ethidium Bromide Working Solution

A 1:200 dilution was made from the stock solution to create the working solution. 1 ml of stock solution was dissolved in 199 ml of distilled water to create a 0.05 mg/ml working solution.

6. 10x MOPS Buffer

Reagent	**Manufacturer**	**Amount**
MOPS	Sigma	4.18 g
1M NaOAC	Sigma	2 ml
0.5M EDTA	Merck	2 ml
DEPC-treated water		96 ml

4.18 g of MOPS was dissolved in 96 ml of DEPC-treated water. Two mililitres of NaOAC and EDTA (pH 8) was added to the MOPS solution.

1x MOPS Buffer

Ten millilitres of 10x MOPS buffer was dissolved in 90 ml of DEPC-treated water.

7. Dilution of primers

Ten microlitres of 100 µmol/l primer stock was dissolved in 90 µl of nuclease free water (Invitrogen). The primer solution was aliquoted in 1.5ml microcentrifuge tubes at a volume of 25 µl. Aliquots were stored at -20^{o}C.

8. dNTP stock

Ten microlitres of each 100 mM stock of dATP, dGTP, dTTP and dCTP was dissolved in 460 µl of nuclease free water. 25 µl aliquots of 2 mM dNTPs were stored at -20^{o}C.

9. 10x TBE Buffer

Reagent	**Manufacturer**	**Amount (g)**
Tris base	Merck	53.89
Boric Acid	Merck	24.96
EDTA Disodium Salt	Merck	1.86

Tris base, boric acid and EDTA was dissolved in 450 ml of distilled water and the pH was adjusted to 8.3. The solution was brought up to a final volume of 500 ml.

1x TBE Buffer

A 1:10 dilution was done where 100 ml of 10x TBE buffer was dissolved in 900 ml of distilled water.

10. 1x TE Buffer

Reagent	**Manufacturer**	**Amount (ml)**
1mM Tris-HCl	Merck	5
500mM EDTA Disodium Salt	Merck	1
Distilled Water		494

A 1 mM Tris-HCl stock solution was prepared by dissolving 7.9 g in 50 ml of distilled water. The solution was adjusted to a pH of 7.5. A 500 mM EDTA stock solution was prepared by dissolving 9.3 g in 50 ml of distilled water with a pH 8.

11. LB Broth

Twenty grams of LB broth (Sigma) dissolved in 1 L of deionised water, autoclaved and stored at 4^{o}C.

12. Preparation of LB Agar Plates

Forty grams of Luria Agar (Sigma) was dissolved in 1 L of deionised water, when cooled ampicillin was added at a concentration of 100 µg/ml (Sigma-Aldrich). 10 ml of luria agar was poured into each petri dish (Carbi Plates) and swirled for even distribution. Plates were stored at 4^{o}C.

13. Glycerol Stock of Plasmids

0.15 ml of 100% glycerol was transferred to 1.5 ml micro-centrifuge tubes and autoclaved. When plasmid colonies were grown for mini-prep, 850 µl of cell suspension was added to the sterilised glycerol. The microcentrifuge was mixed by pipetting 6 times and stored at -80^{o}C.

14. 70% Ethanol

Thirty five millilitres of Absolute Ethanol (Molecular Grade) (Merck) was dissolved in 15 ml of nuclease free water (Invitrogen).

15. 4% Paraformaldehyde with 0.15% Triton X-100

Four grams of paraformaldehyde (Merck) was dissolved in 100 ml of distilled water and filter sterilized. Aliquots of 6 ml in 15 ml centrifuge tubes were prepared and stored at -20^{o}C.

Aliquots were allowed to thaw at room temperature and 9 µl of 1% Triton X-100 (Sigma-Aldrich) was added and ready for use.

16. 10% (m/v) MOWIOL and 23M Glycerol in Tris (0.1M, pH8.5) with DABCO

Reagent	Manufacturer	Amount
MOWIOL	Sigma	2.4 g
0.2M Tris-HCl	Merck	12 ml
Glycerol	Merck	6 ml
Distilled water		6 ml
DABCO	Sigma	0.6 g

MOWIOL was dissolved overnight in 12 ml of Tris-HCl in a closed container, wrapped in foil, by stirring. Glycerol and distilled water was added to the solution and left overnight to stir. 2.5% of DABCO was added to the solution and aliquoted into 1.5 ml microcentrifuge tubes. Aliquots were stored at -20^{o}C.

17. Sodium Butyrate Stock Solution

A 10 mM stock solution was prepared by dissolving 11mg of sodium butyrate (Aldrich) in 10 ml of filter sterilised 100% ethanol.

18. Hexadimethrine Bromide Stock Solution

0.05 g of hexadimethrine bromide (Sigma) was dissolved in 25 ml of sterile distilled water with a concentration of 2 mg/ml.

19. 10x Annexin Binding Buffer

Reagent	Manufacturer	Amount
0.1M HEPES	PAA	20 ml
1.4M NaCl	Merck	16.36 g
25mM $CaCl_2$	BDH Chemical Supplies	0.554 g

HEPES, NaCl and $CaCl_2$ were dissolved in 200 ml of sterile distilled water and filter sterilised. Solution was stored at 4^oC.

1x Annexin Binding Buffer

10 ml of 10x Annexin binding buffer was dissolved in 90 ml of sterilised distilled water.

20. Propidium Iodide

The propidium iodide (Sigma) was dissolved in PBS solution at a concentration of 1 mg/ml.